January 2010

Dissolution, Formation, and Transformation of the Lead Corrosion Product PbO$_2$: Rates and Mechanisms of Reactions that Control Lead Release in Drinking Water Distribution Systems

Yanjiao Xie
Washington University in St. Louis

WASHINGTON UNIVERSITY IN ST. LOUIS

School of Engineering and Applied Science

Department of Energy, Environmental and Chemical Engineering

Dissertation Examination Committee:

Daniel E. Giammar, Chair
William E. Buhro
Young-Shin Jun
Cynthia S. Lo
Jill D. Pasteris
Jay R. Turner

DISSOLUTION, FORMATION, AND TRANSFORMATION

OF THE LEAD CORROSION PRODUCT PbO$_2$:

RATES AND MECHANISMS OF REACTIONS THAT CONTROL

LEAD RELEASE IN DRINKING WATER DISTRIBUTION SYSTEMS

by

Yanjiao Xie

A dissertation presented to
the Graduate School of Arts and Sciences
of Washington University in
partial fulfillment of the requirements for the degree of
Doctor of Philosophy in Energy, Environmental and Chemical Engineering

August 2010

Saint Louis, Missouri

ABSTRACT OF THE DISSERTATION

Dissolution, Formation, and Transformation of the Lead Corrosion Product PbO$_2$:

Rates and Mechanisms of Reactions that Control Lead Release

in Drinking Water Distribution Systems

by

Yanjiao Xie

Doctor of Philosophy in Energy, Environmental & Chemical Engineering

Washington University in St. Louis, 2010

Research Advisor: Professor Daniel Giammar, Chair

As one of the major lead corrosion products in lead service lines, lead(IV) oxide (PbO$_2$) can react with water through reductive dissolution, resulting in elevated lead concentrations in tap water. Limited data are available on the rates and mechanisms of PbO$_2$ dissolution. Information regarding the impact of water chemistry on the rates and mechanisms of PbO$_2$ dissolution can provide potential strategies to control the release of lead from corrosion products to drinking water. The present study investigated effects of water chemistry on the rates and mechanisms of PbO$_2$ dissolution, the equilibrium solubility of PbO$_2$, and the rates of lead release from lead pipes with corrosion scales.

The dissolution rate of pure plattnerite (β-PbO$_2$) was investigated as a function of pH and the concentrations of carbonate, orthophosphate, free chlorine, and monochloramine in continuously stirred tank reactors (CSTR). Complementary batch

experiments were conducted to compare the effects of water chemistry on the PbO_2

dissolution rate for different solid-water contact times. The equilibrium solubility of

plattnerite in the presence of free chlorine was then investigated. Lead release from pipe

scales was determined under different water chemistry conditions at flow or no-flow

conditions to optimize the water chemistry for mitigating lead release. For these

experiments new lead pipes were conditioned in the presence of free chlorine and

carbonate to form corrosion scales.

Dissolution experiments provided direct evidence that the PbO_2 dissolution rate

increases when the disinfectant is switched from free chlorine to monochloramine, which

is consistent with the high lead concentrations observed in Washington D.C. from 2001

to 2004 following such a switch. Lower pH and the presence of carbonate accelerated

PbO_2 dissolution. Addition of orthophosphate as a potential corrosion inhibitor had

multiple effects on PbO_2 dissolution rates. A detailed mechanism and rate model were

proposed for PbO_2 reductive dissolution. Batch experiments showed that the residence

time also played an important role in controlling dissolved lead concentrations. Pipe

scales developed under drinking water conditions contained PbO_2 and hydrocerussite

$(Pb_3(CO_3)_2(OH)_2)$. In experiments with these pipe scales, when compared with stagnant

conditions water flow significantly accelerated the release of both dissolved and total lead

from pipe scales. Among various water chemistry conditions, the dissolved lead was

lowest from corrosion scales in contact with solutions containing orthophosphate. Two

models were proposed to predict lead release from pipe scales.

Acknowledgement

American politics, economy, culture, and society through various events. It is the

McDonnell Academy and ACL members that have made my PhD life colorful and

enjoyable.

Yanjiao Xie

Washington University in St. Louis
August 2010

Table of Contents

List of Tables

List of Figures

xi

Chapter 1. Introduction and overview

1.1. Introduction

1.1.1   Lead Corrosion and Regulation in Water Distribution Systems

Lead pipes have been used to deliver water since the ancient Roman Empire. The

toxic effects of lead have been known as early as the second century B.C [1]. Concerns

about the health effects of lead exposure have increased in the past several decades. Lead

can accumulate in the human body over a lifetime and can be released very slowly [2].

People can be exposed to lead through ingestion of airborne dust, water, food and

soil [3]. The U.S. Environmental Protection Agency (EPA) estimated that 14–20% of

total childhood lead exposure in the United States is from drinking water [4]. The Lead

and Copper Rule (LCR) set the lead action level to 0.015 mg/L in 1991. For this

regulation if 10% of tested homes have lead concentrations above the action level, then

the system must undertake efforts to control corrosion and inform the public. In a recent

incident extremely high lead concentrations in Washington D.C. tap water were

correlated with increased blood lead levels [5]. The problems encountered in

Washington, DC demonstrate the need for research on reactions controlling lead

concentrations in drinking water.

Lead in drinking water comes from the corrosion of lead-containing pipes, solder,

fittings, fixtures, and faucets. Lead pipes were widely used at the beginning of the 20th

century because of their durability and malleability. Brass fittings and faucets used in

distribution systems can also have significant amounts of lead. Since 1986 new

construction cannot use lead pipe. However, many older buildings retain their original

lead service lines. The corrosion of old lead pipes and fittings with time results in the development of lead corrosion products in pipe scales that can leach lead to drinking water [6-8].

1.1.2   Lead Corrosion Products

The formation of lead corrosion products depends on the specific water chemistry of a distribution system. The most common lead phases formed on the inside of pipes are lead(II) carbonates, lead(II) oxides, lead(II) phosphates, and lead(IV) oxides [7, 9]. The lead(II) solids are produced as the elemental lead of the original pipe is oxidized upon contact with oxic or chlorinated water. Figure 1.1 illustrates the formation, transformation, and dissolution of lead corrosion products in pipe scales.

Both scrutinyite (α-PbO_2) and plattnerite (β-PbO_2), formed by oxidation of Pb(II) to Pb(IV), are found in water distribution systems in which free chlorine is used as a secondary disinfectant [10]. Both free chlorine and chloramines are used as residual disinfectants in distribution systems to prevent biological growth throughout the distribution systems. Free chlorine disinfectants, such as sodium hypochlorite (NaOCl)
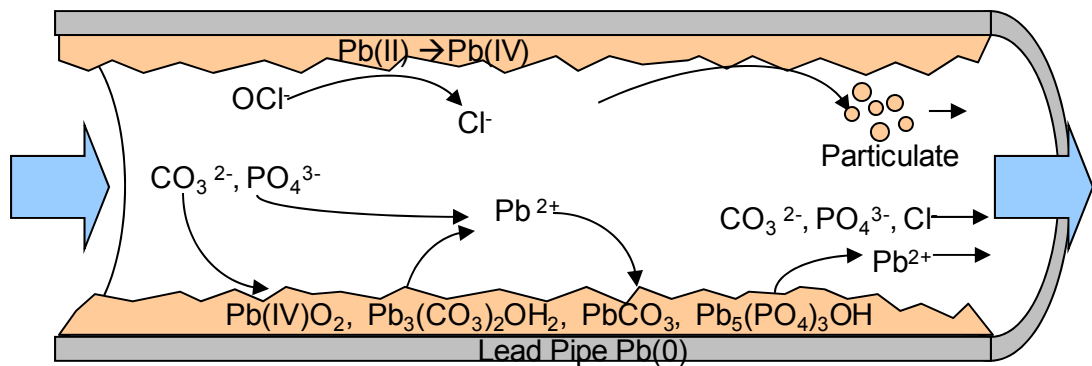
Figure 1.1. A conceptual schematic diagram of the formation of lead corrosion products in distribution systems. (Adopted from Noel and Giammar, 2007)

and chlorine gas (Cl_2), form HOCl and OCl⁻ upon addition to water, which can oxidize elemental lead and lead(II) species to lead(IV) oxides (Figure 1.1). Chloramines, which are among the species known as combined chlorine, are formed by reacting ammonia with free chlorine and cannot oxidize elemental lead and lead(II) species to lead(IV) oxides [11]. Lead(IV) oxides are only present in water distribution systems with the high oxidation-reduction potential (ORP) maintained by free chlorine disinfectants and are not stable with chloramines. Even in some systems with free chlorine, lead(IV) oxides still do not form, which indicates that the formation of lead(IV) oxides may depend on the free chlorine concentration and can be very slow. In water distribution systems with low ORP, lead(II) solids are the dominant corrosion products rather than lead(IV) oxides. Lead(IV) oxides are much less soluble than lead(II) solids, and the low solubility of lead(IV) oxides can maintain very low lead concentrations in drinking water.

1.1.3   Electrochemistry of the Pb(0)/Pb(II)/Pb(IV) System

The oxidation of metallic Pb(0) to Pb(IV) oxides with free chlorine (i.e. HOCl and OCl⁻) proceeds through two steps. The relevant reactions are listed in the Table 1.1. The first step is the oxidation of Pb(0) to Pb(II) via half reactions 1.1 and 1.2, and the overall reaction of the first step is

$$Pb + HOCl + H^+ \rightarrow Pb^{2+} + Cl^- + H_2O$$
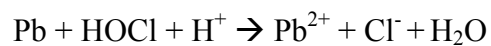
The second step is the oxidation of Pb(II) to Pb(IV) through half reactions 1.2 and 1.3, which can be described by the following overall reaction.

$$HOCl + Pb^{2+} + H_2O \rightarrow PbO_{2\ (s)} + Cl^- + 3H^+$$
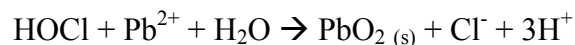
Table 1.1. Relevant half reactions for the oxidation of lead to lead(IV) oxide by free chlorine.

#	Reaction	E_H^0 (V)	Log K[1]
1.1	$Pb^{2+} + 2e^- \rightarrow Pb^0$	4.26	0.13
1.2	$HOCl + 2e^- + H^+ \rightarrow Cl^- + H_2O$	1.48	50.20
1.3	$PbO_{2\,(s)} + 4H^+ + 2e^- \rightarrow Pb^{2+} + 2H_2O$	1.47	49.60

Pb(IV) oxides are only stable at the high ORP (Figure 1.2) provided by free chlorine. In actual distribution systems with free chlorine, the E_H range is from 1.2 to 1.3
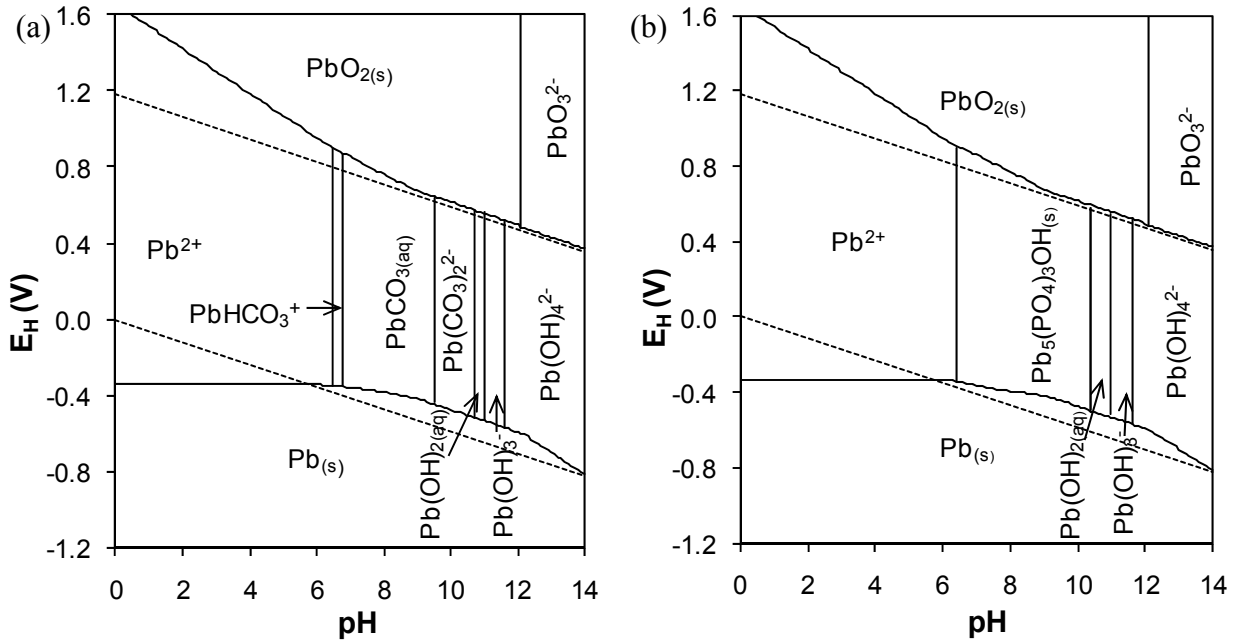
Figure 1.2. Predominance area diagrams showing the dominant lead solid phase or dissolved species as a function pH and oxidation-reduction potential for (a) 30 mg C/L dissolved inorganic carbon (DIC) (2.5×10^{-3} M) and (b) 3 mg C/L DIC (2.5×10^{-4} M) plus 3 mg/L dissolved orthophosphate (9.7×10^{-5} M). The diagrams are constructed for a total lead concentration of 15 µg/L. The dashed lines represent the stability limits of water ($P_{O2} =$ 0.001 atm and $P_{H2} = 1$ atm).

_____

[1] Reaction constants shown in this chapter were taken from MINEQL+ software.

V. However, when chloramine is used as the disinfectant in distribution systems, the E_H is from 0.6 to 0.9 V, which is about 0.5 V lower than with free chlorine [12]. Previous research showed that the ORP from chloramine is not high enough to maintain Pb(IV) oxides [11].

$$NH_2Cl + H_2O + 2e^- \rightarrow Cl^- + OH^- + NH_3 \qquad\qquad E_H^0 = 0.69 \text{ V} \qquad (1.4)$$

In the absence of free chlorine, Pb(IV) oxides will transform to Pb(II) solids or dissolved Pb(II) species. Through energetically favorable reactions, natural organic matter and pure water may reduce Pb(IV) oxides to Pb(II) species (Reaction 1.5) [13-16]. An intermediate species from monochloramine decay can reduce Pb(IV) oxides [17], and iodide, bromide, manganous, and ferrous ions have also been shown to enhance the reductive dissolution of Pb(IV) oxides [18-20].

$$PbO_{2(s)} + H_2O = Pb^{2+} + 0.5O_2 + 2OH^- \qquad\qquad\qquad (1.5)$$

The incident of high lead levels in drinking water of the Washington D.C. area was caused by the breakdown of lead(IV) oxide. In November 2000, the Water and Sewer Authority (WASA) of Washington D.C. switched its disinfectant from free chlorine to chloramines. The change was initiated to comply with the 1998 Disinfection Byproducts Rule (DBR), which restricts the concentrations of disinfection byproducts in water. Chloramine generates less of the regulated disinfection byproducts, such as trihalomethanes and haloacetic acids [10]. After changing the disinfectant, lead concentrations exceeding 0.015 mg/L were measured in drinking water from 2001 to 2004. The lead concentration in tap water of hundreds of homes even exceeded 0.3 mg/L [6]. The switch from chlorine to chloramine is believed to have lowered the ORP and caused the reduction of insoluble Pb(IV) oxides to more soluble Pb(II) species [6, 11, 17].

1.1.4 Equilibrium Solubility of Lead Corrosion Products

The equilibrium solubility of lead corrosion products determines the lead concentration in tap water when water reaches equilibrium with lead corrosion products. The lead concentration at equilibrium depends on the individual lead corrosion products present in pipe scales and the water chemistry. The least soluble lead corrosion product will control the equilibrium dissolved lead concentration. The equilibrium lead concentration with respect to each lead corrosion product can be calculated based on the solubility product of the solid and equilibrium constants for the formation of soluble lead complexes. The total dissolved lead is the sum of the concentrations of the free metal ion Pb^{2+} or Pb^{4+} as well as their complexes with hydroxide, carbonate and other anions.

When lead(IV) is the dominant oxidation state, as controlled by free chlorine, the dissolved lead concentrations controlled by Pb(IV) oxides can be very low (Figure 1.3). Based on equilibrium calculations using Equation 1.6a and 1.6b, the concentration of dissolved free metal ion (Pb^{4+}) from the lead(IV) oxide solid is very low. The total dissolved lead(IV) is the sum of the concentrations of the free metal ion Pb^{4+} and the hydrolysis complexes PbO_3^{2-} and PbO_4^{4-}. The concentrations of the hydrolysis complexes increase with increasing pH and are the dominant lead species above pH 6. Overall, the total dissolved lead(IV) is under the action level (15 ug/L) for an environmentally relevant pH range (Figure 1.3). Despite the widespread observation of lead(IV) oxides in pipe scales, the equilibrium solubility of lead(IV) oxides has not been measured at chemical conditions relevant to drinking water distribution.

$$PbO_{2(s)} + 4H^+ = Pb^{4+} + 2H_2O \qquad (1.6a)$$

$$K_{sp,scrutinyite} = \frac{[Pb^{4+}]}{[H^+]^4} = 10^{-8.26} \qquad (1.6b)$$

6

$$Pb^{4+} + 3H_2O = PbO_3{}^{2-} + 6H^+ \qquad \log(K_{eq}) = -23.04 \qquad (1.7)$$

$$Pb^{4+} + 4H_2O = PbO_4{}^{4-} + 8H^+ \qquad \log(K_{eq}) = -63.8 \qquad (1.8)$$

When Pb(II) is the dominant oxidation state, Pb(II) carbonate, oxide, or phosphate solids can control the dissolved lead concentrations. The following reactions and equations can be used to calculate the dissolved Pb^{2+} concentration in equilibrium with hydrocerussite (1.9) and hydroxylpyromorphite solids (1.10). The equilibrium lead concentration responds to the dissolved carbonate and phosphate concentrations.

$$K_{sp,hydrocerussite} = \frac{[Pb^{2+}]^3[CO_3^{2-}]^2}{[H^+]^2} = 10^{-18.77} \qquad (1.9a)$$

$$Pb_3(CO_3)_2(OH)_{2(s)} + 2H^+ = 3Pb^{2+} + 2CO_3{}^{2-} + 2H_2O \qquad (1.9b)$$
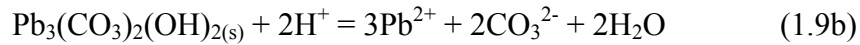
$$K_{hydroxylpyromorphite} = \frac{[Pb^{2+}]^5[PO_4^{3-}]^3}{[H^+]} = 10^{-62.79} \qquad (1.10a)$$

$$Pb_5(PO_4)_3OH_{(s)} + H^+ = 5Pb^{2+} + 3PO_4{}^{3-} + H_2O \qquad (1.10b)$$

As shown in Figure 1.3, the dissolved lead concentrations in equilibrium with a lead(II) carbonate or phosphate are significantly higher than those in equilibrium with lead(IV) oxides.

In actual distribution systems, the water may not be in equilibrium with the corrosion products present since the hydraulic residence time in distribution systems can be insufficient for the water to equilibrate with the solids. The hydraulic residence time is normally minutes to hours. However, it takes days to reach equilibrium for PbO_2 in actual distribution systems. Therefore, equilibrium-based models tend to overpredict dissolved lead concentrations in real distribution systems. Such models are limited by the accuracy of available equilibrium constants, transitions between scale types, byproduct
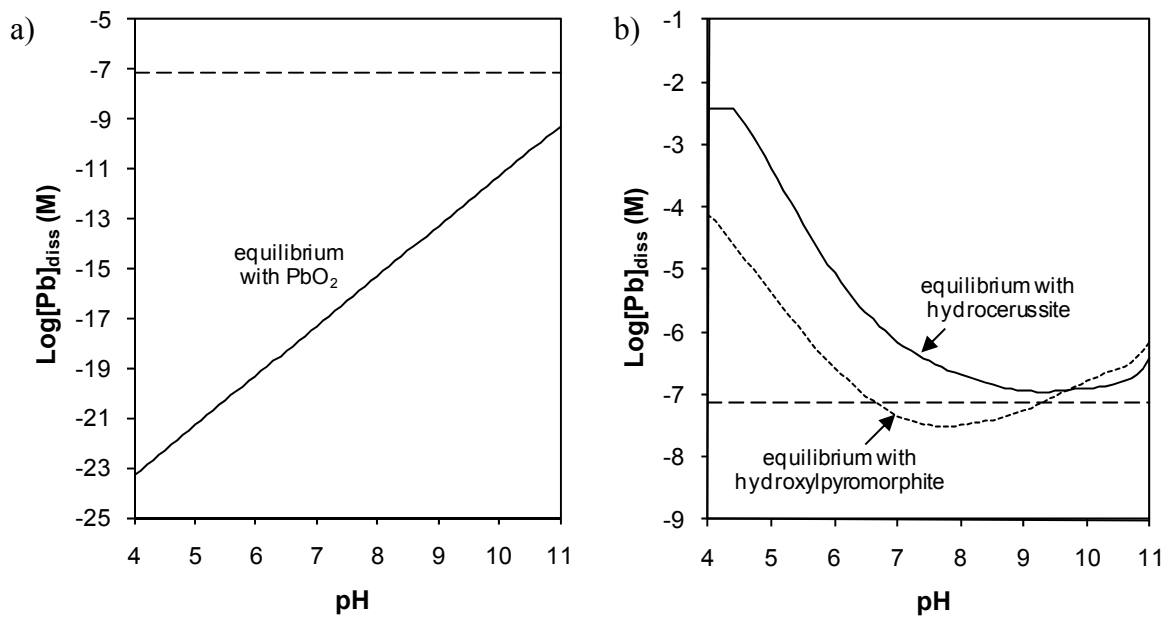
Figure 1.3. Dissolved lead concentration in equilibrium with (a) lead(IV) oxide at sufficiently oxidizing conditions that all lead is present as lead(IV) and (b) the lead(II) carbonate hydrocerussite with 30 mg/L DIC and the lead(II) phosphate hydroxylpyromorphite with 30 mg/L DIC and 3 mg/L orthophosphate. The long dashed line shows the lead action level of 15 μg/L. Note the difference in the y-axis ranges.

release, and reaction kinetics [21, 22]. For systems that are not at equilibrium, measurements of dissolution rates can improve quantitative estimates of soluble lead concentrations in distribution systems.

1.1.5   Dissolution Rates of Lead Corrosion Products

Consideration of the dissolution and transformation rates of lead(IV) oxides can provide more accurate estimates of dissolved lead concentrations in distribution systems than estimates based on equilibrium solubility. The dissolution rates of hydrocerussite and hydroxylpyromorphite have already been determined at various pH and carbonate conditions [23-25], but the dissolution rates of PbO_2 are not known. Previous research investigated the effects of natural organic matter (NOM), chlorine species, manganous, and ferrous, and halide ions on dissolution of PbO_2 in batch systems, but these studies did not quantitatively measure PbO_2 dissolution rates [14, 16-20]. Previous studies all used batch experiments, but the calculation of a dissolution rate from batch studies can be affected by the dissolution of labile surface phases and accumulation of reaction products. Flow-through experiments, which are advantageous for quantifying rates, have not yet been employed to determine the dissolution rates of PbO_2.

1.1.6   Lead Release from Pipe Scales

Previous studies qualitatively showed the effects of stagnation time, flow velocity and water chemistry on lead release from lead pipes. The stagnation time was found to have a substantial effect on lead release from pipes, with most of the release occurring

within the first 24 hours [26]. Flow velocity can influence erosion mechanisms of corrosion and can affect the development of pipe scales [27]. With respect to water chemistry, orthophosphate was demonstrated to inhibit lead release [28, 29]. The effects of pH and carbonate depend on the exact condition and corrosion products that make up the pipe scales [27].

Previous models for lead release from lead pipes accounted for diffusion of lead from the pipe wall and the effects of flow. Lytle and Schock developed a diffusion model to describe the dissolved lead profile with time at stagnant conditions [26]. Cardew extended the diffusion model to laminar flow conditions [30]. These models assumed that equilibrium was always reached at the pipe wall. However, equilibrium is not always reached at short residence times in distribution systems. None of the previous diffusion models used a dissolution rate to predict lead concentrations. A dissolution rate model can provide a way to quantitatively predict the lead release rates from pipe scales, especially when equilibrium is not reached and the dissolution reaction rather than diffusion is the rate-limiting step.

1.1.7 Mitigating Lead Release

Full replacement of any service lines and fittings that are suspected to have lead-containing materials with lead-free alloys is a potential solution to the lead problems in tap water [31]. However, complete replacement is often cost-prohibitive [32]. Considering cost, partial replacement was proposed and tested. However, the partial replacement strategy has been proved to be insufficient for mitigating lead release. After partial replacement, other lead-containing components and the deposition of released

particulate lead to other non-lead segments in the premise plumbing can still release high concentrations of lead [33]. Even water distribution systems that have no lead pipe lines could have lead-containing corrosion scales, because brass fittings can legally have up to 8% by mass lead [34].

Control of the water composition can also be used to limit lead concentrations in tap water. Water distribution systems that have historically used free chlorine as a disinfectant for bacteria and have maintained high free chlorine residuals could have accumulated substantial amounts of Pb(IV) oxides. One way to control lead concentrations in these systems is to provide water chemistry that maintains the stability of the low solubility lead(IV) oxide. Another option to limit lead release is to optimize the DIC and pH in water distribution systems. An optimal DIC and pH can minimize the dissolution rate of the solids in the lead corrosion scales. Changing DIC and pH levels may also lower the lead concentration in distribution systems by precipitation of lead-containing solids. Addition of orthophosphate (PO_4^{3-}) to water distribution systems can also control lead release. Lead phosphate solids are less soluble than lead carbonate solids at most environmentally-relevant conditions. The lead released from Pb(IV) oxide and lead(II) carbonates can precipitate out as lead phosphates in the presence of orthophosphate. Orthophosphate has been used as a corrosion inhibitor in water utilities to control lead release [28]. After the 2001-2004 elevated lead incident, Washington D.C. has used orthophosphate to comply with the Lead and Copper Rule [35].

Combinations of the approaches mentioned above can be used in the future to ensure that water systems meet both the LCR and the Disinfection Byproducts Rule,

while the optimal solution will depend on the water chemistry and the composition of lead corrosion scales of the system.

1.2   Research Objectives

The overall project objective was to measure, evaluate, and predict lead release from pipe scales that contain lead(IV) oxide. The following specific objectives were pursued.

Objective 1: Develop dissolution rate equations for lead(IV) oxide as a function of water chemistry.

Objective 2: Determine the equilibrium solubility of lead(IV) oxide.

Objective 3: Evaluate lead release rates from lead pipes with pipe scales containing lead(IV) oxide and assess whether lead release can be predicted by the dissolution rate equations for lead(IV) oxide.

1.3   Overview of Dissertation

To achieve these objectives, the research approach was organized into three related tasks. Figure 1.4 illustrates how the three tasks are organized. The dissolution rates determined from flow experiments in Task 1 and the equilibrium solubility of PbO_2 measured from batch experiments in Task 2 can be used to interpret the results of lead release from pipe scales in Task 3 and to assess whether dissolution rates of PbO_2 can be used in predicting lead release from pipe scales.
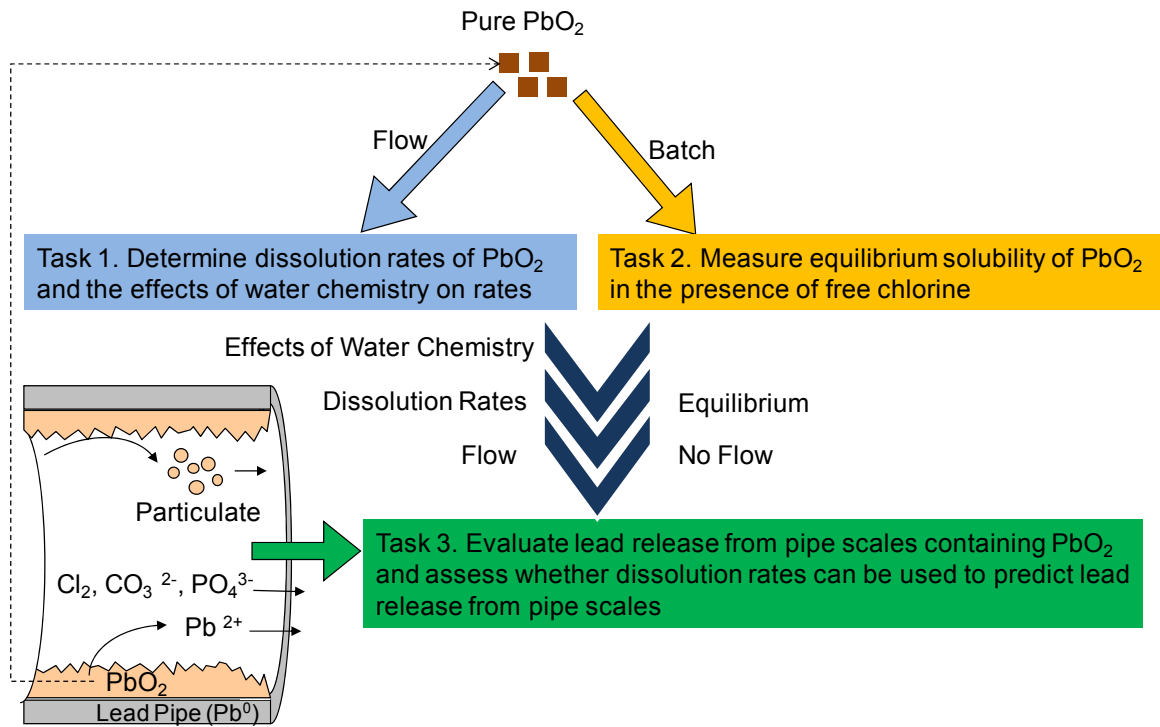
Figure 1.4. Overview of research tasks and their connections.

Task 1: Investigate the effects of water chemistry on the dissolution rates of lead(IV) oxide

Chapters 2, 3, and 4 focus on Task 1. The dissolution rates of lead(IV) oxide were determined as a function of pH, concentrations of DIC, phosphate, free chlorine, and chloramine using continuous flow stirred tank reactors (CSTR). Possible solid transformation was probed by scanning electron microscopy (SEM) and X-ray diffraction (XRD). Complementary batch studies showed the effects of chloramines at long residence times. Dissolution rate equations were proposed to quantify the relationship between the dissolution rate and water chemistry parameters, such as pH, carbonate, and oxidation reduction potential.

Task 2: Measure the equilibrium solubility of lead(IV) oxide in the presence of free chlorine

Task 2 is addressed in sections of Chapter 3. Lead(IV) is predicted to be the dominant oxidation state in the presence of free chlorine. The dissolved lead concentrations in equilibrium with lead(IV) oxide in the presence of free chlorine were measured at different pH values to obtain the Pb(IV) solubility. The equilibrium solubility of lead(IV) oxide in the presence of free chlorine provided more information for control of lead release.

Task 3: Examine lead release from pipe scales containing lead(IV) oxides and develop models to predict lead release from pipe scales

Chapters 5 is related to Task 3. Chapter 5 covers the experimental study of lead release from pipe scales containing lead(IV) oxides, and the Appendix of Chapter 5 presents the modeling of lead release from pipe scales. Corrosion scales were developed on new lead pipes in the presence of free chlorine at environmentally-relevant pH and DIC before the pipes were used for lead release studies. Characterization of the pipe scales using XRD, SEM, and X-ray absorption near edge spectroscopy (XANES) showed lead(IV) oxides and hydrocerussite as the main components of the scales. Lead release from pipe scales was examined at different water chemistry conditions, flow rates, and stagnation times. Different models were developed and compared with the experimental results. The ability of the dissolution rate model for lead(IV) oxide to predict the lead release from pipes was examined.

Chapter 6 summarizes the results from the present study and recommends future work to be done.

References:

1.   Needleman, H., Lead poisoning. *Annual Review of Medicine* **2004,** *55*, 209-222.

2.   Yule, W., Neurotoxicity of lead -- review. *Child Care Health and Development* **1992,** *18*, (5), 321-337.

3.   Moreira, E. G.; Vassilieff, I.; Vassilieff, V. S., Developmental lead exposure: behavioral alterations in the short and long term. *Neurotoxicol. Teratol.* **2001,** *23*, (5), 489-495.

4.   Miranda, M. L.; Kim, D.; Hull, A. P.; Paul, C. J.; Galeano, M. A. O., Changes in blood lead levels associated with use of chloramines in water treatment systems. *Environmental Health Perspectives* **2007,** *115*, (2), 221-225.

5.   Edwards, M.; Triantafyllidou, S.; Best, D., Elevated Blood Lead in Young Children Due to Lead-Contaminated Drinking Water: Washington, DC, 2001-2004. *Environ. Sci. Technol.* **2009,** *43*, (5), 1618-1623.

6.   Edwards, M.; Dudi, A., Role of chlorine and chloramine in corrosion of lead-bearing plumbing materials. *Journal American Water Works Association* **2004,** *96*, (10), 69-81.

7.   Schock, M. R., Understanding Corrosion Control Strategies for Lead. *Journal American Water Works Association* **1989,** *81*, (7), 88-100.

8.   Schock, M. R.; Lytle, D. A.; Sandvig, A. M.; Clement, J.; Harmon, S. M., Replacing polyphosphate with silicate to solve lead, copper, and source water iron problems. *Journal American Water Works Association* **2005,** *97*, (11), 84-93.

9.   Edwards, M.; McNeill, L. S., Effect of phosphate inhibitors on lead release from pipes. *Journal American Water Works Association* **2002,** *94*, (1), 79-+.

10.   Vasquez, F. A.; Heaviside, R.; Tang, Z. J.; Taylor, J. S., Effect of free chlorine and chloramines on lead release in a distribution system. *Journal American Water Works Association* **2006,** *98*, (2), 144-154.

11.   Switzer, J. A.; Rajasekharan, V. V.; Boonsalee, S.; Kulp, E. A.; Bohannan, E. W., Evidence that monochloramine disinfectant could lead to elevated Pb levels in drinking water. *Environ. Sci. Technol.* **2006,** *40*, (10), 3384-3387.

12.   Rajasekharan, V. V.; Clark, B. N.; Boonsalee, S.; Switzer, J. A., Electrochemistry of free chlorine and monochloramine and its relevance to the presence of Pb in drinking water. *Environ. Sci. Technol.* **2007,** *41*, (12), 4252-4257.

13.   Dryer, D. J.; Korshin, G. V., Investigation of the reduction of lead dioxide by natural organic matter. *Environ. Sci. Technol.* **2007,** *41*, (15), 5510-5514.

14.   Lin, Y. P.; Valentine, R. L., The release of lead from the reduction of lead oxide (PbO_2) by natural organic matter. *Environ. Sci. Technol.* **2008,** *42*, (3), 760-765.

15.   Lin, Y. P.; Valentine, R. L., Reduction of lead oxide (PbO_2) and release of Pb(II) in mixtures of natural organic matter, free chlorine and monochloramine. *Environ. Sci. Technol.* **2009,** *43*, (10), 3872-3877.

16.   Shi, Z.; Stone, A. T., PbO_2(s, Plattnerite) reductive dissolution by natural organic matter: reductant and inhibitory subfractions. *Environ. Sci. Technol.* **2009,** *43*, (10), 3604-3611.

17.   Lin, Y. P.; Valentine, R. L., Release of Pb(II) from monochloramine-mediated reduction of lead oxide (PbO_2). *Environ. Sci. Technol.* **2008,** *42*, (24), 9137-9143.

18.   Lin, Y. P.; Washburn, M. P.; Valentine, R. L., Reduction of lead oxide (PbO_2) by iodide and formation of iodoform in the PbO_2/I⁻/NOM system. *Environ. Sci. Technol.* **2008,** *42*, (8), 2919-2924.

19.   Shi, Z.; Stone, A. T., PbO$_2$(s, Plattnerite) reductive dissolution by aqueous manganous and ferrous ions. *Environ. Sci. Technol.* **2009,** *43*, (10), 3596-3603.

20.   Lin, Y. P.; Valentine, R. L., Reductive Dissolution of Lead Dioxide (PbO2) in Acidic Bromide Solution. *Environ. Sci. Technol.* **2010,** *44*, (10), 3895-3900.

21.   Edwards, M.; Jacobs, S.; Dodrill, D., Desktop guidance for mitigating Pb and Cu corrosion by-products. *Journal American Water Works Association* **1999,** *91*, (5), 66-77.

22.   Vasquez, F. A.; Heaviside, R.; Tang, Z. J.; Taylor, J. S., Effect of free chlorine and chloramines on lead release in a distribution system. **2006,** *98*, (2), 144-154.

23.   Giammar, D.; Nelson, K.; Noel, J.; Xie, Y. In *Role of Phosphate in Mitigating Lead Release from Corrosion Products*, Water Quality Technology Conference, Cincinnati, OH, 2008.

24.   Noel, J. D.; Giammar, D. E. In *The influence of water chemistry on dissolution rate of lead corrosion products*, Water Quality Technology Conference, Charlotte, NC, 2007.

25.   Noel, J. D.; Giammar, D. E. In The influence of water chemistry on dissolution rates of Lead(II) carbonate solids found in water distribution systems, Water Quality Technology Conference, Cincinnati, OH, 2008.

26.   Lytle, D. A.; Schock, M. R., Impact of stagnation time on metal dissolution from plumbing materials in drinking water. *Journal Of Water Supply Research And Technology-Aqua* **2000,** *49*, (5), 243-257.

27.   Schock, M. R., Internal corrosion and deposition control. In *Water quality and treatment*, Fifth ed.; Letterman, R. D., Ed. McGraw-Hill, Inc.: New York, New York, 1999.

28.   Edwards, M.; McNeill, L. S., Effect of phosphate inhibitors on lead release from pipes. *J. Am. Water Works Assoc.* **2002,** *94*, (1), 79-90.

29.   Nadagouda, M. N.; Schock, M.; Metz, D. H.; DeSantis, M. K.; Lytle, D.; Welch, M., Effect of Phosphate Inhibitors on the Formation of Lead Phosphate/Carbonate Nanorods, Microrods, and Dendritic Structures. *Crystal Growth & Design* **2009,** *9*, (4), 1798-1805.

30.   Cardew, P. T., Development of a convective diffusion model for lead pipe rigs operating in laminar flow. *Water Res.* **2006,** *40*, (11), 2190-2200.

31.   Renner, R., Lead pipe replacement should go all the way. *Environ. Sci. Technol.* **2007,** *41*, (19), 6637-6638.

32.   Renner, R., "Catch-22" makes it tough to get the lead out. *Environmental Science & Technology* **2006,** *40*, (10), 3130-3131.

33.   Renner, R., Reaction to the Solution Lead Exposure Following Partial Service Line Replacement. *Environmental Health Perspectives* **2010,** *118*, (5), A203-A208.

34.   Kimbrough, D. E., Brass corrosion as a source of lead and copper in traditional and all-plastic distribution systems. *J. Am. Water Works Assoc.* **2007,** *99*, 70-76.

35.   Standard, D. S., On-line orthophosphate monitoring. Automated dosing optimize Washington, DC's lead reduction program. *J. Am. Water Works Assoc.* **2006,** *98*, (10), 38-40.

Reproduced in part from with permission from [Xie, Y., Wang, Y., Singhal, V., and Giammar, D.E. (2010) Effects of pH and carbonate concentration on dissolution rates of the lead corrosion product PbO_2. Environmental Science & Technology 44(3), 1093-1099]. Copyright [2010] American Chemical Society.

Chapter 2. Effects of pH and carbonate concentration on dissolution rates of the lead corrosion product PbO$_2$

Abstract

Lead(IV) oxide is a corrosion product that can develop on lead pipes and affect lead concentrations in drinking water. Continuously-stirred flow-though reactors were used to quantify the dissolution rates of plattnerite (β-PbO$_2$) at different pH values and dissolved inorganic carbon (DIC) concentrations. Organic pH buffers were not used, because several were found to be reductants for PbO$_2$ that accelerated its dissolution. Most plattnerite dissolution rates were on the order of 10^{-10} mol/min-m^2. The rate of dissolution increased with decreasing pH and with increasing DIC. The effect of DIC is consistent with a reductive dissolution mechanism that involves the reduction of Pb(IV) to Pb(II) at the plattnerite surface followed by the formation of soluble Pb(II)-carbonate complexes that accelerate Pb(II) release from the surface. Under the experimental conditions, dissolved lead concentrations were controlled by the dissolution rate of plattnerite and not by its equilibrium solubility. A dissolution rate model was developed and can be used to predict dissolution rates of plattnerite as a function of pH and DIC.

2.1.   Introduction

Concerns about the adverse health effects of lead exposure motivated the development of the 1991 Lead and Copper Rule, which set the action level for lead in drinking water to 0.015 mg/L *(1)*. Lead concentrations in drinking water are controlled by the dissolution of lead corrosion products developed on lead-containing pipes, solders, and fittings used in service lines and premise plumbing. These corrosion products include Pb(II) carbonates and oxides and Pb(IV) oxides *(2)*. The stability and dissolution of lead corrosion products are strongly affected by water chemistry.

The observations of high lead levels in Washington D.C. tap water from 2001 to 2004 demonstrate the need for information on reactions controlling lead concentrations in drinking water *(3, 4)*. These high concentrations are believed to have been caused by the reductive dissolution of PbO_2 due to a switch of the residual disinfectant from free chlorine to chloramines, a switch that was made to reduce the formation of chlorinated disinfection by-products (DBPs). The change lowered the oxidation reduction potential (ORP) of the water and caused the reduction of low solubility PbO_2 to more soluble Pb(II) species *(5-7)*.

Both scrutinyite (α-PbO_2) and plattnerite (β-PbO_2), which are formed by oxidation of Pb(II) to Pb(IV), are found in water distribution systems that have maintained a high concentration of free chlorine as a residual disinfectant *(8, 9)*. The dissolution rate of PbO_2 is particularly relevant to assessing the rates of lead release when the concentration or type of the residual disinfectant is changed *(8)*. When PbO_2 is stable at the high oxidation-reduction potential provided by free chlorine, dissolved lead concentrations can

be maintained at low levels. When the free chlorine is not present, the dissolution rate of

PbO_2 is anticipated to be controlled by the water chemistry in the distribution system *(5)*.

Lead release from PbO_2 is affected by pH, carbonate, chloramines, and chemical

reductants that include natural organic matter (NOM) and Fe(II) and Mn(II) species *(10-*

14). A typical range of dissolved inorganic carbon (DIC) in drinking water is 0-50 mg

C/L *(15)*. The reaction of PbO_2 with the reductants produces soluble Pb(II) species and

increases dissolved lead concentrations. These previous studies demonstrated chemical

reduction of PbO_2, but they did not quantify the dissolution rates. Dissolution rates are

needed to predict lead concentrations in premise plumbing when equilibrium is not

reached.

The objective of this study was to quantify the dissolution rates of plattnerite as a

function of pH and DIC concentration. Based on these measurements, additional

objectives were to identify likely dissolution mechanisms and to assess equilibrium

versus kinetic control of dissolved lead concentrations.

2.2.　　Materials and Methods

2.2.1　Materials

The plattnerite (β-PbO_2) (Fisher Scientific) consisted of black primary particles

ranging in size from 50 to 500 nm as determined by scanning electron microscopy (SEM)

(Figure S1 of the Supporting Information). The solid was indentified as pure plattnerite

by X-ray Diffraction (XRD) (Figure S2 of the Supporting Information). Its specific

surface area was determined as 3.6 m^2/g by N_2 adsorption and the BET isotherm. All

chemicals used were reagent grade or better. Ultrapure water (resistivity > 18.2 MΩ-cm) was used to prepare solutions.

2.2.2. Analytical Methods

XRD was performed on a Rigaku Geigerflex D-MAX/A diffractometer using Cu-Ka radiation. Electron microscopy was performed on a JOEL 7001LVF field emission SEM. Dissolved lead concentrations were determined by inductively coupled plasma mass spectroscopy (ICP-MS) (Agilent 7500ce). The pH of solutions was measured with a glass pH electrode and pH meter (Accumet).

2.2.3. Measurement of Dissolution Rates

Plattnerite dissolution rates were quantified using small (84 mL) stirred flow-through reactors that were loaded with 1 g/L plattnerite and sealed with 0.22 μm nitrocellulose filter membranes (Figure S3 of the Supporting Information). The influent was supplied to the reactors with a peristaltic pump set at a flow rate to provide a hydraulic residence time of 30 minutes. In separate experiments with plattnerite, filtration with 0.025 μm membranes gave similar dissolved lead concentration results as filtration with 0.22 μm membranes. Lin and Valentine also demonstrated that after filtration of similarly sized PbO_2 with 0.2 μm membranes, the dissolved and total lead concentrations were similar *(10)*.

The influent compositions were controlled to evaluate the effects of pH and DIC concentration on the dissolution rates. The dissolution rates were determined for pH values of 7.5, 8.5 and 10 and DIC concentrations of 0, 10, and 50 mg-C/L (carbonate alkalinity from 0 to 5.6 mM). Effluent samples were collected periodically, preserved by acidification to 2% HNO_3, and analyzed for dissolved lead. Volumetric flow rate and pH were periodically measured throughout each experiment. Each experimental condition was run in duplicate or triplicate with a procedural blank run under the same conditions as the other reactors but without any solid added. Prior to running dissolution experiments, a tracer study was performed, which determined that the solution in the reactors was well-mixed. The solids remaining in the reactors after the dissolution experiment were analyzed by XRD and SEM.

The reactor influents were prepared in 10 L plastic bags (Tedlar) to ensure no transfer of CO_2 into or out of solution. To minimize uptake of CO_2, the ultrapure water in each influent was purged with nitrogen immediately before being pumped into the bags. The influent pH was adjusted by the addition of NaOH or HNO_3 solution. DIC concentrations were provided by the addition of volumes of 1.0 M $NaHCO_3$. An aliquot of 1.0 M $NaNO_3$ was then injected into the bag to set the ionic strength at 0.01 M. Experiments were conducted at room temperature (22±2°C).

To provide constant pH for the plattnerite experiments with influent solutions that did not have sufficient buffering capacity provided by DIC, solutions of either NaOH or HNO_3 were added to the influent from a syringe pump to continuously adjust the pH as necessary. For these experiments the effluent pH was continuously measured using a small flow-through cell (15 mL) with a pH electrode so that acid or base additions could

be adjusted in near real-time. Organic pH buffers were not used because preliminary experiments found that they could reduce PbO_2 and accelerate PbO_2 dissolution (Figure S4 of the Supporting Information).

Dissolution rates were determined by operating the flow-through reactors for durations equivalent to 48 or more hydraulic residence times (24 hours). By continuously flushing the products of dissolution from the reactor, the effluent dissolved lead concentration approaches a steady-state value (C_{ss}) that is controlled by the dissolution rate of the solid phase and is below the equilibrium solubility (C_{eq}). This process is illustrated conceptually in Figure S5 of the Supporting Information. Equilibrium concentrations were calculated using MINEQL+ version 4.5 *(16)*. This approach is different from batch experiments in which the dissolved concentrations increase until they reach equilibrium solubility; the accumulation of reaction products and the presence of initial labile phases in batch experiments can complicate the quantification of rates *(17-19)*. In a flow-through experiment for rate quantification, the steady-state effluent concentration needs to be significantly less than the equilibrium solubility of the dissolving solid.

The experimentally-measured dissolution rate (R_{exp} in mol/m^2-min) is quantified by Equation 2.1,

$$R_{exp} = \frac{(C_{out} - C_{in})}{A \cdot [\ solids\ ] \cdot t_{res}} \qquad (2.1)$$

where C_{out} and C_{in} are the influent and effluent lead concentration respectively (mol/L), t_{res} is the hydraulic residence time (min), *[solid]* is the solid concentration in the reactor (g/L), and A is the specific surface area of the solid (m^2/g). The steady-state concentration was determined as the average of at least 5 consecutive samples that varied

23

by less than 30% and spanned at least 5 residence times. With C_{in} below detection limits, Equation 2.1 simplifies to Equation 2.2.

$$R_{exp} = \frac{C_{ss}}{A \cdot [\,solids\,] \cdot t_{res}}$$ (2.2)

A model for surface-controlled dissolution rates *(20)* was used to calculate the dissolution rate constant k (mol/m^2-min) from the rate by accounting for the distance of the solution in the reactor from the predicted equilibrium solubility of the solid, as expressed as a function of the Gibbs free energy of reaction (ΔG) (Equation 2.3). Dissolution is surface-controlled for most minerals under well-mixed laboratory conditions; exceptions are for extremely soluble minerals, which plattnerite is not *(21)*.

$$R_{mod\,el} = k \cdot f(\Delta G) = R_{exp}$$ (2.3)

For a reversible elementary reaction,

$$f(\Delta G) = (1 - e^{\frac{\Delta G}{RT}})$$ (2.4)

The value of ΔG can be related to the saturation index (SI) (Equations 2.5-2.6).

$$\Delta G = RT \ln\left(\frac{IAP}{K_{sp}}\right) = 2.303RT \log\left(\frac{IAP}{K_{sp}}\right) = 2.303RT \cdot SI$$ (2.5)

$$SI = log\left(\frac{IAP}{K_{sp}}\right)$$ (2.6)

where R is the ideal gas constant (8.314 J mol^{-1} K^{-1}), T is absolute temperature (K), and IAP and K_{sp} are the ion activity product and equilibrium solubility product for the solid, respectively. A final dissolution rate expression (Equation 2.7) is used with the parameter Ω as an empirical coefficient, set to 1 in these calculations, to account for the non-elementary nature of the reactions *(20)*.

$$Rate = k(1 - e^{\frac{\Delta G}{RT}})^{\Omega} = k(1 - 10^{SI})^{\Omega} \tag{2.7}$$

Additional discussion of this model is in the Supporting Information.

2.2 Results and Discussion

2.2.1 Plattnerite Dissolution Rates

The effluent dissolved lead concentrations and pH versus time are shown for all experiments in Figure 2.1. Effluent concentrations were consistently at steady-state over the final 7-10 hours of each experiment, and these concentrations were used to determine the dissolution rates that are summarized in Table 2.1.
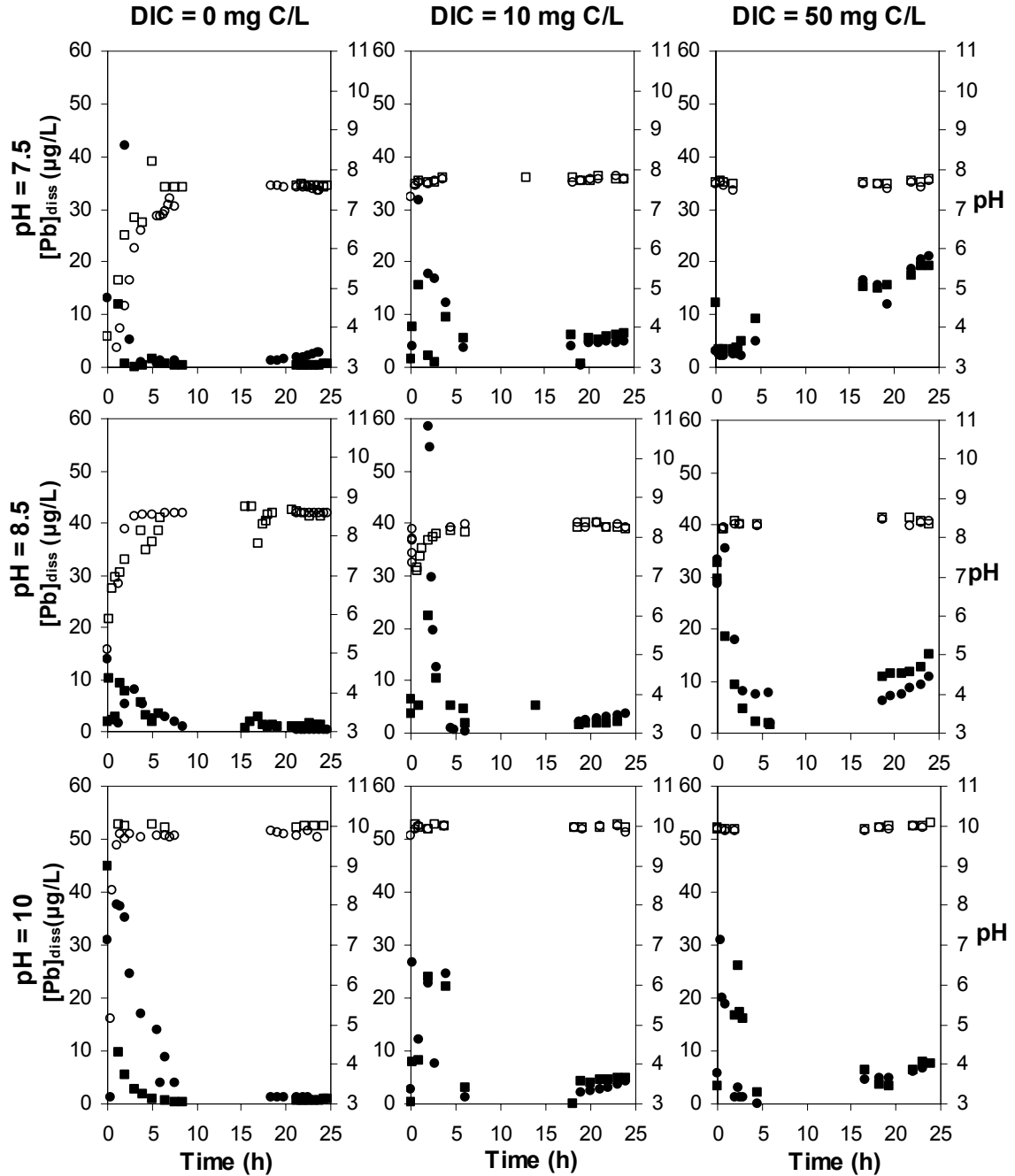
Figure 2.1. Effluent lead concentrations (shown as ■ and ●) and pH (shown as □ and ○) from flow-through reactors over time for different DIC levels at pH 7.5, 8.5, and 10. Duplicate experiments (represented by rectangles and circles) were conducted at the hydraulic residence time of 30 minutes. Samples were not taken during the middle of the run (9 to 15 hours).

In several experimental conditions, especially at 50 mg C/L DIC, the effluent lead

concentrations had a slightly upward trend (<30% increase) in the final 7-10 hours.

26

While this slight increase introduces uncertainty to the dissolution rates reported for these conditions, the average concentration were taken as approximating steady-state for calculation of rates. As is often observed for flow-through dissolution experiments, concentrations during the initial operation of the reactors were more variable *(18)*; potential factors affecting initially greater dissolution are discussed in a later section. During the period from 9-15 hours the reactors were not sampled. The duplicate or triplicate experiments were generally in agreement; the largest differences were for the experiments with the lowest Pb concentrations, which were near its detection limit. Variability was also introduced by the challenges of maintaining a constant pH in the absence of buffering from inorganic carbon. The weighted averages of the pH over the period for the steady-state lead effluent concentration were within 0.3 pH units of the target value, and the pH measurements varied by less than 0.5 pH units over this period.

Table 2.1. Conditions and results of plattnerite dissolution experiments

Experiment ID*	Influent Composition pH	DIC (mg/L as C)	Measured pH†	Residence time (min)	effluent lead (nM)	Equilibrium lead (nM)	Steady-state Dissolution rate x 10^{10} (mol/min·m^2)	Rate constant x 10^{10} (mol/min·m^2)§
1A	7.5	0.0	7.58	30	2	8318	0.19	0.19
1B	7.5	0.0	7.52	30	12	8318	1.09	1.09
2A	8.5	0.0	8.57	30	6	389	0.53	0.54
2B	8.5	0.0	8.58	30	1	389	0.10	0.10
3A	10.0	0.0	9.94	30	6	41	0.56	0.66
3B	10.0	0.0	9.98	30	3	41	0.32	0.35
3C	10.0	0.0	9.78	30	6	41	0.54	0.63
4A	7.5	10.0	7.78	30	28	21380	2.64	2.64
4B	7.5	10.0	7.78	30	23	21380	2.12	2.12
5A	8.5	10.0	8.27	30	15	1585	1.37	1.39
5B	8.5	10.0	8.26	30	12	1585	1.17	1.18
6A	10.0	10.0	9.95	30	15	85	1.44	1.76
6B	10.0	10.0	9.97	30	22	85	2.05	2.75
7A	7.5	50.0	7.62	30	84	72444	7.87	7.88
7B	7.5	50.0	7.68	30	83	72444	7.77	7.78
8A	8.5	50.0	8.36	30	42	7413	3.90	3.92
8B	8.5	50.0	8.42	30	60	7413	5.63	5.67
9A	10.0	50.0	9.94	30	27	676	2.52	2.63
9B	10.0	50.0	9.99	30	28	676	2.61	2.72

*The letters A-C identify replicate experiments.
†The weighted average of the effluent pH during the steady-state period is indicated.
§Rate constants were calculated from the measured dissoluton rate and Equation 2.3

2.2.2. Effect of pH and DIC on Plattnerite Dissolution

Dissolution rates were higher at pH 7.5 than 8.5 when other parameters were held constant (Figure 2.2). Further increasing the pH to 10 resulted in very slight increases in the dissolution rate at 0 and 10 mg C/L DIC and to a decrease for 50 mg C/L DIC.

Dissolution rates increased with increasing DIC for all 3 pH values (Figure 2.2). The effect of simultaneously increasing pH and DIC is to increase the dissolution rate at

the experimental conditions. These results reveal that DIC has a stronger effect than pH

on the dissolution rates of plattnerite under the experimental conditions. The formation

of soluble Pb(II)-carbonate complexes can explain the accelerated dissolution in the

presence of DIC. At equilibrium at pH 7.5, the species $PbCO_{3(aq)}$, $Pb(CO_3)_2^{2-}$ and

$PbHCO_3^+$ comprise 61% of the dissolved lead at 10 mg-C/L DIC and 86% of the

dissolved lead concentration at 50 mg-C/L DIC. At pH 10, 17-26% of the dissolved lead

can be attributed to these soluble Pb-carbonate complexes; the lower percentage of these

complexes at higher pH is due to a higher percentage of lead hydroxyl complexes,

resulting in an increase of dissolution rate from pH 8.5 to 10 at low DIC levels (i.e.

$PbOH^+$ and $Pb(OH)_{2(aq)}$).
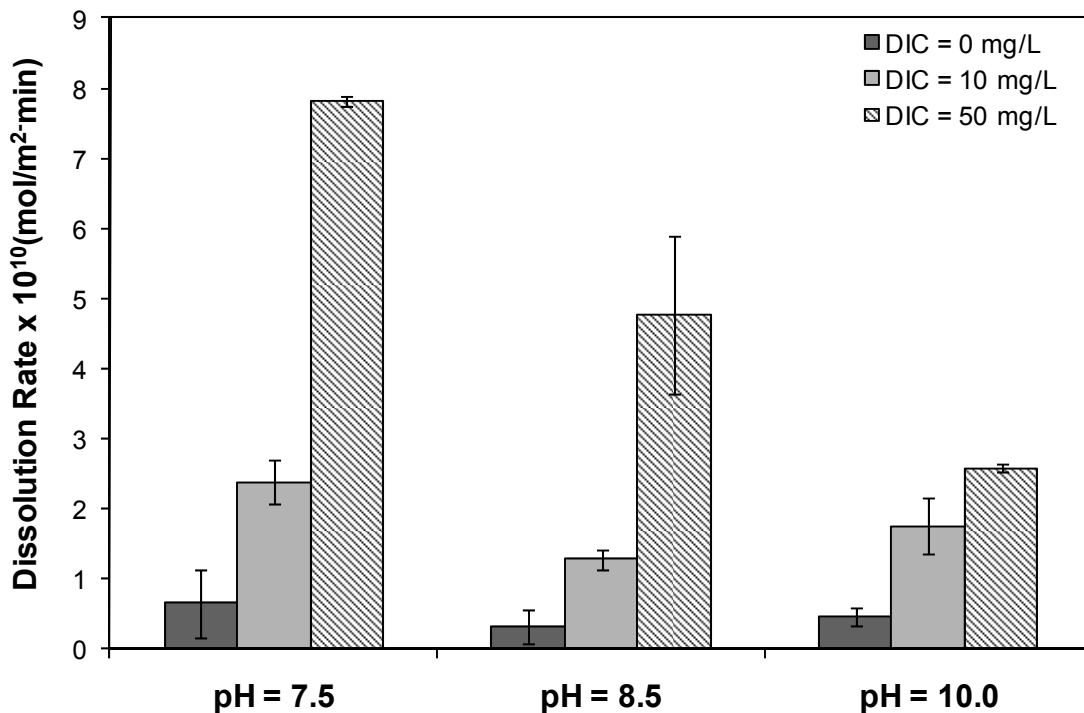
Figure 2.2. Dissolution rate of plattnerite as a function of pH and DIC (concentrations given in mg-C/L) determined using reactors with 1 g/L plattnerite suspension and a residence time of 0.5 hour.

Although DIC accelerates dissolution, the steady-state lead concentration only exceeded the 15 μg/L (72 nM) standard for the highest dissolution rate. However, the dissolved lead concentration is a function of the dissolution rate, the reaction time, and reactive surface area of PbO_2. For reaction times longer than the 30 minute residence time in the flow-through experiments, dissolved lead concentrations will be higher. Previous studies demonstrated that dissolved lead concentrations do increase with contact time, solid loading, and DIC concentration. In the study of Lin and Valentine *(10, 11, 22)*, the dissolved lead concentration reached 25 μg/L after 28 days with 4 mg/L PbO_2 at pH 7.0 and 12 mg-C/L DIC, 50 μg/L after 21 days with 10 mg/L PbO_2 at pH 7.0 and 12 mg-C/L DIC, and 52 μg/L after 7 days with 10 mg/L PbO_2 at pH 7.0 and 60 mg-C/L DIC. Dryer and co-workers *(12)* observed dissolved lead concentrations as high as 500 μg/L after 53 days with 31 mg/L PbO_2 at pH 7.0 and 1.2 mg-C/L DIC.

Dissolution rates of PbO_2 determined from the flow-through experiments were comparable to those calculated from the results of previous batch experiments. In the work of Lin and Valentine *(10)*, the dissolved lead concentration was around 6 μg/L in the batch reactor after 1 day at the condition of pH 7.0, 12 mg-C/L DIC and 12 mg/L plattnerite with 4.14 g/m^2 specific surface area, and it increased linearly versus time. Thus, the calculated dissolution rate at this condition is $4.0 \cdot 10^{-10}$ mol/min-m^2. The average dissolution rate in the present study at similar conditions of pH 7.5 and 10 mg-C/L DIC was $2.4 \cdot 10^{-10}$ mol/min-m^2. The slightly higher rate in the study of Lin and Valentine could be caused by a lower pH or a higher DIC than in the present study. From Dryer and Korshin's batch experiment with 100 nm-sized scrutinyite, a dissolution rate of $4.8 \cdot 10^{-9}$ mol/min-m^2 can be calculated based on the dissolved lead concentration after 1

day of reaction at pH 7.0 and 1.2 mg-C/L DIC *(12)*. This rate is one order of magnitude higher than the dissolution rate in the present work and the study of Lin and Valentine. The higher rate could be caused by two reasons. First, filtration with 0.45 µm membranes may allow more particulate lead to pass into the "dissolved" samples than filtration with 0.20-0.22 µm in our experiments and those of Lin and Valentine *(10)*. Second, the two polymorphs of PbO_2, plattnerite and scrutinyite, could have intrinsically different dissolution rates due to differences in their crystalline structures.

For comparable conditions, the dissolution rates of plattnerite are about two orders of magnitude less than those of hydrocerussite ($Pb_3(CO_3)_2(OH)_2$) *(23)*   . Plattnerite is much more effective at maintaining steady-state dissolved lead concentrations below the action level.

2.2.3   Dissolution During Initial Period of Reactor Operation

During the earliest period of reactor operation, the effluent lead concentration is more variable and the concentrations are often significantly higher than at later times (Figure 2.1). The high lead concentrations could be caused in part by a lower pH during the initial reactor operation (Figure 2.1). The pH values below the target values were most pronounced for experiments without DIC to provide buffering capacity, and both the period of low pH and high lead concentrations persisted the longest for these DIC-free conditions. However initial periods of high lead concentrations were also observed for experiments that quickly reached the target pH and remained stable at that value. The high initial concentrations may also result from the initial dissolution of a labile surface phase. Dissolution of labile surface phases, which are related to rates of active site

production and dissolution, on metal oxides was previously observed and explained by Samson et al *(18)*. In the present study, a dry solid was added to the water at time of zero and the initial pH was adjusted in the first several hours from a lower pH to the target pH. Such perturbations of the initial surface could cause dissolution of labile surface phases and an initially higher dissolution rate. Additional evidence for dissolution of labile surface phases and not simply pH variation as the cause of the high lead concentrations was that the high lead concentrations were spread over 5 hours, while the pH fluctuation generally lasted less than one hour for experiments that included DIC.

Possible loss of small lead-containing particles (particle size < 0.22 μm) might also contribute to the initial high lead concentrations; however, electron micrographs of plattnerite before and after reactions showed that the distribution of primary particle sizes was similar and that the particles existed in aggregates larger than 0.22 μm (Figure 2-S1). XRD confirmed that the remaining solids after reaction were still plattnerite (Figure 2-S2).

2.2.4.   Equilibrium Versus Kinetic Control of Dissolved Lead Concentrations

The steady-state concentrations were well below the equilibrium solubility of any possible solids at all three pH values investigated (Figure 2.3). Solids considered were plattnerite as well as the Pb(II) carbonate solids cerussite and hydrocerussite that will ultimately govern the dissolved lead concentration as the Pb(IV) in plattnerite is reduced and released to solution. The undersaturation of the solution with respect to all possible solids is consistent with X-ray diffraction results that observed only plattnerite in solid samples collected at the conclusion of dissolution experiments. An estimate of the time

needed for the concentration to reach 99% of the equilibrium in a batch experiment with

1 g/L PbO$_2$ at pH 7.5 and 10 mg-C/L DIC is 5.5 days; this estimate is conservative

because it assumes a constant dissolution rate of 2.4×10^{-10} mol/min-m^2, and the actual

rate would decrease as equilibrium is approached.
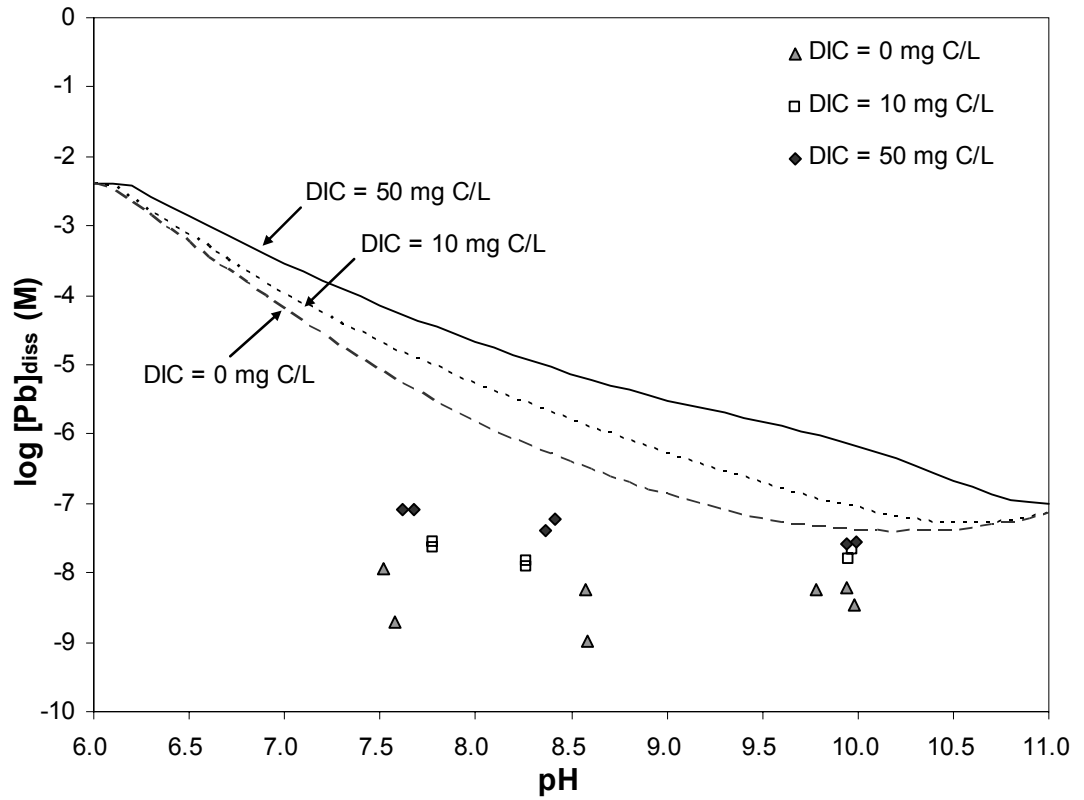
Figure 2.3. Steady-state (points) and predicted equilibrium (lines) lead concentrations for plattnerite dissolution as a function of pH and DIC. The solution was assumed to have 1.26 μM dissolved oxygen, which would be in equilibrium with 0.1% gaseous oxygen.

The dissolved lead concentrations in equilibrium with plattnerite were calculated

by assuming equilibrium with water acting as a reductant. The relevant oxidation-

reduction dissolution half reactions are:

$$PbO_{2(s)} + 4H^+ + 2e^- = Pb^{2+} + 2H_2O \quad \log K_1 = 49.60 \quad E_H^0 = 1.46 \ V \quad (2.8)$$

$$2H_2O = O_{2(aq)} + 4H^+ + 4e^- \quad \log K_2 = -86.00 \quad E_H^0 = -1.27 \ V \quad (2.9)$$

Therefore, the overall reaction and equilibrium constant are

$$2H^+ + PbO_{2(s)} = Pb^{2+} + \tfrac{1}{2} O_{2(aq)} + H_2O \quad \log K = 6.60 \tag{2.10}$$
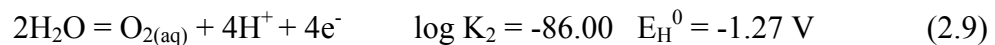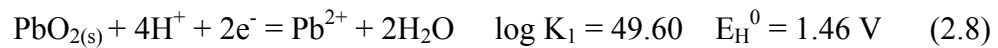
$$K = \frac{\{Pb^{2+}\}\{O_2\}^{1/2}}{\{H^+\}^2} = 10^{6.60} \tag{2.11}$$

The equilibrium Pb^{2+} activity was calculated using Equation 2.11 assuming 0.1% partial pressure of gaseous oxygen (1.26 µmol/L dissolved oxygen), and the Pb^{2+} concentration was calculated from its activity. The activity coefficients were calculated from ionic strength using the Davies equation. The equilibrium dissolved Pb(II) concentration was calculated as the sum of all dissolved Pb(II) species. Concentrations of Pb(II) complexes were calculated using the reactions and equilibrium constants in Tables 2-S2 and 2-S4 of the Supporting Information. The solution was purged by nitrogen immediately before it was pumped into the Tedlar bags, which should have decreased the dissolved oxygen concentration to below 1.26 µmol/L. Therefore, the equilibrium dissolved Pb(II) concentration should be equal to or higher than the values calculated for 0.1% P_{O_2} that are shown in Figure 2.3. The reduction of PbO_2 will produce O_2 in the reactor, but based on steady-state lead concentrations, the highest O_2 concentration generated would only be 0.042 µmol/L.

Dissolution in the flow-through reactors occurred at conditions that are far from equilibrium. For such conditions, the Gibbs free energy of reaction (ΔG) is very negative. Consequently, $f(\Delta G)$ in Equation 2.3 is close to 1 and Equation 2.3 can be simplified to Equation 2.12.

$$Rate = k \cdot 1 = k \tag{2.12}$$

In this manner, the dissolution rates and the rate constants are the same.

Although the increase in DIC leads to an increase in the predicted equilibrium dissolved lead concentration, this change in the equilibrium concentration is not the cause of the faster dissolution with DIC. The reaction was sufficiently far from equilibrium so that $f(\Delta G)$ was approximately 1 both with and without DIC. Consequently, the presence of DIC leads to a greater value for the rate constant (k) and indicates that the effect of DIC is to accelerate the rate of the reaction occurring on the surface of the solid.

2.2.5. Mechanism of Plattnerite Dissolution

Dissolution of plattnerite at conditions without free chlorine to maintain the stability of Pb(IV) occurs through steps of reduction and dissolution, but the sequence of these two steps is unknown. Previous research demonstrated that dissolved lead from plattnerite dissolution is exclusively Pb(II) by comparing dissolved lead concentrations measured by graphite furnace atomic absorption spectroscopy with those determined by anodic stripping voltammetry *(10)*. A conceptual model showing two hypothesized reductive dissolution mechanisms is presented in Figure 2.4. Mechanism A involves the reduction of Pb(IV) to Pb(II) at the surface of the solid followed by the release of the Pb(II) to solution. Mechanism B starts with the release of Pb(IV) to solution followed by the reduction to dissolved Pb(II). The acceleration of the dissolution rate by the presence of carbonate provides support for the pathway involving reduction at the plattnerite surface. The formation of soluble Pb(II)-carbonate complexes can accelerate dissolution by extracting Pb(II) that had formed on the solid surface; there are not soluble Pb(IV)-carbonate complexes, and were reduction to occur in solution, then the addition of DIC would not have changed the dissolved lead concentration.

35

The dissolution of plattnerite is kinetically limited at all, or nearly all, of the combinations of pH and DIC studied. The rate-limiting step appears to be the detachment of Pb(II) from the plattnerite surface. Ligand-enhanced dissolution or desorption are possible models for PbO_2 reductive dissolution in the presence of CO_3^{2-} *(24)*. Pb(II) can adsorb to PbO_2 above pH 7 *(13)*, and complexation with carbonate can lead to its desorption. Carbonate also acted as a dissolution-enhancing ligand in hematite dissolution *(25)*. Similar effects of carbonate on UO_2 dissolution were reported in a study that found UO_2 dissolution to occur in two steps *(26)*. First, U(IV) is oxidized to U(VI) on the surface of UO_2, and then U(VI)-CO_3 complexes form and dissolve into solution.

Recent studies showed that Fe(II), Mn(II), NOM, hydroquinone, and decomposition intermediates of monochloramine can act as reductants for PbO_2 reductive dissolution *(10-14, 22, 27)*. The reductive dissolution rates of PbO_2 in the presence of these reductants decrease in the following order: hydroquinone > Mn(II) > Fe(II) > NOM NOM > monochloramine-intermediates.
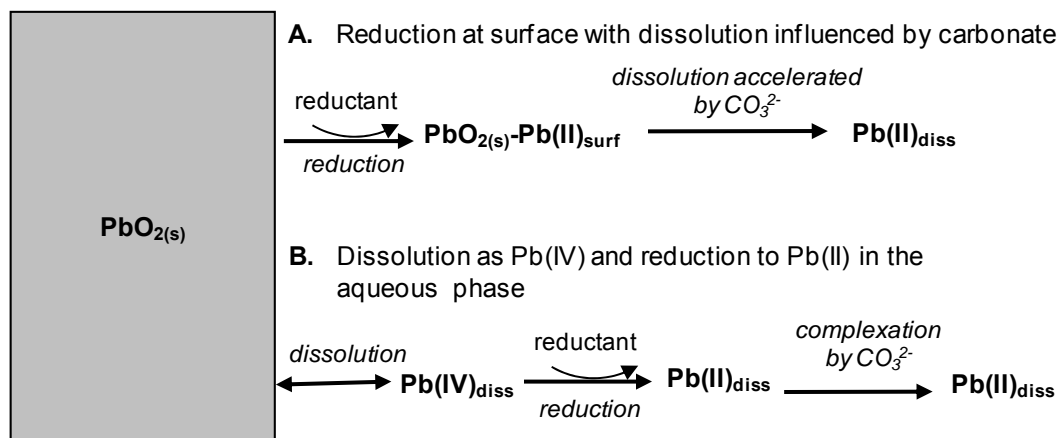
Figure 2.4. Conceptual model of PbO_2 dissolution showing two possible mechanisms and the potential role of carbonate.

In the work of Shi and Stone, dissolution rates were higher with higher reductant concentration, so the reduction step was rate-limiting at their conditions *(13)*. In one of their experiments, aqueous Fe(II) was reacted with PbO_2 before the addition of hydroquinone. The Fe^{III} (hydr)oxide produced by Fe(II) addition apparently blocked the PbO_2 surface from subsequent reaction with hydroquinone, which provides support for Mechanism A with Fe(III) production on the PbO_2 surface. Mechanism B is precluded by their observation because Fe^{III} (hydr)oxide formed from bulk aqueous reaction would not block the PbO_2 surface sites. Additional measurements, such as XPS and dissolved Pb(IV) measurement, could more definitively establish the actual mechanism.

According to the proposed mechanism, the sequence of dissolution reactions is:

$$PbO_2 + 2H^+ = Pb(II)_{surf}^{2+} + \tfrac{1}{2}O_2 + H_2O \tag{2.13}$$

$$Pb(II)_{surf}^{2+} + CO_3^{2-} = Pb(II) - CO_{3surf} \tag{2.14}$$

$$Pb(II) - CO_{3surf} = PbCO_{3(aq)} \tag{2.15}$$
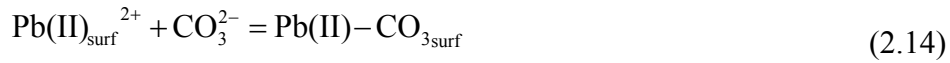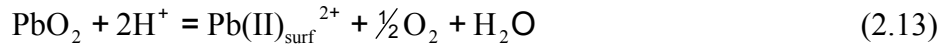
Steps 2.14 and 2.15 illustrate the role of DIC in the formation of $PbCO_{3(aq)}$, which is the dominant but not the only soluble lead carbonate complex. Based on the hypothesized dissolution mechanism, the dissolution rate constant (k) can be described as a function of pH and carbonate (Equations 2.16-2.17),

$$k = c \times [H^+]^a \times [CO_3^{2-}]^b \tag{2.16}$$

$$\log k = a \times \log[H^+] + b \times \log[CO_3^{2-}] + \log c \tag{2.17}$$

Least squares optimization of the experimental data to Equation 2.17 yielded values of 0.820, 0.655, and 2.91×10^{-10} mol/min-m^2 for coefficients a-c, respectively. The optimization of the parameters for the rate model used only data in the presence of DIC. The model fits the experimental dissolution rates well (Figure 2.5) with an R-

squared value of 0.84. The point (3.9, 5.6) off the 1:1 line was for one of the duplicates

at the condition of pH 8.5 and 50 mg-C/L DIC. Because the effluent lead concentration

for this experiment still had a slightly increasing trend after 24 hours of reaction, the

actual rate could be higher than 3.9×10^{-10} mol/min-m^2 and may fit the model better.
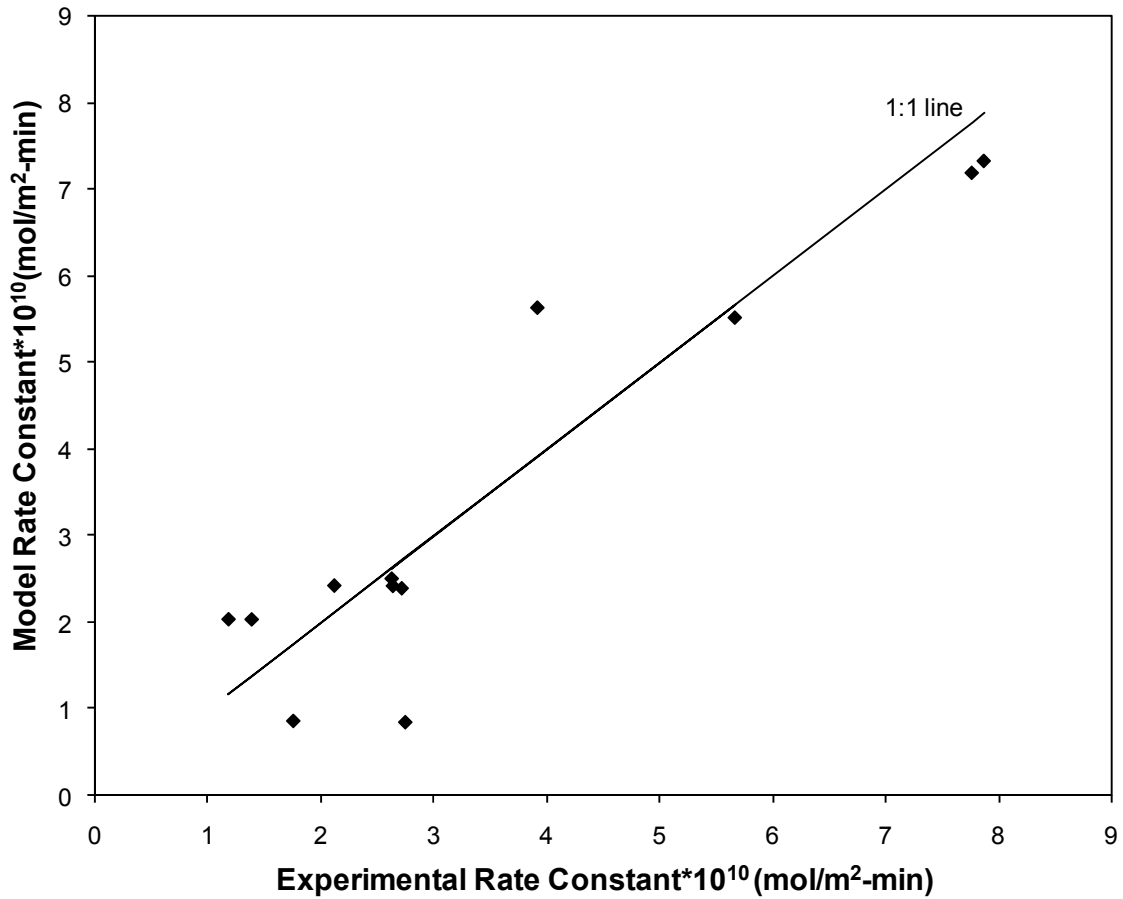
Figure 2.5. Empirical model for the plattnerite dissolution rate constant. The 1:1 line is shown for reference.

2.3   Environmental Implications

The slow dissolution of PbO$_2$ makes dissolution rates as important, if not more

important, than equilibrium solubility for predicting dissolved lead concentrations in tap

water when plattnerite is present as a corrosion product. It can take days for PbO$_2$

dissolution reactions to reach equilibrium. For plattnerite, most steady-state effluent concentrations for a 30 minute residence time were below the lead action level. Water in contact with PbO_2 for long stagnation times could have higher lead concentrations, but during flow of water through a pipe with PbO_2, low concentrations of lead would be reached due to the slow dissolution rate of PbO_2.

Promoting the formation of PbO_2 can be an effective method for achieving low lead concentrations, but this requires a free chlorine residual to provide the high oxidation-reduction potential needed. Many utilities have switched from free chlorine to monochloramine as the residual disinfectant to limit production of DBPs and meet the associated drinking water regulations. In balancing control of lead concentrations and DBPs, some treatment systems may find an optimal solution by maintaining free chlorine and taking other steps to limit DBP formation.

Increasing carbonate alkalinity has been a strategy to limit lead corrosion, but for plattnerite such increases in alkalinity may actually increase dissolved lead concentrations. Higher alkalinity can be beneficial when hydrocerrusite or cerussite is dominant; however, if PbO_2 is dominant, then increasing DIC can promote its dissolution and increase lead concentrations in drinking water. Thus, information about the identity of corrosion products present on lead-containing pipes and fittings is critical to identifying optimal lead corrosion control treatment.

Acknowledgements

Literature Cited:

(1)   U.S.EPA, Maximum Contaminant Level Goals and National Primary Drinking Water Regulations for Lead and Copper. Final Rule. *Federal Register* **1991,** *56*, 26460.
(2)   Schock, M.R.; Hyland, R.N.; Welch, M.M., Occurrence of contaminant accumulation in lead pipe scales from domestic drinking-water distribution systems. *Environ. Sci. Technol.* **2008,** *42*, (12), 4285-4291.
(3)   Renner, R., DC's water linked to elevated lead levels. *Environ. Sci. Technol.* **2007,** *41*, 10-11.
(4)   Renner, R., Plumbing the depths of DC's drinking water crisis. *Environ. Sci. Technol.* **2004,** *38*, (12), 224A-227A.
(5)   Switzer, J.A.; Rajasekharan, V.V.; Boonsalee, S.; Kulp, E.A.; Bohannan, E.W., Evidence that monochloramine disinfectant could lead to elevated Pb levels in drinking water. *Environ. Sci. Technol.* **2006,** *40*, (10), 3384-3387.
(6)   Edwards, M.; Dudi, A., Role of chlorine and chloramine in corrosion of lead-bearing plumbing materials. *J. Am. Water Works Assoc.* **2004,** *96*, (10), 69-81.
(7)   Boyd, G.R.; Dewis, K.M.; Korshin, G.V.; Reiber, S.H.; Schock, M.R.; Sandvig, A.M.; Giani, R., Effects of changing disinfectants on lead and copper release. *J. Am. Water Works Assoc.* **2008,** *100*, (11), 75-87.
(8)   Vasquez, F.A.; Heaviside, R.; Tang, Z.J.; Taylor, J.S., Effect of free chlorine and chloramines on lead release in a distribution system. *J. Am. Water Works Assoc.* **2006,** *98*, (2), 144-154.
(9)   Lytle, D.A.; Schock, M.R., Formation of Pb(IV) oxides in chlorinated water. *J. Am. Water Works Assoc.* **2005,** *97*, (11), 102-114.
(10)   Lin, Y.P.; Valentine, R.L., The release of lead from the reduction of lead oxide (PbO_2) by natural organic matter. *Environ. Sci. Technol.* **2008,** *42*, (3), 760-765.
(11)   Lin, Y.P.; Valentine, R.L., Release of Pb(II) from monochloramine-mediated reduction of lead oxide (PbO_2). *Environ. Sci. Technol.* **2008,** *42*, (24), 9137-9143.
(12)   Dryer, D.J.; Korshin, G.V., Investigation of the reduction of lead dioxide by natural organic matter. *Environ. Sci. Technol.* **2007,** *41*, (15), 5510-5514.

(13)   Shi, Z.; Stone, A.T., PbO$_2$(s, Plattnerite) reductive dissolution by aqueous manganous and ferrous ions. *Environ. Sci. Technol.* **2009,** *43*, (10), 3596-3603.

(14)   Shi, Z.; Stone, A.T., PbO$_2$(s, Plattnerite) reductive dissolution by natural organic matter: reductant and inhibitory subfractions. *Environ. Sci. Technol.* **2009,** *43*, (10), 3604-3611.

(15)   Schock, M.R., Understanding Corrosion Control Strategies for Lead. *J. Am. Water Works Assoc.* **1989,** *81*, (7), 88-100.

(16)   Schecher, W. D.; McAvoy, D. C. *MINEQL+: A chemical equilibrium modeling system, version 4.5*, Environmental Research Software: Hallowell, ME, 1998.

(17)   Kraemer, S.M.; Hering, J.G., Influence of solution saturation state on the kinetics of ligand-controlled dissolution of oxide phases. *Geochim. Cosmochim. Acta* **1997,** *61*, (14), 2855-2866.

(18)   Samson, S.D.; Eggleston, C.M., The depletion and regeneration of dissolution-active sites at the mineral-water interface: II. Regeneration of active sites on alpha-Fe$_2$O$_3$ at pH 3 and pH 6. *Geochim. Cosmochim. Acta* **2000,** *64*, (21), 3675-3683.

(19)   Oelkers, E.H., An experimental study of forsterite dissolution rates as a function of temperature and aqueous Mg and Si concentrations. *Chemical Geology* **2001,** *175*, 485-494.

(20)   Lasaga, A. C., *Kinetic theory in the earth sciences*. Princeton University Press: Princeton, New Jersey, 1998; p 811.

(21)   Morel, F.M.M.; Hering, J.G., *Principles and applications of aquatic chemistry*. Wiley Inter-science: New York, NY, 1993.

(22)   Lin, Y.P.; Valentine, R.L., Reduction of lead oxide (PbO$_2$) and release of Pb(II) in mixtures of natural organic matter, free chlorine and monochloramine. *Environ. Sci. Technol.* **2009,** *43*, (10), 3872-3877.

(23)   Noel, J.D.; Giammar, D.E. The influence of water chemistry on dissolution rate of lead corrosion products. *Proceedings of AWWA Water Quality Technology Conference, Charlotte*, NC, 2007.

(24)   Stumm, W., Reactivity at the mineral-water interface: Dissolution and inhibition. *Colloid Surf. A-Physicochem. Eng. Asp.* **1997,** *120*, (1-3), 143-166.

(25)   Bruno, J.; Stumm, W.; Wersin, P.; Brandberg, F., On the Influence of Carbonate in Mineral Dissolution .1. The Thermodynamics and Kinetics of Hematite Dissolution in Bicarbonate Solutions at T = 25-Degrees-C. *Geochim. Cosmochim. Acta* **1992,** *56*, (3), 1139-1147.

(26)   Ulrich, K.U.; Singh, A.; Schofield, E.J.; Bargar, J.R.; Veeramani, H.; Sharp, J.O.; Bernier-Latmani, R.; Giammar, D.E., Dissolution of biogenic and synthetic UO$_2$ under varied reducing conditions. *Environ. Sci. Technol.* **2008,** *42*, (15), 5600-5606.

(27)   Lin, Y.P.; Washburn, M.P.; Valentine, R.L., Reduction of lead oxide (PbO$_2$) by iodide and formation of iodoform in the PbO$_2$/I$^-$/NOM system. *Environ. Sci. Technol.* **2008,** *42*, (8), 2919-2924.

Chapter 2. Supporting Information

Contents: Five tables (S1-S4)

Six figures (S1-S5)

Dissolution Rate Model

The dissolution rate can be quantified by performing a lead mass balance on the CFSTR (Equation 1),

$$\frac{dm}{dt} = V \cdot \frac{dC}{dt} = QC_{in} - QC_{out} + R \cdot A \cdot [\,solids\,] \cdot V \qquad (1)$$

where R = net dissolution rate normalized by surface area (mol/m^2-min)

V = reactor volume (L)

Q = flow rate (L/min)

C_{out}, C_{in} = effluent and influent concentrations (M)

A = specific surface area (m^2/g solid)

[solid] = solid concentration (g/L)

From Equation 1, experimental dissolution rates can be derived as a function of residence time, reactor volume, and lead concentrations in the effluent and influent (C_{in} = 0) in the following equation when the reactor behavior reaches steady-state (i.e. dC/dt = 0)

$$R_{exp} = \frac{(C_{out} - C_{in})}{A \cdot [solids] \cdot t_{res}} = \frac{C_{ss}}{A \cdot [solids] \cdot t_{res}} \qquad (2)$$

where t_{res} = residence time of flow-through experiments (h) (t_{res} = V/Q)

Based on the dissolution rate model developed by Lasaga, the dissolution rate in flow-through reactors can be predicted by Equation 3 based on a reaction rate law *(1)*.

$$R_{model} = k \cdot f(\Delta \overline{G}) \qquad (3)$$

Where R_{model} = model net dissolution rate normalized by surface area (mol/m^2-min)

k = intrinsic rate constant (mol/m^2·h)

$\Delta\overline{G}$ = molar Gibbs free energy of reaction (J/mol)

For reversible elementary reactions,

$$f(\Delta\overline{G}) = 1 - e^{\frac{\Delta\overline{G}}{RT}} \qquad (4)$$

where R = gas constant (8.314 J/K·mol)

T = temperature (K)

since

$$\Delta\overline{G} = RT\ln(\frac{IAP}{K_{eq}}) \qquad (5)$$

where IAP = ion activity product

K_{eq} = equilibrium constant

In the case of lead(IV) oxide, based on the reductive dissolution reaction,

$$PbO_{2(s)} + 2H^+ = Pb^{2+} + 0.5O_2 + H_2O \qquad (6)$$
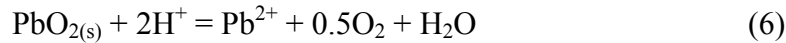
the ion activity product is expressed as Equation 6 assuming concentrations are equal to activities.

$$IAP = [Pb^{2+}][O_2]^{1/2}[H^+]^{-2} \qquad (7)$$

Thus, Equation 4 can be written as

$$f(\Delta\overline{G}) = 1 - \frac{IAP}{K_{eq}} = 1 - \frac{[Pb^{2+}]_{out}[O_2]^{1/2}[H^+]^{-2}}{[Pb^{2+}]_{eq}[O_2]^{1/2}[H^+]^{-2}} = 1 - \frac{C_{out}}{C_{eq}} \qquad (8)$$

By setting the influent concentration to be zero, Equations 2 and 3 can be combined to derive the dissolution rate constant k.

$$R_{\exp} = R_{\text{model}} = \frac{C_{out}}{A \cdot [solids] \cdot t_{res}} = k \cdot f(\Delta \overline{G}) = k \cdot (1 - \frac{C_{out}}{C_{eq}}) \tag{9}$$

At steady-state,

$$C_{ss} = C_{out} = k \cdot A \cdot [solids] \cdot t_{res} \cdot (1 - \frac{C_{ss}}{C_{eq}}) \tag{10}$$

Solve Equation 10,

$$C_{ss} = \frac{k \cdot A \cdot [solids] \cdot V \cdot C_{eq}}{C_{eq} \cdot Q + k \cdot A \cdot [solids] \cdot V} \tag{11}$$

The effluent lead concentration versus time can then be calculated by solving Equation 1 with Equation 9 used for the dissolution rate:

$$C_{out} = C_{ss} + (C_0 - C_{ss}) \cdot e^{-\frac{k \cdot A \cdot [solids]}{C_{ss}} t} \tag{12}$$

where C_{ss} = steady-state effluent concentration from the flow-through reactor (mol/L)

C_0 = initial effluent concentration at t = 0, which is 0 for the present experiments.

Equation 12 also helps illustrate the initial curvature of the effluent concentrations during the early phase of the experiment (Figure S4).

Effect of Organic pH Buffers on Plattnerite Dissolution

Initial plans were to use organic buffers for pH stabilization. Before using organic buffers, their effects on PbO_2 dissolution were investigated. Solutions of the buffers N-cyclohexyl-3-aminopropanesulfonic acid (CAPS), 4-(2-hydroxyethyl)-1-piperazineethanesulfonic acid (HEPES), and 2-(N-morpholino)ethanesulfonic acid (MES) (Acros Organics) at 1 mM concentration were contacted with 0.24 g/L plattnerite in stirred polypropylene bottles with no headspace. These buffers, which are all sulfonic acids with amine groups, were chosen because they do not form strong complexes with metals. Their structures and the final pH values in experiments with them are shown in Table S1 of the Supporting Information. The pH and dissolved lead concentrations were measured over 48 hours; samples for dissolved lead were filtered (0.45 μm PTFE membranes) and acidified (2% HNO_3) prior to analysis. Because two of the buffers (HEPES and MES) accelerated plattnerite dissolution (results shown in next section), no organic buffers were used in the experiments.

Organic pH buffers were not used in the plattnerite experiments because of their ability to accelerate plattnerite dissolution. The organic buffers (HEPES and MES) increased the dissolution of plattnerite dramatically compared to a buffer-free control experiment (Figure S5). The dissolved lead concentration in contact with CAPS buffer was not significantly different from that in the control experiment. The accelerated dissolution was probably due to the reduction of PbO_2 by the organic buffers to produce more soluble Pb(II) species *(2)*, which is similar to the effect of NOM on PbO_2 dissolution *(3, 4)*.

Table 2-S1. Molecular structure and pK_a values of pH buffers and final pH in batch experiments reacting the buffers with plattnerite.
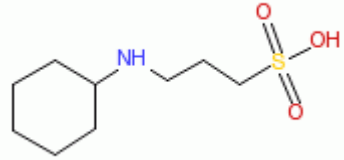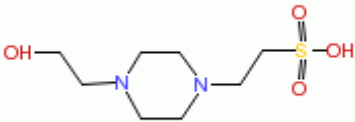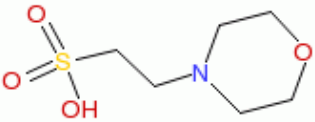
Name	pH	pK_a	Structure
Control	4.80		
CAPS	4.93	10.4	
HEPES	6.20	7.5	
MES	5.12	6.1	

Table 2-S2. Equilibrium constants for aqueous species

#	Reaction	Log K	Source
1	$H_2O \rightarrow H^+ + OH^-$	-13.998	MINEQL+
2	$CO_{2(g)} + H_2O \rightarrow H_2CO_3^*$	-1.459	MINEQL+
3	$H_2CO_3^* \rightarrow 2H^+ + CO_3^{2-}$	-16.68	MINEQL+
4	$HCO_3^- \rightarrow H^+ + CO_3^{2-}$	-10.33	MINEQL+
5	$Pb^{2+} + H_2O \rightarrow PbOH^+ + H^+$	-7.597	MINEQL+
6	$Pb^{2+} + 2H_2O \rightarrow Pb(OH)_2^0 + 2H^+$	-17.12	Benjamin
7	$Pb^{2+} + 3H_2O \rightarrow Pb(OH)_3^- + 3H^+$	-28.06	Benjamin
8	$Pb^{2+} + 4H_2O \rightarrow Pb(OH)_4^{2-} + 4H^+$	-39.70	Benjamin
9	$Pb^{2+} + CO_3^{2-} \rightarrow PbCO_3^0$	6.478	MINEQL+
10	$Pb^{2+} + 2CO_3^{2-} \rightarrow Pb(CO_3)_2^{2-}$	9.38	MINEQL+
11	$Pb^{2+} + CO_3^- + H^+ \rightarrow PbHCO_3^+$	13.20	MINEQL+
12	$2Pb^{2+} + 3H_2O \rightarrow Pb_2(OH)^{3+} + H^+$	-6.397	MINEQL+
13	$3Pb^{2+} + 4H_2O \rightarrow Pb_3(OH)_4^{2+} + 4H^+$	-23.888	MINEQL+
14	$4Pb^{2+} + 4H_2O \rightarrow Pb_4(OH)_4^{4+} + 4H^+$	-19.988	MINEQL+
15	$HOCl + 2e^- + H^+ \rightarrow Cl^- + H_2O$	50.20	Benjamin
16	$Pb^{4+} + 2e^- \rightarrow Pb^{2+}$	28.64	Benjamin
17	$O_{2(aq)} + 4H^+ + 4e^- \rightarrow 2H_2O$	86.00	Benjamin
18	$2H^+ + 2e^- \rightarrow H_{2(aq)}$	3.10	Benjamin
19	$Pb^{4+} + 3H_2O \rightarrow PbO_3^{2-} + 6H^+$	-23.04	Calculated
20	$Pb^{4+} + 4H_2O \rightarrow PbO_4^{4-} + 8H^+$	-63.80	Calculated

Benjamin = *(5)* MINEQL+ = *(6)*

The equilibrium constant for Reactions 19 and 20 were calculated by first

determining the Gibbs free energy of the reaction by the summation of the molar Gibbs

free energies of formation ($G_{f,i}^0$) for each component (i). The Gibbs free energies of

formation are listed in Table S3.

Table 2-S3. Chemical potentials for various aqueous species.

Species	$G_{f,i}^0$ (J/mol)	Source
$Pb_3O_{4(s)}$	-601,200	Benjamin
$Pb_2O_{3(s)}$	-411,769	Pourbaix
$PbO_{2(s)}$	-218,987	Pourbaix
Pb^{2+}	-24,309	Pourbaix
$HPbO_2^-$	-338,898	Pourbaix
Pb^{4+}	302,498	Pourbaix
PbO_3^{2-}	-277,562	Pourbaix
PbO_4^{4-}	-282,084	Pourbaix
H^+	0.00	Benjamin
OH^-	-157,300	Benjamin
H_2O	-237,180	Benjamin

Benjamin = *(5)* Pourbaix = *(7)*

For example the Gibbs free energy for Reaction 19 can be calculated as,

$$\Delta G_r = \sum_{i=1}^{k} G_{f,i}^0 N_i \tag{1}$$

where ΔG_r = Gibbs free energy of reaction (J/mol)

$G_{f,i}^0$ = Gibbs free energy of formation of species (i), joules per mole

(J/mol)

N_i = stoichiometric coefficient

$$\Delta G_{r,19} = G_{f,PbO_3^{2-}}^0 + 6 * G_{f,H^+}^0 - G_{f,Pb^{4+}}^0 - 3 * G_{f,H_2O}^0 = 131,481 \text{ J}$$

$$\tag{2}$$

The equilibrium constant can then be calculated by Equation 3:

$$LogK_{eq} = -\frac{\Delta G_r}{2.303RT} \qquad (3)$$

Where R is the equilibrium gas constant (J/mol•K), and T is temperature (K).

$$Log(K_{eq}) = -\frac{131,481}{2.303RT} - = -23.04 \qquad (4)$$

Table 2-S4. Solubility products of selected lead solids

#	Solid	Reaction	Log K	Source
21	Massicot	$PbO_{(s)} + 2H^+ \rightarrow Pb^{2+} + H_2O$	12.91	MINEQL+
22	Litharge	$PbO_{(s)} + 2H^+ \rightarrow Pb^{2+} + H_2O$	12.72	MINEQL+
23	$Pb(OH)_{2(s)}$	$Pb(OH)_{2(s)} + 2H^+ \rightarrow Pb^{2+} + 2H_2O$	12.40	Stumm & Morgan
24	Cerussite	$PbCO_{3(s)} \rightarrow Pb^{2+} + CO_3^{2-}$	-13.13	Benjamin
25	Hydrocerussite	$Pb_3(CO_3)_2(OH)_{2(s)} + 2H^+ \rightarrow 3Pb^{2+} + 2CO_3^{2-} + 2H_2O$	-18.77	MINEQL+
26	$Pb_3(PO_4)_{2(s)}$	$Pb_3(PO_4)_{2(s)} \rightarrow 3Pb^{2+} + 2PO_4^{3-}$	-44.50	Benjamin
27	$PbHPO_{4(s)}$	$PbHPO_{4(s)} \rightarrow Pb^{2+} + PO_4^{3-} + H^+$	-37.80	MINEQL+
28	Hydroxyl-pyromorphite	$Pb_5(PO_4)_3OH_{(s)} + H^+ \rightarrow 5Pb^{2+} + 3PO_4^{3-} + H_2O$	-62.79	MINEQL+
29	Plattnerite	$PbO_{2\ (s)} + 4H^+ + 2e^- \rightarrow Pb^{2+} + 2H_2O$	49.60	MINEQL+
30	Plattnerite	$Pb(IV)O_{2(s)} + 4H^+ \rightarrow Pb^{4+} + 2H_2O$	-8.91	Calculated

Benjamin = *(5)* MINEQL+ = *(6)* Stumm & Morgan = *(8)*
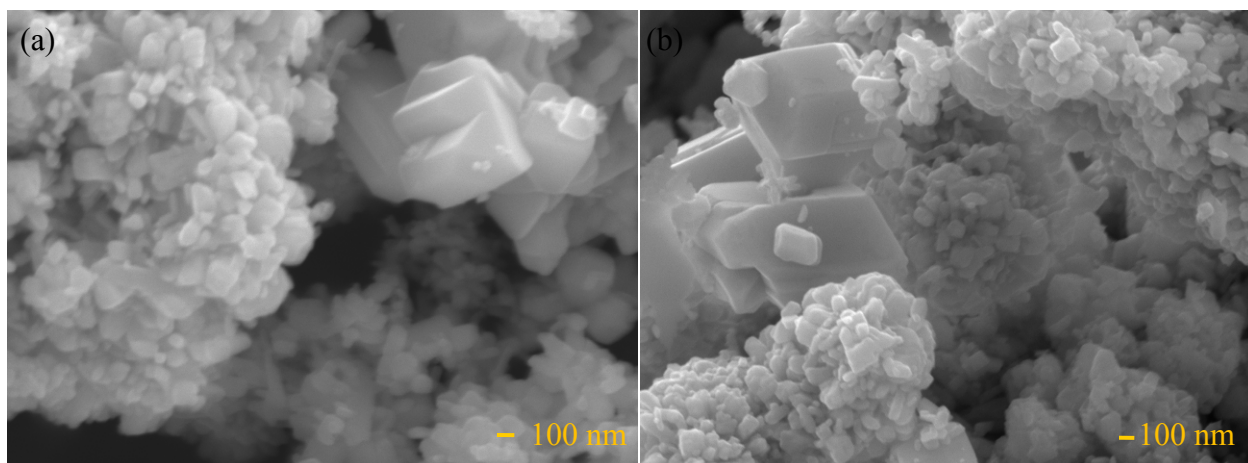
Figure 2-S1. Scanning electron micrograph of plattnerite before reaction (a) and after one day of reaction at pH 7.5 DIC 0 (b).
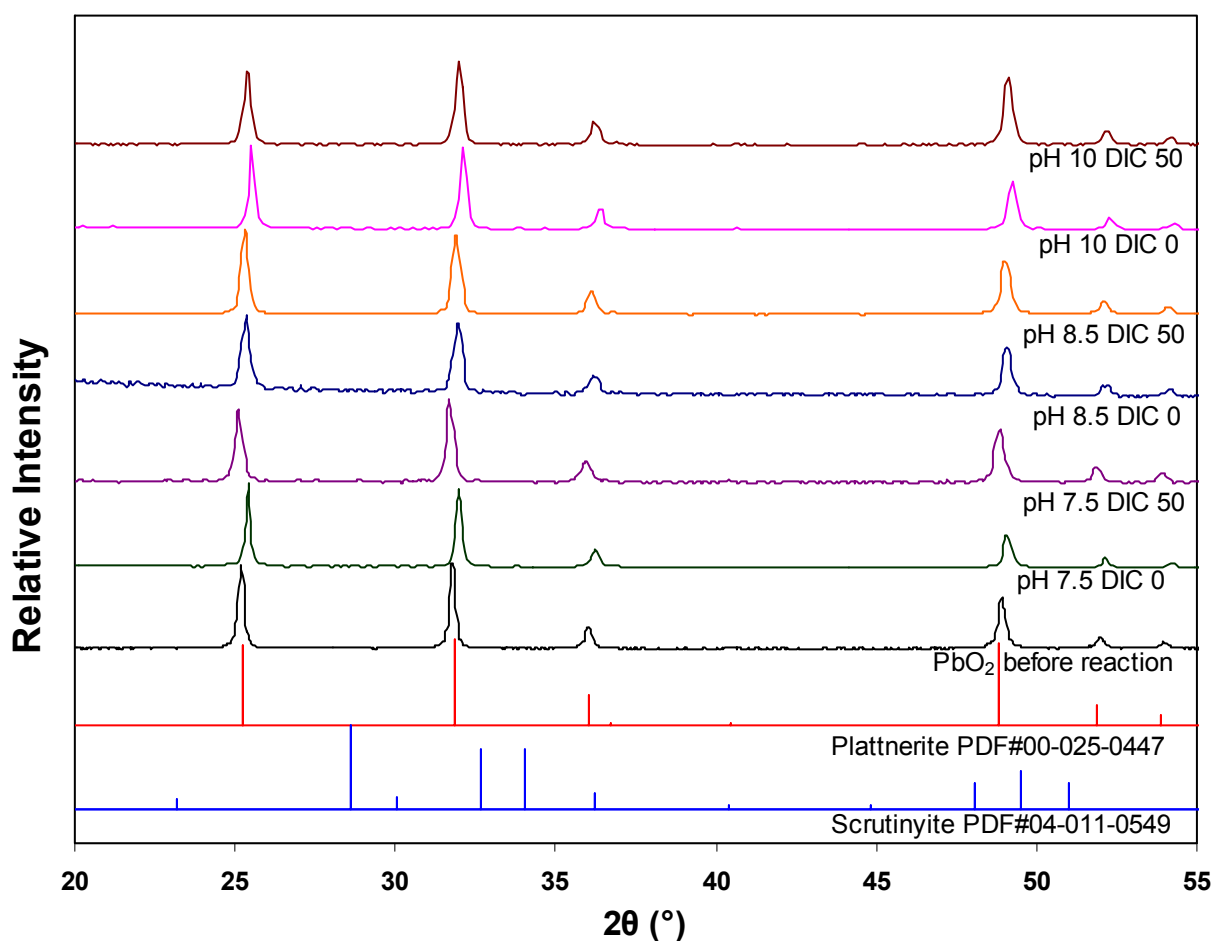
Figure 2-S2. X-ray diffraction (XRD) patterns of plattnerite before and after reaction at denoted conditions. The reference patterns for plattnerite (PDF# 00-025-0447) and scrutinyite (PDF# 04-011-0549) are included for comparison.
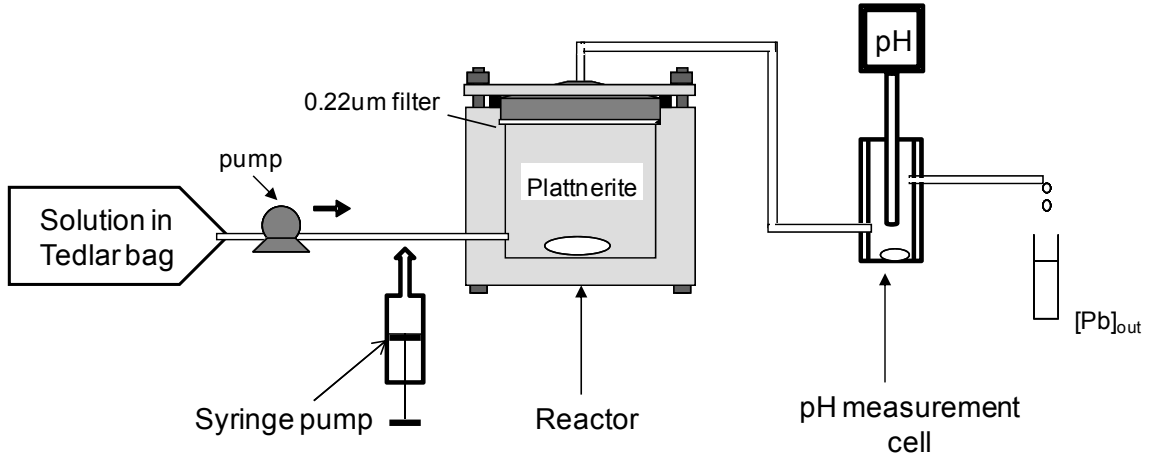
Figure 2-S3. Experimental system for dissolution rate measurements. The Tedlar bag initially contains 5 L of solution, and the reactor volume is 84 mL.
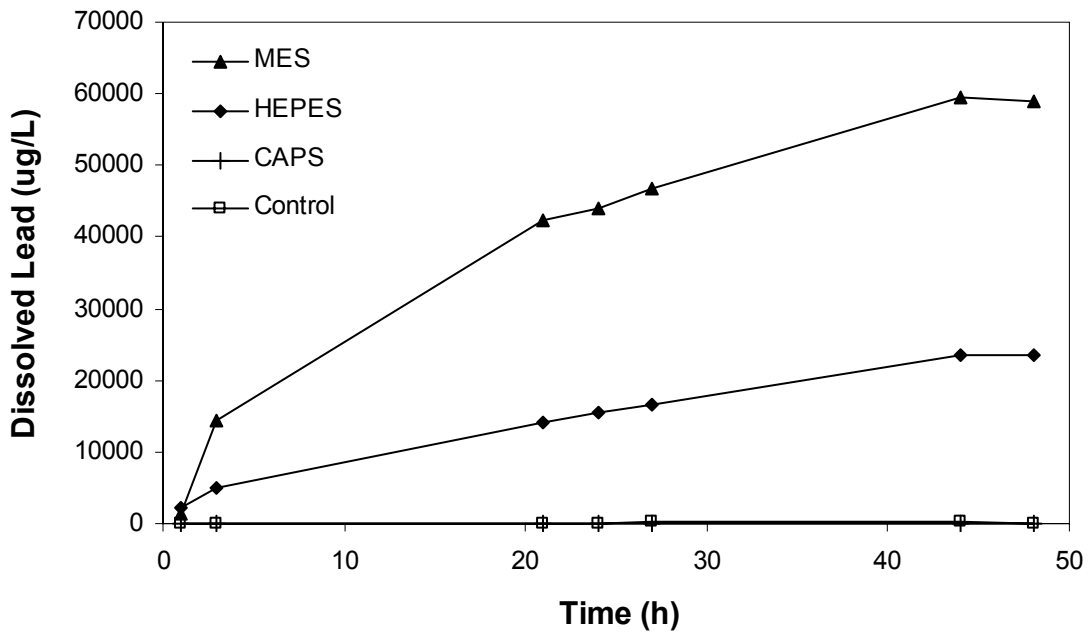
Figure 2-S4. Lead release from PbO_2 upon reaction with organic pH buffers. $PbO_2 = 1$ mM, organic buffer = 1 mM.
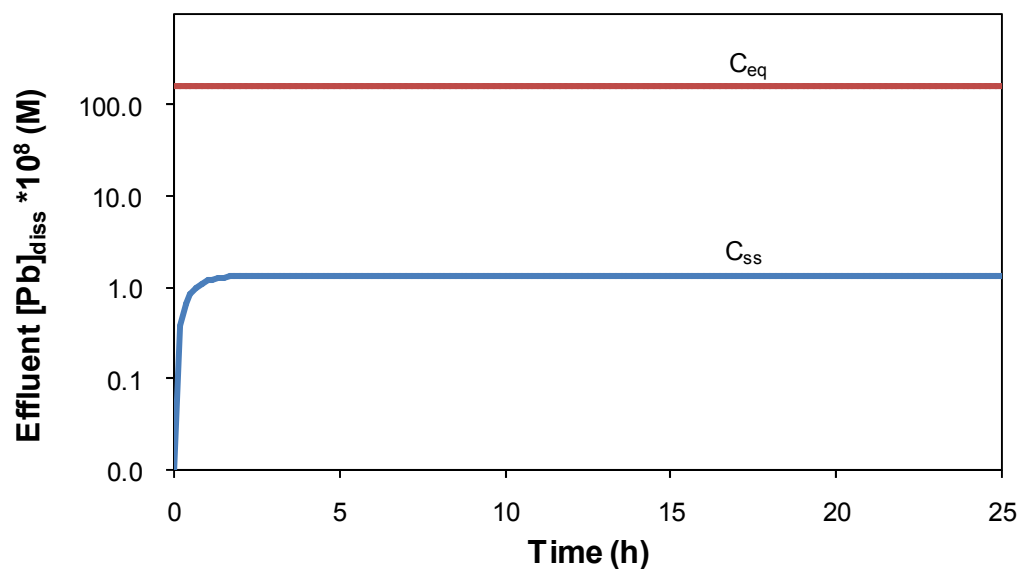
Figure 2-S5. Illustration of the dissolved lead effluent from a flow-through reactor. The illustration is for a hydraulic residence time of 0.5 hour at pH 8.5, DIC 10 mg C/L and 1 g/L plattnerite. The equilibrium solubility (C_{eq}) and steady-state concentration (C_{ss}) are identified.

Literature Cited:

(1)   Lasaga, A. C., *Kinetic theory in the earth sciences*. Princeton University Press: Princeton, New Jersey, 1998; p 811.

(2)   Xie, Y.; Noel, J. D.; Giammar, D. E. Impact of water chemistry on the formation, stabilization, and dissolution rates of PbO_2. *Proceedings of AWWA Water Quality Technology Conference*, Cincinnati, OH, 2008.

(3)   Dryer, D. J.; Korshin, G. V., Investigation of the reduction of lead dioxide by natural organic matter. *Environ. Sci. Technol.* **2007,** *41*, (15), 5510-5514.

(4)   Lin, Y. P.; Valentine, R. L., The release of lead from the reduction of lead oxide (PbO_2) by natural organic matter. *Environ. Sci. Technol.* **2008,** *42*, (3), 760-765.

(5)   Benjamin, M. M., *Water Chemistry*. 1st ed.; McGraw-Hill: New York, NY, 2002.

(6)   Schecher, W. D.; McAvoy, D. C. *MINEQL+: A chemical equilibrium modeling system, version 4.0*, 4.0; Environmental Research Software: Hallowell, ME, 1998.

(7)   Pourbaix, M., *Atlas of Electrochemical Equilibrium in Aqueous Solutions*. Second ed.; National Association of Corrosion Engineers: Houston, TX, 1974.

(8)   Stumm, W.; Morgan, J. J., *Aquatic chemistry*. Third ed.; John Wiley & Sons, Inc.: New York, NY, 1996; p 1022.

Chapter 3. Impact of Chlorine Disinfectants on Dissolution of the Lead Corrosion Product PbO$_2$

Results of this Chapter have been accepted by *Environmental Science and Technology* in August 2010

Abstract

Plattnerite (β-PbO$_2$) is a corrosion product that develops on lead pipes that have been in contact with free chlorine present as a residual disinfectant. The reductive dissolution of PbO$_2$ can cause elevated lead concentrations in tap water when the residual disinfectant is switched from free chlorine to monochloramine. The objectives of this study are to determine PbO$_2$ dissolution rates in the presence of chlorine disinfectants and PbO$_2$ equilibrium solubility in the presence of free chlorine, which are valuable for quantitatively predicting lead release from PbO$_2$. The effects of free chlorine and monochloramine on the dissolution rates of plattnerite were quantified in completely-mixed continuous-flow reactors at relevant pH and dissolved inorganic carbon conditions. PbO$_2$ dissolution rates decreased in the following order: no disinfectant > monochloramine > chlorine, which was consistent with the trend in the redox potential caused by monochloramine and chlorine. The results indicate that lead release from PbO$_2$ corrosion products on lead pipe will increase following a switch from free chlorine to monochloramine. Compared with experiments without disinfectant, monochloramine inhibited plattnerite dissolution in continuous-flow experiments. Although free chlorine maintained steady-state lead concentrations below the action level of 15 μg/L in flow-through experiments, in batch experiments lead concentrations exceeded the action level for longer residence times and approached an equilibrium value that was several orders of magnitude higher than that predicted from available thermodynamic data.

3.1   Introduction

The Lead and Copper Rule (LCR) set an action level of 15 µg/L (7.2×10^{-8} M) for lead in drinking water *(1)*. Release of lead from corrosion products that develop on plumbing materials can cause elevated lead concentrations in tap water. Lead corrosion products include lead(II) carbonates and oxides and lead(IV) oxides (PbO_2) *(2-4)*. PbO_2 rarely exists in natural environments, but it can develop in distribution systems that use free chlorine (i.e., HOCl and OCl⁻) as the residual disinfectant *(4)*. According to the available thermodynamic data, PbO_2 is less soluble than the lead(II) solids *(5, 6)* and very low lead concentrations are expected for systems with PbO_2 and free chlorine present to maintain a high redox potential. However, the equilibrium solubility of PbO_2 has not been experimentally measured at conditions relevant to drinking water distribution.

PbO_2 stability is strongly influenced by the disinfectant, free chlorine or chloramines (e.g, monochloramine, NH_2Cl). The Disinfection-By-Product Rule requires low disinfection-by-product concentrations, which is often achieved by switching the residual disinfectant from free chlorine to chloramines *(7)*. Following such a water treatment change, high lead concentrations were observed in Washington D.C. tap water *(8, 9)*. However, in other distribution systems high lead concentrations were not observed *(7)*. Lin and Valentine showed that an intermediate species in monochloramine decay can accelerate lead release from PbO_2 *(10)*. Switzer and co-workers reported that free chlorine can oxidize elemental lead to PbO_2 while monochloramine cannot *(11)*. Lead concentrations in tap water can be affected by the contact time of water with lead corrosion products. Water is only in contact with the corrosion products for a short time (seconds to minutes) at flowing conditions, while contact times of days can occur when

water is stagnant in lead-containing pipes or fittings. Most investigations of PbO_2 dissolution have been batch studies *(12, 13)* that provide important information on dissolved lead accumulation for long contact times. Compared with batch studies, flow-through experiments can be used to quantify the dissolution rates without the influence of reaction products on the dissolution rate *(14-16)*. Knowledge of PbO_2 dissolution rates will be useful for predicting lead concentrations in pipes when equilibrium has not been reached.

The objectives of this study were to (1) quantify the effects of free chlorine and monochloramine on the dissolution rate of plattnerite under flowing-water conditions; (2) elucidate PbO_2 dissolution mechanisms; and (3) determine PbO_2 solubility in the presence of free chlorine at environmentally relevant pH values. In this study, PbO_2 dissolution rates in the presence of chlorine disinfectants were determined, and the mechanism of the effects of chlorine disinfectants on rates and a quantitative rate model based on redox potential were proposed. The equilibrium solubility of PbO_2 in the presence of free chlorine was studied and compared with the prediction using thermodynamic constants.

3.2   Experimental Section

3.2.1   Materials

PbO_2 (Acros Organics) was identified as pure plattnerite (β-PbO_2) by X-ray diffraction (XRD). Primary particles (50 nm to 2 μm) formed aggregates larger than 1 μm. A specific surface area of 3.6 m^2/g was determined from the BET N_2-adsorption

isotherm. A solution of NaOCl (Fisher Chemical, 6% w/w) was used as the source of free chlorine. Monochloramine solutions were prepared by mixing volumes of 6% w/w NaOCl and 0.15 M NH_4Cl (Aqua Solutions) solutions in ultrapure water to achieve a 0.79 Cl_2:N molar ratio (4:1 Cl_2:N mass ratio), which is in the range used in drinking water distribution *(17)*. Under these conditions the dominant form of chloramines is monochloramine (NH_2Cl). All solutions were prepared from reagent grade chemicals and ultrapure water (>18.2 MΩ-cm resistivity, Milli-Q, Millipore Corp., Milford, MA).

3.2.2   Analysis Methods

XRD was performed on a Rigaku Geigerflex D-MAX/A diffractometer using Cu-Ka radiation. The instrument has a vertical goniometer and a scintillation counter. A JEOL 7001LVF field emission scanning electron microscope (SEM) was used to characterize the morphology of the solids. Dissolved lead concentrations were determined by inductively coupled plasma mass spectrometry (ICP-MS) (Agilent 7500ce). Solution pH was measured with a glass pH electrode and pH meter (Accumet). Free chlorine and monochloramine concentrations were measured using the standard DPD colorimetric method (4500-Cl Chlorine G) with a spectrophotometer (Perkin-Elmer Lambda 2S) *(18)*.

3.2.3.   Flow-through Experiments

Plattnerite dissolution rates were quantified using 84 mL continuous-flow stirred tank reactors (CSTR) with a hydraulic residence time of 30 minutes. The reactors were

loaded with 1 g/L plattnerite and sealed with 0.22 μm nitrocellulose filter membranes. Selected effluent samples were further filtered with 0.02 polyethersulfone membranes. All effluent samples were preserved by acidification to 2% HNO_3 and analyzed for dissolved lead by ICP-MS. In the flow-through experiments lead concentrations after 0.02 and 0.22 μm filtration were similar.

Influent compositions were controlled to evaluate the effects of chlorine and chloramines on plattnerite dissolution rates at environmentally relevant conditions. Six conditions were studied (2 pH values with no disinfectant, 2 mg/L as Cl_2 monochloramine, and 2 mg/L as Cl_2 free chlorine) in duplicate experiments (Table 1), and solid-free experiments were conducted as procedural blanks. Additional two conditions of 1 and 0.1 mg/L free chlorine at pH 7.5 were investigated in duplicate to study the effect of free chlorine concentrations on plattnerite dissolution rates. These reactors were previously used to determine plattnerite dissolution rates as a function of pH and DIC in the absence of any chlorine species *(19)*. Flow rate, pH, and chlorine/monochloramine concentrations were periodically measured throughout each experiment. Experiments were conducted at room temperature (21 ± 1 ºC).

The reactor influents were prepared in 10 L plastic (Tedlar) bags to avoid transfer of CO_2 into or out of solution. Ultrapure water was purged with nitrogen before being pumped into the bags. Dissolved inorganic carbon (DIC) was provided by the addition of $NaHCO_3$. Monochloramine solutions were prepared immediately before each experiment and were shielded from light by aluminum foil to minimize the chloramines decomposition. An aliquot of 1.0 M $NaNO_3$ solution was injected to set the ionic strength at 0.01 M. The influent pH was adjusted last by the addition of NaOH or HNO_3.

Dissolution rates were determined by operating the flow-through reactors for 48 or more hydraulic residence times (24 hours). By continuously flushing the products of dissolution from the reactors, the effluent dissolved lead concentrations approach steady-state concentrations that are controlled by the rates of dissolution of the solid phase. This approach is different from batch experiments in which the dissolved concentrations increase until they reach equilibrium solubility; the accumulation of reaction products and the presence of initial labile phases in batch experiments can complicate the quantification of rates *(14-16)*. In a flow-through experiment, the steady-state effluent concentration will be less than the equilibrium solubility of the dissolving solid. A tracer study confirmed that the reactor solutions were well-mixed.

After the 24-hour period of flow, each reactor remained sealed and stirred with no flow for another 24 hours. At the conclusion of this batch mode, the pH and concentrations of lead, free chlorine, and monochloramine were measured. The solids remaining at the end of each experiment were characterized by XRD. The batch mode of the experiments provides complementary information regarding the effects of chlorine disinfectants on PbO_2 dissolution at longer residence times than during the period with flow.

For a flow-through reactor at steady-state the dissolution rate can be quantified by Equation 3.1,

$$Rate = \frac{Q \cdot t \cdot C_{ss}}{t \cdot A \cdot [solids] \cdot V} = \frac{C_{ss}}{t_{res} \cdot A \cdot [solids]} \qquad (3.1)$$

where *Rate* is the dissolution rate (mol m^{-2} min^{-1}); C_{ss} is the steady-state effluent lead concentration (mol/L); Q is flow rate (m^3 min^{-1}); t is the elapsed reaction time, V is the volume of the reactor (m^3); t_{res} is the hydraulic residence time (min); *[solid]* is the solid

concentration in the reactor (g/L); and A is the specific surface area of the solid (m^2/g).

No lead was added to the influent, and samples of the influent had lead concentrations

below the detection limit (30 ng/L). The steady-state effluent concentration was

determined as the average concentration of at least 5 samples that did not vary by more

than 30% and spanned at least 5 residence times.

3.2.4. PbO_2 Equilibrium Solubility Batch Experiments

Batch experiments were conducted in duplicate in carbonate-free solutions at

three pH values (6, 7.5, and 8.5) to evaluate equilibrium PbO_2 solubility in the presence

of free chlorine. To avoid the influence of carbonate on PbO_2 dissolution, experiments

were performed in a glove box filled with argon that was in contact with a concentrated

solution of NaOH to absorb traces of CO_2. The pH of the suspensions was adjusted to the

desired value each day for one month by adding 0.5 M NaOH or HNO_3 solution; the pH

variations were within $\pm$ 0.2 pH units. No buffer was used. The free chlorine

concentrations were monitored and, if necessary, readjusted to the target value. Aqueous

samples were collected every day, filtered with 0.02 μm polyethersulfone membranes,

and acidified in preparation for ICP-MS analysis of dissolved lead. After 1 month the

remaining solids were collected for X-ray diffraction analysis.

In the presence of free chlorine, Pb(IV) is predicted to be dominant. The

equilibrium dissolved lead concentration was calculated as the sum of all dissolved

species. The equilibrium concentrations of Pb^{4+} and Pb(IV) complexes were calculated

using the reactions and equilibrium constants in Tables S1 and S2 of the Supporting

Information.

3.3   Results and Discussion

3.3.1   Effects of Monochloramine and Chlorine on Dissolution Rates in Flow-through Experiments

Both monochloramine and free chlorine slowed PbO_2 dissolution. Lead concentrations reached steady-state within 19 hours (Figure 3.1), and these concentrations were used in Equation 3.1 to calculate dissolution rates (Table 3.1).
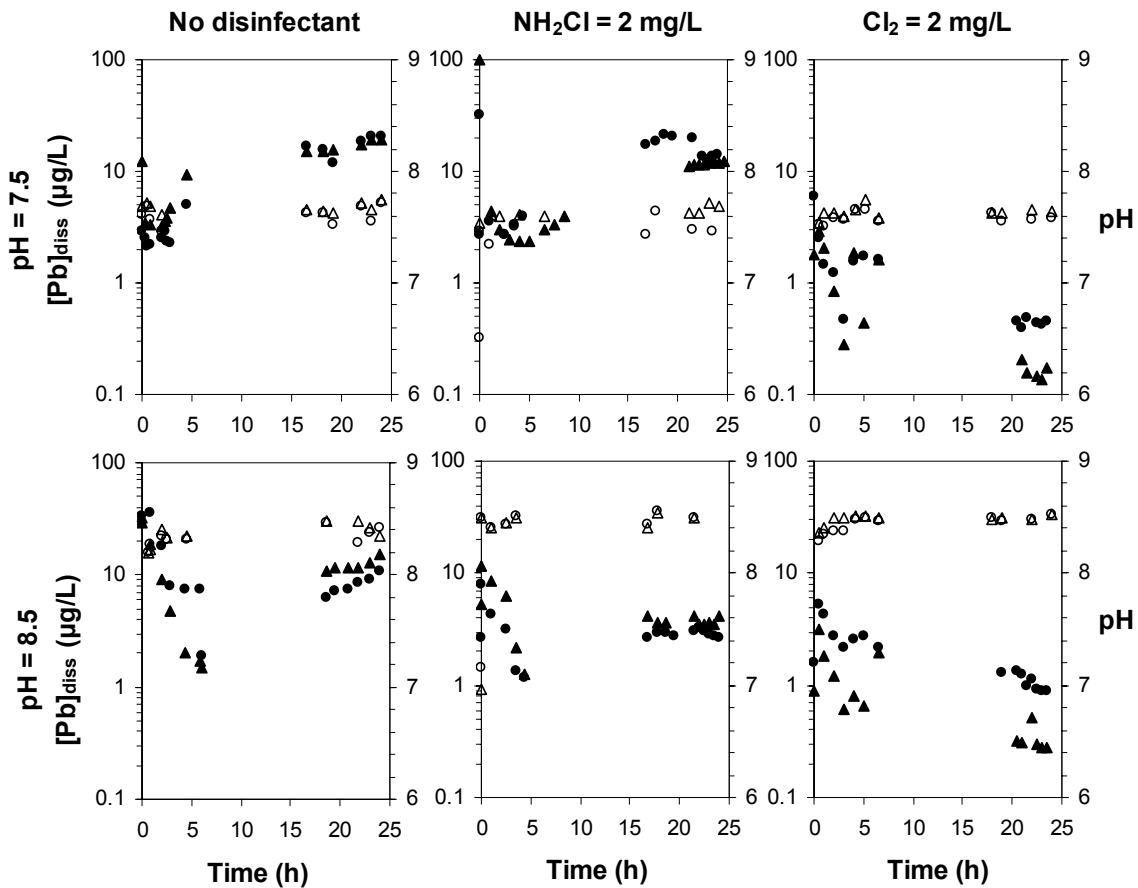
Figure 3.1. Effluent lead concentrations (shown as ▲ and ●) and pH (shown as Δ and ○) from flow-through reactors in the absence and presence of monochloramine or free chlorine. Duplicate experiments (represented by triangles and circles) were conducted at the hydraulic residence time of 30 minutes. Samples were not taken during the middle of the experiments (9 to 15 hours). Note: monochloramine concentration is 2 mg/L as Cl_2.

Table 3.1. Conditions and results of plattnerite dissolution experiments

| Experiment ID | pH | Influent Composition | | | Residence Time (min) | effluent Lead (nM) | Steady-state Dissolution Rate x 10^{10} (mol/min·m^2) |
		DIC (mg/L as C)	Chloramine (mg/L as Cl$_2$)	Free Chlorine (mg/L as Cl$_2$)			
1A	7.5	50.0	0.0	0.0	30	83.8	7.87
1B	7.5	50.0	0.0	0.0	30	82.7	7.77
2A	8.5	50.0	0.0	0.0	30	41.5	3.90
2B	8.5	50.0	0.0	0.0	30	59.9	5.63
3A	7.5	50.0	2.0	0.0	30	77.5	7.28
3B	7.5	50.0	2.0	0.0	30	57.2	5.37
4A	8.5	50.0	2.0	0.0	30	14.0	1.32
4B	8.5	50.0	2.0	0.0	30	17.6	1.65
5A	7.5	50.0	0.0	2.0	30	2.12	0.20
5B	7.5	50.0	0.0	2.0	30	0.97	0.09
6A	8.5	50.0	0.0	2.0	30	4.67	0.44
6B	8.5	50.0	0.0	2.0	30	1.60	0.15
7A	7.5	50.0	0.0	1.0	30	3.26	0.31
7B	7.5	50.0	0.0	1.0	30	6.04	0.57
8A	7.5	50.0	0.0	0.1	30	5.59	0.52
8B	7.5	50.0	0.0	0.1	30	12.46	1.17

Dissolution rates decreased in the following order: no disinfectant > monochloramine > free chlorine (Figure 3.2a). Free chlorine inhibited dissolution most significantly and maintained effluent lead concentrations well below the action level. Dissolution rates decreased with increasing free chlorine concentration, and the rates in the presence of all concentrations of free chlorine were lower than the rates in the presence of monochloramine (Figure 3.2b). Monochloramine also kept the lead concentration below the action level, although effluent concentrations were close to 15 μg/L at pH 7.5 and DIC 50 mg/L. As determined by X-ray diffraction, the remaining solids after two days of reaction were still plattnerite.
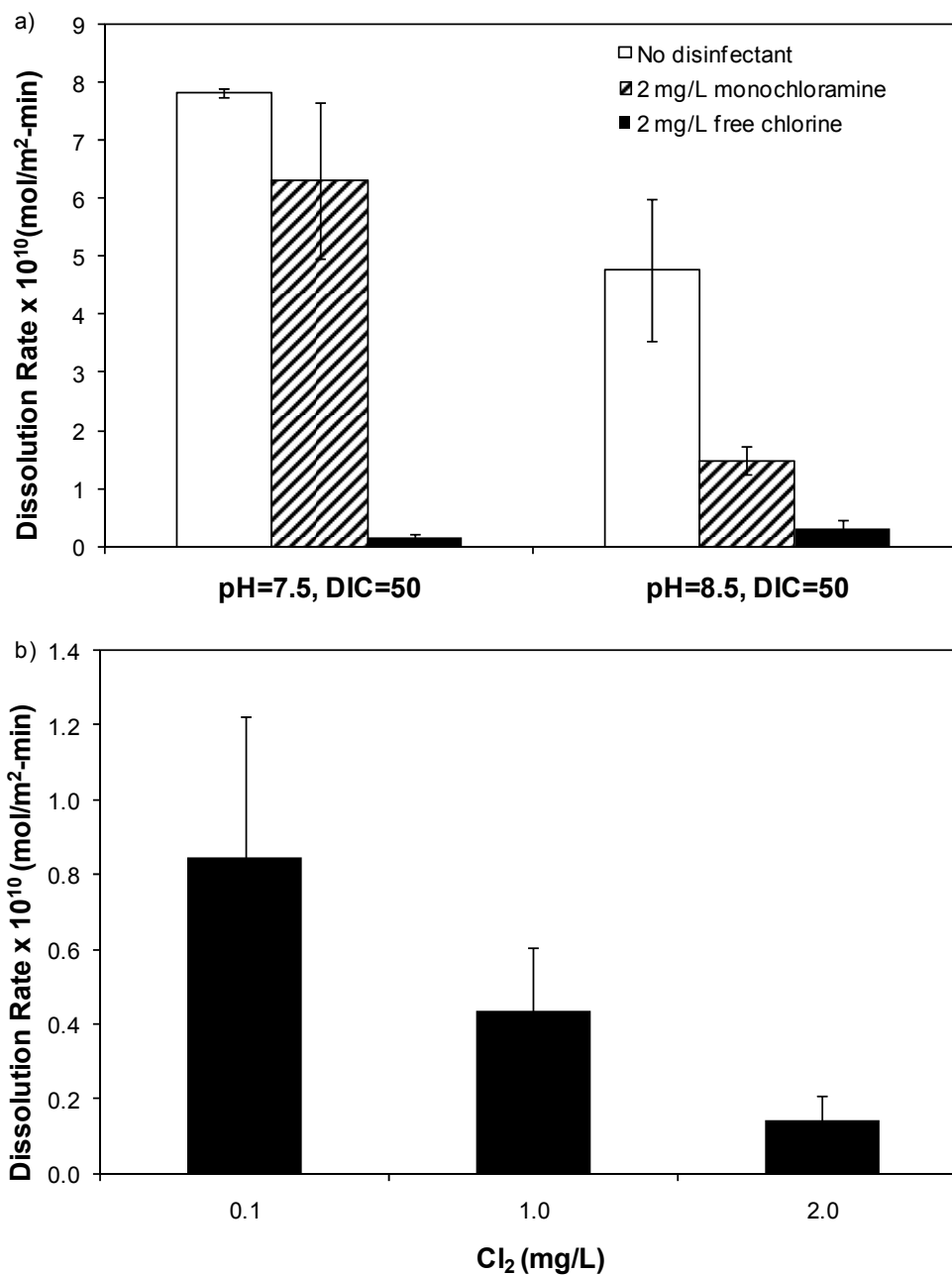
Figure 3.2. a) Dissolution rates of plattnerite determined from flow-through experiments using no disinfectant, 2 mg/L monochloramine as Cl_2, and 2 mg/L free chlorine. b) Dissolution rates of plattnerite determined from flow-through experiments using different concentrations of free chlorine (0.1, 1, and 2 mg/L). DIC denotes the dissolved inorganic carbon concentration in mg C/L. The error bars represent one sample standard deviation. The pH indicated is the target pH of the influents.

In the presence of monochloramine, the PbO_2 dissolution was faster at lower pH, which is consistent with previous observations in the absence of chlorine species *(19)*. In the presence of free chlorine, dissolution rates at pH 7.5 and 8.5 were not significantly different. The different effects of pH observed with and without free chlorine could result from different dissolution mechanisms. In the absence of free chlorine, PbO_2 reductive dissolution occurs in two sequential steps: first, PbO_2 is reduced to Pb(II) on the surface; second, surface Pb(II) is released into solution *(19)*. In the presence of free chlorine, PbO_2 is expected to dissolve by directly releasing Pb(IV) to solution; however, as will be discussed in the section on batch dissolution experiments, the effects may be more complicated.

The pH values were stable and steady-state effluent concentrations were usually established. Prior to reaching steady-state, the effluent pH and dissolved lead concentrations varied during the early period after initiation of flow. The starting solution was pure water with a lower pH than the influent, and the effluent pH gradually increased and stabilized at the influent pH within one hour. The lower initial pH and dissolution of the smallest particles or initial labile surface phases probably caused the lead concentrations in the first few hours that were higher than the later steady-state values. In one of the replicates with pH 8.5 and 50 mg/L DIC, a gradual decrease in pH caused a slight increase in the effluent lead concentrations. For this experiment, the average of the last five samples was used to represent the steady-state concentration in the rate calculation; however, because steady-state was not achieved, this rate may represent only a lower bound. In one of the replicates with 2 mg/L monochloramine, pH

7.5, and 50 mg/L DIC, the small shift in lead concentration right before the steady-state period was caused by a pH fluctuation.

3.3.2 Control of PbO₂ Dissolution Rate by Redox Potential

Dissolution of PbO_2 in the well-mixed reactors is limited by surface reaction [19], and it can involve chemical reduction. The relationship between redox potential and the PbO_2 dissolution rate can be related as follows,

$$Rate = A \cdot e^{-\frac{\Delta G^{\neq}}{RT}}$$

(3.2)

where $\Delta G^{\neq}$ is the Gibbs free energy of activation, A is a positive constant, R is the ideal gas constant (8.314 J mol^{-1} K^{-1}), and T is temperature (K). When electron transfer is the rate limiting step, the transition state is energetically closer to the products than the precursors. The Gibbs free energy of activation is then proportional to the Gibbs free energy change of the reaction (ΔG_r) [20].

$$\Delta G^{\neq} = a\Delta G_r + constant$$

(3.3)

where a is a positive constant. Since ΔG_r is proportional to the difference in the redox potentials of the PbO_2/Pb^{2+} couple ($E_{H,PbO_2/Pb^{2+}}$) and the dominant aqueous redox couple ($E_{H,aq}$), which is O_2/H_2O, NH_2Cl/Cl^- or $HOCl/Cl^-$, the dissolution rate is then proportional to the difference in redox potentials.

$$\Delta G_r = -nF\Delta E = -nF(E_{H,PbO_2/Pb^{2+}} - E_{H,aq})$$

(3.4)

$$Rate = A \cdot e^{\frac{anF}{RT}(E_{H,PbO_2/Pb^{2+}} - nE_{H,aq})} + constant'$$

(3.5)

where F is the Faraday constant (96500 C mol^{-1}) and n is the number of electrons

transferred during the overall reaction. The difference between the redox potential of the

PbO_2/Pb^{2+} couple and the dominant aqueous redox couple controls the driving force for

PbO_2 dissolution.

In Equation 3.5 the dissolution rate decreases with increasing E_H of the dominant

aqueous redox couple. In the absence of chlorine and monochloramine, the O_2/H_2O

couple dominates the redox potential of the solution. The relevant half reactions are:

$$PbO_{2(s)} + 4H^+ + 2e^- = Pb^{2+} + 2H_2O \quad \log K_1 = 49.60 \qquad E_H^0 = 1.46 \text{ V} \qquad (3.6)$$

$$O_{2(aq)} + 4H^+ + 4e^- = 2H_2O \qquad \log K_2 = 86.00 \qquad E_H^0 = 1.27 \text{ V} \qquad (3.7)$$
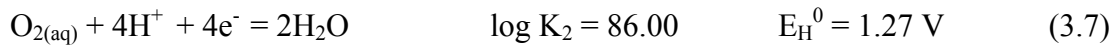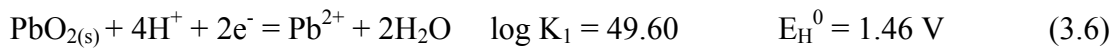
When monochloramine is present it controls the redox potential of the system, and the E_H

of the solution can be calculated from Reaction 3.8.

$$NH_2Cl + 2e^- + 2H^+ = Cl^- + NH_4^+ \qquad \log K_5 = 47.46 \qquad E_H^0 = 1.40 \text{ V} \qquad (3.8)$$
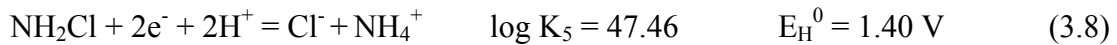
Similarly, free chlorine can control the redox potential of the system, and the E_H of the

solution can be calculated from Reaction 3.9.

$$HOCl + 2e^- + H^+ = Cl^- + H_2O \qquad \log K_5 = 50.20 \qquad E_H^0 = 1.48 \text{ V} \qquad (3.9)$$
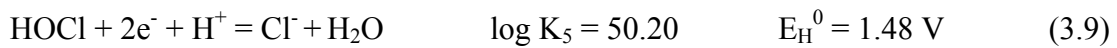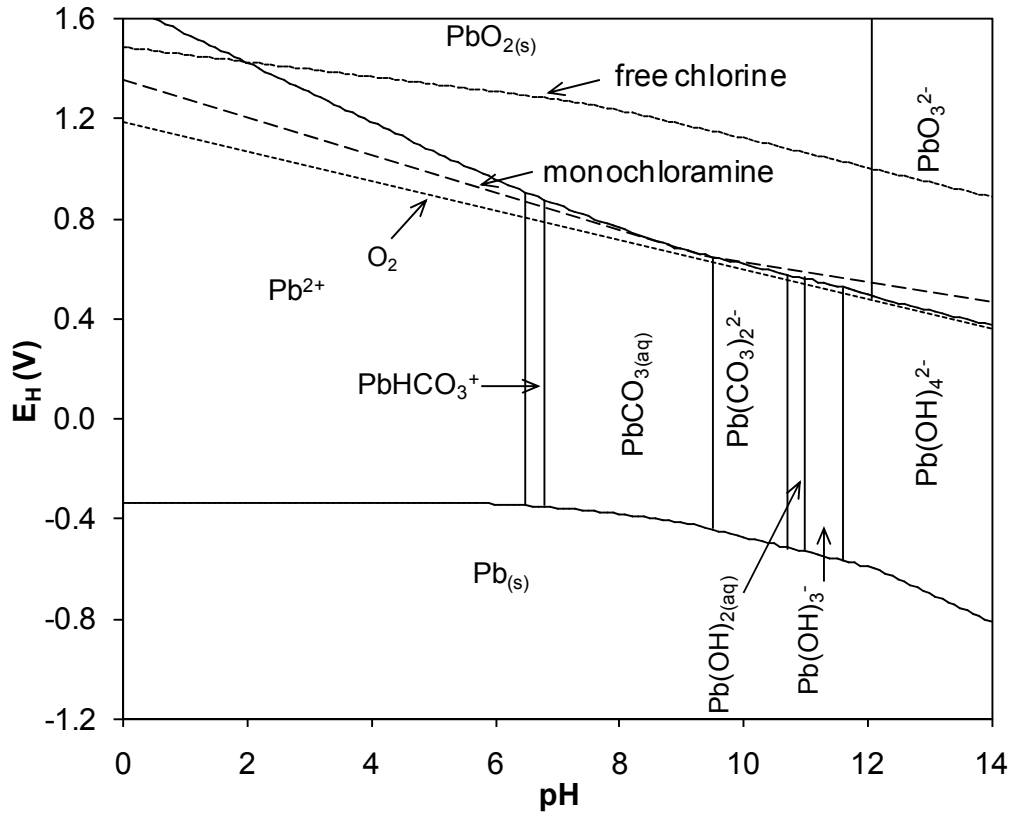
Figure 3.3. E_H-pH diagram for the Pb(IV)-Pb(II)-Pb(0) system with a total lead concentration of 15 μg/L and 30 mg/L of dissolved inorganic carbon. The short-dashed lines denote the the E_H provided by 1.26 μM dissolved oxygen (in equilibrium with 0.001 atm O_2). The long-dashed line indicates the E_H provided by monochloramine at a concentration of 2 mg/L as Cl_2 with a Cl_2:N ratio of 0.79. The free chlorine line represent the E_H provided by free chlorine at a concentration of 2 mg/L as Cl_2.

The E_H increases in the following order: no disinfectant < monochloramine < free chlorine (Figure 3.3), and increases with increasing free chlorine concentration. Thus, it is not surprising that PbO_2 dissolution rates decreased in the order of solutions that provided higher E_H. Least squares optimization of the experimental data to Equation 5 yielded parameters that allow the equation (Eq 3.10) to fit the rates well with an R-squared value of 0.95 (Figure 3.4).

$$Rate = 1.2 \times 10^{-10} e^{119.7 \left(\frac{E_{H, \, PbO_2}}{Pb^{2+}} - E_{H,aq} \right)} + 4.3 \times 10^{-11} \tag{3.10}$$
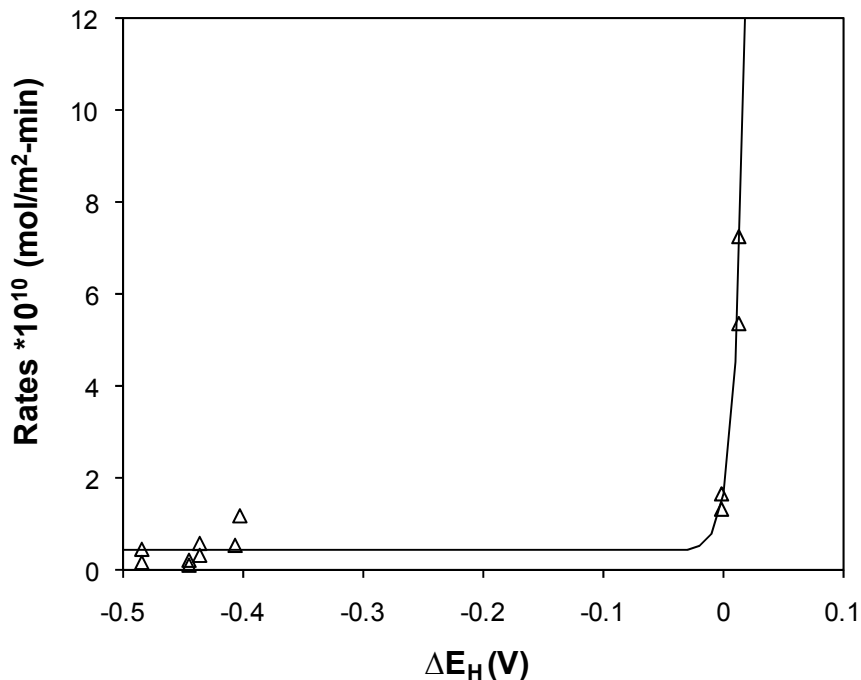
Figure 3.4. Least square fitting of experimental data to Equation 3.5. Only experimental data in the presence of free chlorine or monochloramine are used in the fitting.

In the presence of free chlorine, the steady-state concentrations in the flow-through experiments were much lower than the lead concentrations reached in the PbO_2 batch experiments discussed in a subsequent section (Table 3.1 and Figure 3.5). These differences in the lead concentrations indicate that the flow-through experiments with free chlorine were far from equilibrium. The effect of free chlorine on the PbO_2 dissolution rate is consequently confirmed to be through control of dissolution kinetics and not equilibrium. Because the PbO_2 dissolution rates responded to the redox potential of the solution set by the NH_2Cl/Cl^- or the $HOCl/Cl^-$ couple, the reduction step was rate-limiting in the presence of free chlorine or monochloramine.
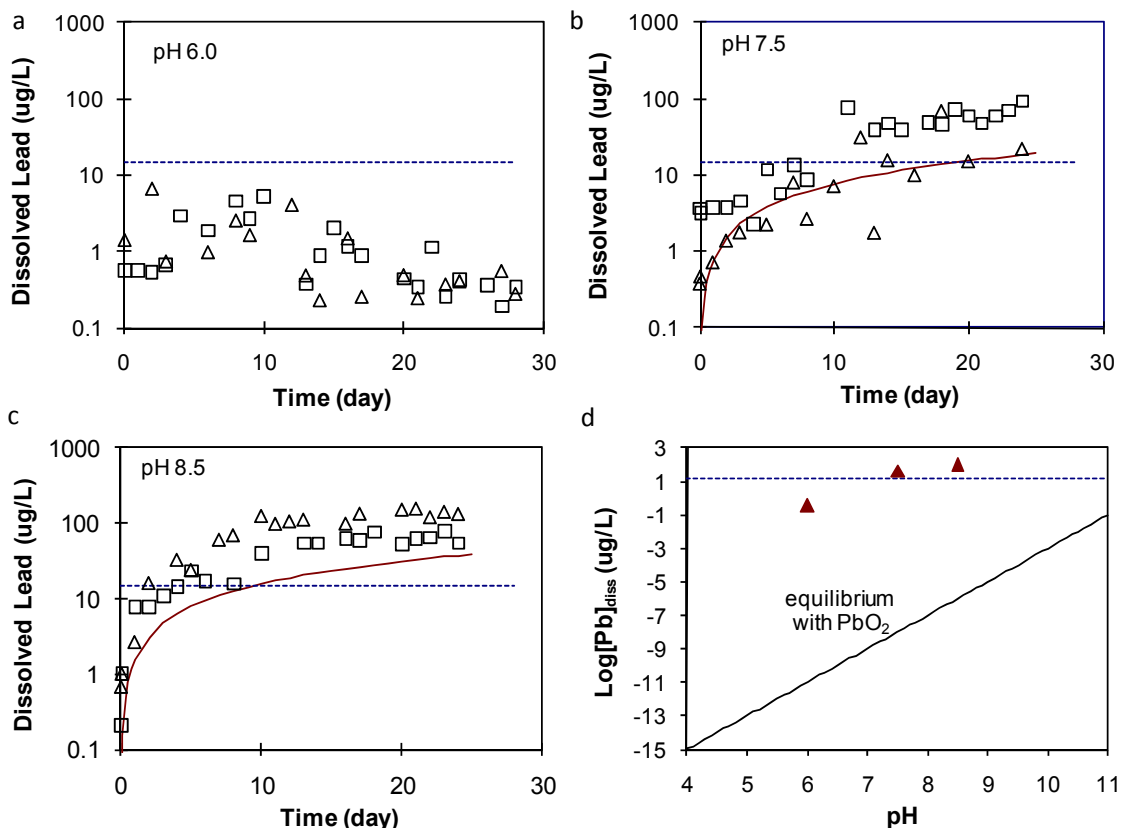
Figure 3.5. a-c) Experimental and predicted dissolved lead concentrations with time in PbO$_2$ batch dissolution experiments. Experiments were performed at 2 mg/L free chlorine, 50 mg/L plattnerite, and pH values of 6.0, 7.5 and 8.5. Replicate experimental lead concentrations are shown as Δ and □. The solid lines represent the predicted lead concentrations assuming dissolution at the rates determined from the flow-through experiments. Panel d presents the predicted (solid line) and measured (triangular points) equilibrium solubility of PbO$_2$ versus pH. In all panels dashed lines represent the lead action level of 15 μg/L.

Previous studies measured an increase in redox potential upon addition of monochloramine *(21, 22)*. However, a measured ORP from monochloramine was lower than that from the thermodynamic prediction *(21-23)*, and there is still uncertainty in the equilibrium constants for Reactions 3.6 and 3.8 *(6, 11, 23)*. Consequently, while monochloramine and free chlorine can qualitatively be demonstrated to lower the plattnerite dissolution rate, definitive quantification of the effects of chlorine species on

the dissolution rate need more accurate equilibrium constants for PbO_2 and

monochloramine and redox potential measurements.

3.3.3. Effects of Monochloramine and Free chlorine on PbO_2 Dissolution in Batch vs. Flow-through Experiments

Relative to conditions with no disinfectant, monochloramine was able to decrease

the PbO_2 dissolution rate in flow-through experiments, but during the 1-day batch period

immediately following the flow-through period, monochloramine decayed and

accelerated PbO_2 dissolution (Figure 3.6). The contrasting observations between batch

and flow conditions may be explained by differences in the nature of the reaction times

(much shorter at flow conditions) and can be attributed to two separate effects of

monochloramine. The first effect is increasing the redox potential, which inhibits the

reduction step. The second effect is the reduction of PbO_2 to Pb(II) by an intermediate

species involved in monochloramine decomposition. Lin and Valentine found that such

an intermediate species could accelerate the reduction of PbO_2 *(10)*. The second effect is

more significant in a batch system because the reactive intermediate species can

accumulate over time in a way that does not occur in a flow-through system. The extent

of monochloramine decay during a residence time of 30 min in the flow-through mode

was negligible (< 0.02 mg/L), while the decline of monochloramine during 24 hours in

the batch mode was about 50%. In fact, for the batch mode, the decay of

monochloramine correlated well with the dissolved lead concentration (Figure 3.6). The

slope of this correlation was 0.04, which was similar to that of 0.05 - 0.21 observed by

Lin and Valentine. The differences in slopes could be caused by different water

71

chemistry conditions and PbO_2 specific surface areas *(10, 24)* or uncertainty in the slope

obtained in the presented study due to limited data points. The positive x-axis intercept

in Figure 3.6, which indicates partial PbO_2 reduction without an increase in dissolved

lead, could result from production of Pb(II) that remained adsorbed to the PbO_2 surface.

Pb(II) can appreciably adsorb to PbO_2 at pH 7.5 and 8.5 *(25)*. This adsorption would be

stronger in the present study because of a higher PbO_2 loading (1 g/L) than in Lin and

Valentine's work (10 mg/L).
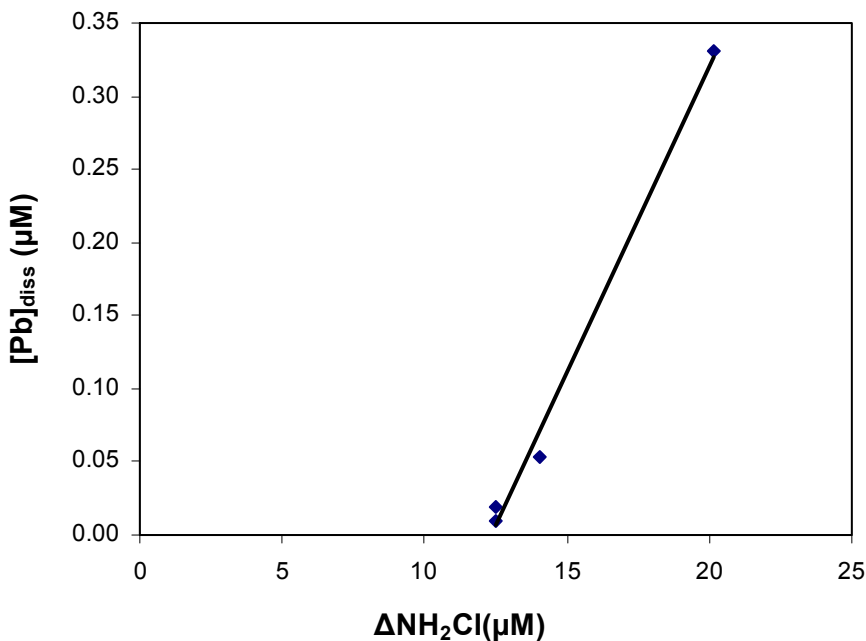
Figure 3.6. Dissolved lead concentration versus ΔNH_2Cl after 24 hours of reaction in the batch mode following the flow-through experiments. The linear regression y = 0.042x - 0.52 fits the experimental data well with an R-squared value of 0.99.

During the 1-day batch period immediately following the flow-through period,

free chlorine slightly decayed (within 10%) and dissolved lead concentration increased.

However, the decay of free chlorine did not correlate linearly with the dissolved lead

concentrations in the 1-day batch experiments following the flow-through period.

3.3.4 Equilibrium Solubility of Plattnerite

In batch experiments designed to measure equilibrium PbO_2 solubility in the presence of free chlorine, for most conditions the dissolved lead concentrations increased with time until they reached plateaus after 17 days (Figure 3.5a-c). The lead concentrations exceeded the action level (15 μg/L) after 4 days for pH 8.5 and after 10 days for pH 7.5. The plateau lead concentrations probably represent equilibrium between PbO_2 and the solution. Pb(IV) is calculated to dominate in the presence of free chlorine. However, available thermodynamic data for calculating equilibrium solubility of PbO_2 were not determined from solubility studies at environmentally-relevant conditions. Pourbaix calculated the Gibbs free energies for $PbO_{2(s)}$ and Pb(IV) aqueous species (Table 3-S3 of the Supporting Information) and the solubility product of PbO_2 based on electric potential measurements made by Glasstone at very acidic and very basic conditions *(5, 26)*. The equilibrium solubility of PbO_2 calculated using these thermodynamic data increases with increasing pH (Figure 3.5d), and experimentally measured solubility is indeed higher at higher pH. However, the measured lead concentrations were orders of magnitude higher than the predicted values ($\log[Pb]_{diss}$ < -13). This observation raises questions about the applicability of the thermodynamic constants for PbO_2 and Pb(IV) aqueous species to conditions relevant to environmental systems. The thermodynamic constants could be one reason for the discrepancy between the experimental and predicted PbO_2 equilibrium solubility.

Another reason for the higher experimental than predicted PbO_2 solubility could be the presence of dissolved Pb(II). In previous work Lin and Valentine used a Pb(II)-

specific analysis method to detect 5-10 µg/L dissolved Pb(II) from PbO_2 dissolution in the presence of free chlorine *(24)*. If the rate of PbO_2 reduction by water is faster than the oxidation of Pb(II) species by free chlorine, then Pb(II) concentrations could be maintained even in the presence of free chlorine. Oxidation reactions are generally faster with HOCl than with OCl⁻ *(27)*, and HOCl is more abundant at lower pH values. Therefore, the oxidation of Pb(II) species by free chlorine could cause lower lead concentrations at lower pH values. Further work is needed to experimentally determine the equilibrium solubility of PbO_2 and aqueous lead speciation in the presence of free chlorine at environmentally-relevant conditions.

3.3.5 Comparison of PbO_2 Dissolution Rates from Batch and Flow-through Experiments

In batch experiments the initial dissolution was faster than at longer reaction times (Figure 3.5a-c), which is consistent with the observation in flow-through experiments. The high initial lead release rate in batch experiments could have been caused by the fast dissolution of initial labile surface phases and very small PbO_2 particles. Owing to the initial high lead release rates, the measured lead concentrations in batch experiments were higher than the concentrations predicted by applying the steady-state dissolution rates from the flow-through experiments to the batch experiments (shown by the solid lines in Figure 3.5a-c).

3.4 Environmental Implications

The study provided direct evidence that the PbO_2 dissolution rate is enhanced when the residual disinfectant is switched from free chlorine to monochloramine, which is consistent with observations of higher lead concentrations in Washington D.C. tap water following such a switch. At flowing conditions, the increase in the rate was due to the decreased redox potential. Free chlorine can effectively control the lead concentration from PbO_2 dissolution at flowing conditions, but the results of batch experiments suggest that free chlorine may not be able to control the lead concentration under the action level for very long stagnation times. However, PbO_2 dissolution is still very slow with free chlorine present; 4-10 days were required for lead concentrations to exceed 15 $\mu g/L$ for relatively high PbO_2 loadings of 1 g/L. The available thermodynamic data for PbO_2 and Pb(IV) species failed to predict the measured PbO_2 equilibrium solubility in the presence of free chlorine, and calculations of lead concentrations based on these data will underestimate actual concentrations.

Chloramines can affect lead release from plattnerite in two opposing ways: (a) through PbO_2 reduction by an intermediate species from decomposition of monochloramine and (b) through increasing the redox potential to decrease the thermodynamic driving force for reduction. The contact time of monochloramine with PbO_2 and the Cl_2:N ratio in monochloramine formation will determine which mechanism is more important. Residence time plays an important role in controlling the lead concentrations in tap water disinfected with monochloramine or free chlorine. The actual concentrations of chlorine species will vary with location in a distribution system. The rate equation developed in this study may ultimately allow PbO_2 dissolution rates to be

estimated based on the specific concentrations of monochloramine or free chlorine for a
given system and location.

Acknowledgements

Literature Cited

(1)   U.S.EPA, Maximum Contaminant Level Goals and National Primary Drinking
Water Regulations for Lead and Copper. Final Rule. *Federal Register* **1991,** *56*, 26460.
(2)   Schock, M.R.; Hyland, R.N.; Welch, M.M., Occurrence of contaminant
accumulation in lead pipe scales from domestic drinking-water distribution systems.
Environ. Sci. Technol. **2008,** *42*, (12), 4285-4291.
(3)   Liu, H.Z.; Korshin, G.V.; Ferguson, J. F., Investigation of the kinetics and
mechanisms of the oxidation of cerussite and hydrocerussite by chlorine. *Environ. Sci.
Technol.* **2008,** *42*, (9), 3241-3247.
(4)   Lytle, D.A.; Schock, M.R., Formation of Pb(IV) oxides in chlorinated water. *J.
Am. Water Works Assoc.* **2005,** *97*, (11), 102-114.
(5)   Pourbaix, M., *Atlas of Electrochemical Equilibria in Aqueous Solutions*. Second
ed.; National Association of Corrosion Engineers: Houston, TX, 1974.
(6)   Schock, M.; Giani, R. Oxidant/disinfectant chemistry and impacts on lead
corrosion, *Proceedings of Water Quality Technology Conference*, San Antonio, TX,
2004; San Antonio, TX, 2004.
(7)   Wilczak, A.; Hokanson, D.R.; Trussell, R.R.; Boozarpour, M.; Degraca, A.F.,
Water conditioning for LCR compliance and control of metals release in San Francisco's
water system. *J. Am. Water Works Assoc.* **2010,** *102*, (3), 52-64.

(8)   Edwards, M.; Dudi, A., Role of chlorine and chloramine in corrosion of lead-bearing plumbing materials. *J. Am. Water Works Assoc.* **2004,** *96*, (10), 69-81.

(9)   Renner, R., Plumbing the depths of DC's drinking water crisis. *Environ. Sci. Technol.* **2004,** *38*, (12), 224A-227A.

(10)   Lin, Y.P.; Valentine, R.L., Release of Pb(II) from monochloramine-mediated reduction of lead oxide (PbO_2). *Environ. Sci. Technol.* **2008,** *42*, (24), 9137-9143.

(11)   Switzer, J.A.; Rajasekharan, V.V.; Boonsalee, S.; Kulp, E. A.; Bohannan, E. W., Evidence that monochloramine disinfectant could lead to elevated Pb levels in drinking water. *Environ. Sci. Technol.* **2006,** *40*, (10), 3384-3387.

(12)   Dryer, D.J.; Korshin, G.V., Investigation of the reduction of lead dioxide by natural organic matter. *Environ. Sci. Technol.* **2007,** *41*, (15), 5510-5514.

(13)   Lin, Y.P.; Valentine, R.L., The release of lead from the reduction of lead oxide (PbO_2) by natural organic matter. *Environ. Sci. Technol.* **2008,** *42*, (3), 760-765.

(14)   Samson, S.D.; Eggleston, C.M., The depletion and regeneration of dissolution-active sites at the mineral-water interface: II. Regeneration of active sites on alpha-Fe_2O_3 at pH 3 and pH 6. *Geochim. Cosmochim. Acta* **2000,** *64*, (21), 3675-3683.

(15)   Oelkers, E.H., An experimental study of forsterite dissolution rates as a function of temperature and aqueous Mg and Si concentrations. *Chemical Geology* **2001,** *175*, 485-494.

(16)   Kraemer, S.M.; Hering, J.G., Influence of solution saturation state on the kinetics of ligand-controlled dissolution of oxide phases. *Geochim. Cosmochim. Acta* **1997,** *61*, (14), 2855-2866.

(17)   Jafvert, C.T.; Valentine, R.L., Reaction scheme for the chlorination of ammoniacal water. *Environ. Sci. Technol.* **1992,** *26*, (3), 577-586.

(18)   American Public Health Association, A.W.W.A., Water Environment Federation, *Standard Methods for the Examination of Water and Wastewater*. Twentieth ed.; 1999.

(19)   Xie, Y.; Wang, Y.; Singhal, V.; Giammar, D.E., Effects of pH and carbonate concentration on dissolution rates of the lead corrosion product PbO_2 *Environ. Sci. Technol.* **2010,** *44*, (3), 1093-1099.

(20)   Schwarzenbach, R.P.; Gschwend, P.M.; Imboden, D.M., *Environmental Organic Chemistry*. John Wiley & Sons, Inc.: Hoboken, New Jersey, 2003.

(21)   Boyd, G.R.; Dewis, K.M.; Korshin, G.V.; Reiber, S.H.; Schock, M.R.; Sandvig, A.M.; Giani, R., Effects of changing disinfectants on lead and copper release. *J. Am. Water Works Assoc.* **2008,** *100*, (11), 75-87.

(22)   Vasquez, F.A.; Heaviside, R.; Tang, Z.J.; Taylor, J.S., Effect of free chlorine and chloramines on lead release in a distribution system. *J. Am. Water Works Assoc.* **2006,** *98*, (2), 144-154.

(23)   Rajasekharan, V.V.; Clark, B.N.; Boonsalee, S.; Switzer, J.A., Electrochemistry of free chlorine and monochloramine and its relevance to the presence of Pb in drinking water. *Environ. Sci. Technol.* **2007,** *41*, (12), 4252-4257.

(24)   Lin, Y.P.; Valentine, R.L., Reduction of lead oxide (PbO_2) and release of Pb(II) in mixtures of natural organic matter, free chlorine and monochloramine. *Environ. Sci. Technol.* **2009,** *43*, (10), 3872-3877.

(25)   Shi, Z.; Stone, A.T., PbO_2(s, Plattnerite) Reductive Dissolution by Aqueous Manganous and Ferrous Ions. *Environ. Sci. Technol.* **2009,** *43*, (10), 3596-3603.

(26)   Glasstone, S., Physical chemistry of the oxides of lead. Part V. The electromotive behaviour of lead dioxide. *Journal of the Chemical Society* **1922,** *122*, 1469-1480.
(27)   Lahoutifard, N.; Lagrange, P.; Lagrange, J., Kinetics and mechanism of nitrite oxidation by hypochlorous acid in the aqueous phase. *Chemosphere* **2003,** *50*, (10), 1349-1357.

Chapter 3. Supporting Information

Table 3-S1. Equilibrium constants for aqueous species

#	Reaction	Log K	Source
1	$H_2O \rightarrow H^+ + OH^-$	-13.998	MINEQL+
2	$CO_2(g) + H_2O \rightarrow H_2CO_3^*$	-1.459	MINEQL+
3	$H_2CO_3^* \rightarrow 2H^+ + CO_3^{2-}$	-16.68	MINEQL+
4	$HCO_3^- \rightarrow H^+ + CO_3^{2-}$	-10.33	MINEQL+
5	$Pb^{2+} + H_2O \rightarrow PbOH^+ + H^+$	-7.597	MINEQL+
6	$Pb^{2+} + 2H_2O \rightarrow Pb(OH)_2^0 + 2H^+$	-17.12	Benjamin
7	$Pb^{2+} + 3H_2O \rightarrow Pb(OH)_3^- + 3H^+$	-28.06	Benjamin
8	$Pb^{2+} + 4H_2O \rightarrow Pb(OH)_4^{2-} + 4H^+$	-39.70	Benjamin
9	$Pb^{2+} + CO_3^{2-} \rightarrow PbCO_3^0$	6.478	MINEQL+
10	$Pb^{2+} + 2CO_3^{2-} \rightarrow Pb(CO_3)_2^{2-}$	9.38	MINEQL+
11	$Pb^{2+} + CO_3^- + H^+ \rightarrow PbHCO_3^+$	13.20	MINEQL+
12	$2Pb^{2+} + 3H_2O \rightarrow Pb_2(OH)^{3+} + H^+$	-6.397	MINEQL+
13	$3Pb^{2+} + 4H_2O \rightarrow Pb_3(OH)_4^{2+} + 4H^+$	-23.888	MINEQL+
14	$4Pb^{2+} + 4H_2O \rightarrow Pb_4(OH)_4^{4+} + 4H^+$	-19.988	MINEQL+
15	$Pb^{4+} + 3H_2O \rightarrow PbO_3^{2-} + 6H^+$	-23.06	Pourbaix
16	$Pb^{4+} + 4H_2O \rightarrow PbO_4^{4-} + 8H^+$	-63.94	Pourbaix
17	$HOCl \rightarrow OCl^- + H^+$	-7.60	Benjamin
18	$HOCl + 2e^- + H^+ \rightarrow Cl^- + H_2O$	50.20	Benjamin
19	$Pb^{2+} \rightarrow Pb^{4+} + 2e^-$	-28.64	Benjamin
20	$O_{2(aq)} + 4H^+ + 4e^- \rightarrow 2H_2O$	86.00	Benjamin
21	$2H^+ + 2e^- \rightarrow H_{2(aq)}$	3.10	Benjamin
22	$NH_2Cl + 2e^- + 2H^+ \rightarrow Cl^- + NH_4^+$	47.46	Switzer
23	$NH_2Cl + H_2O + 2e^- \rightarrow Cl^- + OH^- + NH_3$	23.39	Switzer

Benjamin = (1)
MINEQL+ = *(2)*
Switzer = *(3)*
Pourbaix = *(4)*

Table 3-S2. Solubility products of selected lead solids

#	Solid	Reaction	Log K	Source
24	Massicot	$PbO_{(s)} + 2H^+ \rightarrow Pb^{2+} + H_2O$	12.91	MINEQL+
25	Litharge	$PbO_{(s)} + 2H^+ \rightarrow Pb^{2+} + H_2O$	12.72	MINEQL+
26	$Pb(OH)_{2(s)}$	$Pb(OH)_{2(s)} + 2H^+ \rightarrow Pb^{2+} + 2H_2O$	12.40	Stumm & Morgan
27	Cerussite	$PbCO_{3(s)} \rightarrow Pb^{2+} + CO_3^{2-}$	-13.13	Benjamin
28	Hydrocerussite	$Pb_3(CO_3)_2(OH)_{2(s)} + 2H^+ \rightarrow 3Pb^{2+} + 2CO_3^{2-} + 2H_2O$	-18.77	MINEQL+
29	$Pb_3(PO_4)_{2(s)}$	$Pb_3(PO_4)_{2(s)} \rightarrow 3Pb^{2+} + 2PO_4^{3-}$	-44.50	Benjamin
30	$PbHPO_{4(s)}$	$PbHPO_{4(s)} \rightarrow Pb^{2+} + PO_4^{3-} + H^+$	-37.80	MINEQL+
31	Hydroxyl-pyromorphite	$Pb_5(PO_4)_3OH_{(s)} + H^+ \rightarrow 5Pb^{2+} + 3PO_4^{3-} + H_2O$	-62.79	MINEQL+
32	Plattnerite	$PbO_{2\ (s)} + 4H^+ + 2e^- \rightarrow Pb^{2+} + 2H_2O$	49.60	MINEQL+
33	PbO_2	$Pb(IV)O_{2(s)} + 4H^+ \rightarrow Pb^{4+} + 2H_2O$	-8.26	Pourbaix

Benjamin = (1); MINEQL+ = (2); Stumm & Morgan = (5); Pourbaix = (4)

Table 3-S3. Chemical potentials of various solids and aqueous species.

Species	$G^0_{f,i}$ (J/mol)	Source
$Pb_3O_{4(s)}$	-601,200	Benjamin
$Pb_2O_{3(s)}$	-411,769	Pourbaix
$PbO_{2(s)}$	-218,987	Pourbaix
Pb^{2+}	-24,309	Pourbaix
$HPbO_2^-$	-338,898	Pourbaix
Pb^{4+}	302,498	Pourbaix
PbO_3^{2-}	-277,562	Pourbaix
PbO_4^{4-}	-282,084	Pourbaix
H^+	0.00	Benjamin
OH^-	-157,300	Benjamin
H_2O	-237,180	Benjamin

Benjamin = (1)
Pourbaix = (4)
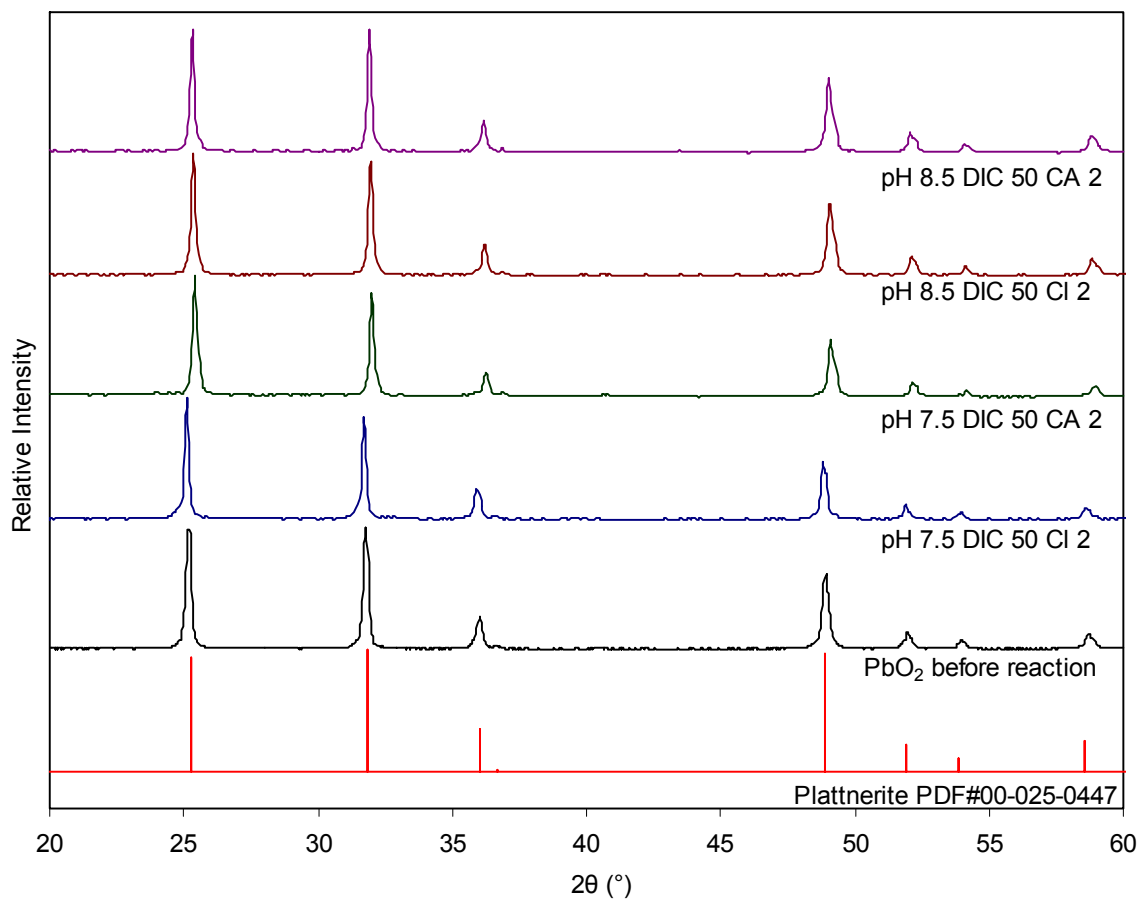
Figure 3-S1. X-ray diffraction (XRD) pattern of plattnerite before and after reactions for selected experiments. (The reference pattern PDF# 00-025-047). Cl denotes experiments in the presence of free chlorine, while CA represents experiments with monochloramine.
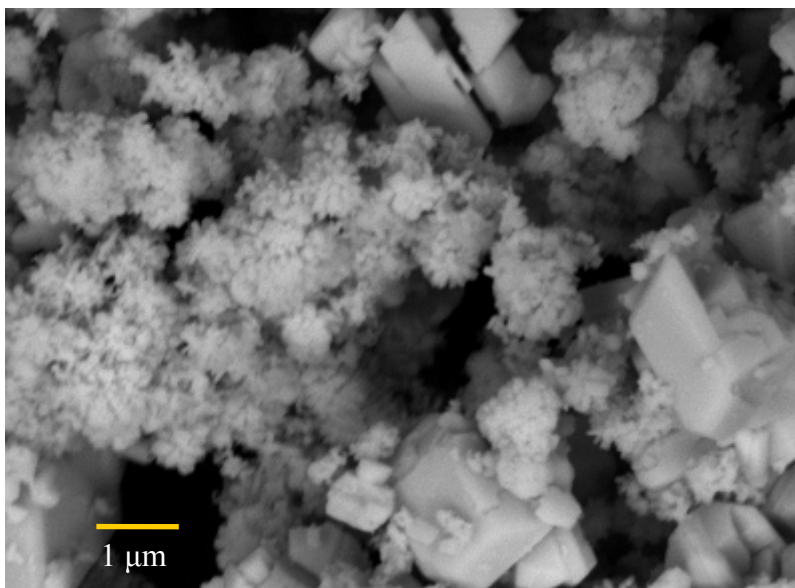
Figure 3-S2. Scanning electron micrograph of plattnerite used in experiments.

Literature Cited:

1.   Benjamin, M. M., *Water Chemistry*. 1st ed.; McGraw-Hill: New York, NY, 2002.
2.   Schecher, W. D.; McAvoy, D. C., *MINEQL+: A chemical equilibrium modeling system, version 4.5*. Environmental Research Software: Hallowell, ME, 1998.
3.   Switzer, J. A.; Rajasekharan, V. V.; Boonsalee, S.; Kulp, E. A.; Bohannan, E. W., Evidence that monochloramine disinfectant could lead to elevated Pb levels in drinking water. *Environ. Sci. Technol.* **2006,** *40*, (10), 3384-3387.
4.   Pourbaix, M., *Atlas of Electrochemical Equilibrium in Aqueous Solutions*. Second ed.; National Association of Corrosion Engineers: Houston, TX, 1974.
5.   Stumm, W.; Morgan, J. J., *Aquatic chemistry*. Third ed.; John Wiley & Sons, Inc.: New York, NY, 1996; p 1022.

Chapter 4.   Effects of orthophosphate on PbO$_2$ dissolution rates

Results of this Chapter will be submitted to *Water Research*

Abstract

Plattnerite is a corrosion product that develops on lead pipes that have been in contact with free chlorine present as a residual disinfectant. The dissolution of plattnerite may control the dissolved lead concentration in tap water. Orthophosphate has been used as a lead corrosion inhibitor in many U.S. utilities. In this study the effects of phosphate on the dissolution rates of plattnerite were quantified in completely-mixed continuous-flow reactors at relevant pH, chloramines, and dissolved inorganic carbon conditions. Phosphate decreased the release of lead from the dissolution of plattnerite by the formation of hydroxylpyromorphite ($Pb_5(PO_4)_3OH$). At selected conditions, the rate of plattnerite dissolution was also inhibited by phosphate adsorption to PbO_2.

Keywords: orthophosphate corrosion inhibitor, PbO_2 dissolution, lead corrosion, distribution system

4.1. Introduction

Motivated by concerns about the adverse health effects of lead, the Lead and Copper Rule (LCR) was passed in 1991 and set an action level of 15 µg/L for lead in drinking water (U.S.EPA 1991). If 10% of the tested homes have lead concentrations above the action level, then the system must undertake efforts to control corrosion and inform the public.

Release of lead from corrosion products that develop on plumbing materials can cause elevated lead concentrations in tap water. Lead corrosion products include lead(II) carbonates, lead(II) oxides, and lead(IV) oxides (PbO_2). Both plattnerite (β-PbO_2) and scrutinyite (α-PbO_2) have been observed in distribution systems that used free chlorine as disinfectants (Schock and Giani 2004). The switch of residual disinfectant from free chlorine to chloramines in November 2000 enhanced reductive dissolution of PbO_2 and caused tap water lead concentrations as high as 48000 µg/L in Washington, DC from 2001 to 2004 (Edwards and Dudi 2004; Schock and Giani 2004). Elevated blood levels in young children were correlated with the elevated tap water lead concentrations during the Washington, DC lead incident (Edwards et al. 2009).

Orthophosphate addition is an established corrosion control strategy that has been effective in mitigating lead concentrations in Washington, DC. (Schock 1999; U.S.EPA 2007). The effect of orthorphosphate is attributed to the precipitation of low solubility lead phosphate solids such as hydroxylpyromorphite ($Pb_5(PO_4)_3OH$) (Edwards and McNeill 2002; Nadagouda et al. 2009). Hydroxylpyromorphite has been found as a corrosion product in actual distribution systems and in laboratory experiments with lead

compounds in the presence of phosphate (Lytle et al. 2009; Noel and Giammar 2008; Schock et al. 2006).

Recent investigations of PbO_2 dissolution have all been batch studies (Lin and Valentine 2008a; b; 2010; Shi and Stone 2009a; b). While batch studies are useful for determining effects of water chemistry on PbO_2 dissolution, they are not ideal for quantifying dissolution rates because they are sensitive to the initial environment and are affected by accumulation of reaction products. Dissolution rates are valuable for predicting lead concentrations when equilibrium is not reached, as can occur in plumbing with intermittent periods of flow. Since more than 5 days can be required for the reductive dissolution of PbO_2 to reach equilibrium (Xie et al. 2010), tap water lead concentrations are unlikely to be at equilibrium with PbO_2. The objectives of this study were to quantify the effect of phosphate on the dissolution rate of plattnerite and to identify potential mechanisms for any observed effects.

4.2. Materials and Methods

4.2.1. Materials

PbO_2 (Fisher Scientific) with primary particle sizes of 50 to 500 nm was identified as pure plattnerite (β-PbO_2) by X-Ray diffraction (XRD) (Xie et al. 2010). Its specific surface area was 3.6 m^2/g based on the BET N_2-adsorption isotherm. A phosphate stock solution was prepared from NaH_2PO_4. DIC was provided by the addition of $NaHCO_3$. Chloramine solutions were prepared by mixing volumes of 6% (w/w) NaOCl and 0.15 M NH_4Cl solutions in ultrapure water to achieve a 0.79 Cl_2:N molar ratio (4:1 Cl_2:N mass ratio), which is in the range used in drinking water

distribution (Jafvert and Valentine 1992). Under these conditions the dominant form of chloramine is monochloramine (NH$_2$Cl). All solutions were prepared from reagent grade chemicals and ultrapure water (Milli-Q water, >18.2 MΩ-cm resistivity, Millipore Corp., Milford, MA).

4.2.2. Analysis Methods

XRD was performed on a Rigaku Geigerflex D-MAX/A diffractometer using Cu-Kα radiation. The instrument has a vertical goniometer and a scintillation counter. A JEOL 7001LVF field emission scanning electron microscope (SEM) was used to characterize the morphology and composition of the solids before and after reaction. Dissolved lead concentrations were determined by inductively coupled plasma mass spectroscopy (ICP-MS) (Agilent 7500ce). Solution pH was measured with a glass pH electrode and pH meter (Accumet). Free chlorine and chloramine concentrations were measured using the standard DPD colorimetric method (4500-Cl Chlorine G) with a spectrophotometer (Perkin-Elmer Lambda 2S) (American Public Health Association 1999).

4.2.3. Measurement of Dissolution Rates

Plattnerite dissolution rates were quantified using 84 mL continuously stirred flow-through reactors that were loaded with 1 g/L plattnerite and had 30 min hydraulic residence times. Details of reactor operation have been described previously (Xie et al. 2010). The influent compositions were controlled to evaluate the effects of

orthophosphate and chloramines on plattnerite dissolution rates at environmentally relevant pH and dissolved inorganic carbon (DIC) conditions. A series of eight compositions all containing 50 mg/L DIC were studied. The eight compositions examined two pH values (7.5 and 8.5), the presence or absence of 2 mg/L as Cl_2 monochloramine, and the presence or absence of 1 mg/L as P orthophosphate. Each experimental condition was run in duplicate or triplicate reactors with a procedural blank that consisted of a solid-free reactor. Supplementary experiments in the absence of DIC were also conducted. Effluent samples were collected, preserved by acidification to 2% HNO_3, and analyzed for dissolved lead by ICP-MS. Flow rate and pH were periodically measured throughout each experiment.

The reactor influents were prepared in 10 L plastic (Tedlar) bags to avoid transfer of CO_2 into or out of solution. Ultrapure water was purged with nitrogen immediately before being pumped into the bags. The influent pH was adjusted by the addition of NaOH or HNO_3. Chloramine solutions were prepared immediately before each dissolution experiment. Solutions that contained chloramines were shielded from light by alumnium foil to minimize the decomposition of chloramines. An aliquot of 1.0 M $NaNO_3$ solution was injected to set the ionic strength at 0.01 M.

Dissolution rates were determined by operating the flow-through reactors for durations equivalent to 48 or more hydraulic residence times (24 hours). By continuously flushing the products of dissolution from the reactor, the effluent dissolved lead concentration approaches a steady-state concentration that is controlled by the rate of dissolution of the solid phase (Xie et al. 2010). This approach is different from batch experiments in which the dissolved concentrations increase until they reach equilibrium

solubility; the accumulation of reaction products and the presence of initial labile phases

in batch experiments can complicate the quantification of rates. After the 24-hour period

of flow, each reactor remained sealed and stirred with no flow for another 24 hours. At

the conclusion of this batch mode, the pH and concentrations of dissolved lead,

orthophosphate, and monochloramine were measured. The solids remaining at the end of

each experiment were characterized by XRD and SEM.

For a flow-through reactor the dissolution rate can be quantified by Equation 4.1,

$$Rate = \frac{C_{ss}}{t_{res} \cdot [solid] \cdot A}$$

(4.1)

where *Rate* is the dissolution rate (mol/m^2-min); C_{ss} is the steady-state effluent lead

concentration (mol/L); t_{res} is the hydraulic residence time (min); *[solid]* is the solid

concentration in the reactor (g/L); and *A* is the specific surface area of the solid (m^2/g).

No lead was added to the influent, and samples of the influent had lead concentrations

below the detection limit (30 ng/L). The steady-state effluent concentration was

determined as the average of the effluent concentrations for at least 5 samples that did not

vary by more than 30% and spanned at least 5 residence times.

For comparison with experimentally measured dissolved lead concentrations, the

equilibrium solubility of plattnerite and hydroxylpyromorphite were calculated.

Calculations were performed with MINEQL+ (version 4.5) (Schecher and McAvoy

1998a). The reactions considered and their equilibrium constants are given in the

Appendix.

4.3. Results and Discussion

4.3.1 Effect of Phosphate on Plattnerite Dissolution

At almost all conditions studied, the addition of 1 mg P/L ($3.2 \cdot 10^{-5}$ M) phosphate inhibited plattnerite dissolution (Figure 4.1). The effect was most pronounced at pH 8.5 without chloramine and at pH 7.5 with chloramine. Dissolution rates for a given condition were almost always higher at pH 7.5 than 8.5, which is consistent with previous studies (Xie et al. 2010). When both phosphate and chloramines were present, the rates at pH 7.5 and 8.5 were very similar. Dissolution rates were also consistently lower in the presence of chloramine than in the absence of chloramine, although not significantly lower when both phosphate and chloramine were present. The inhibition of dissolution
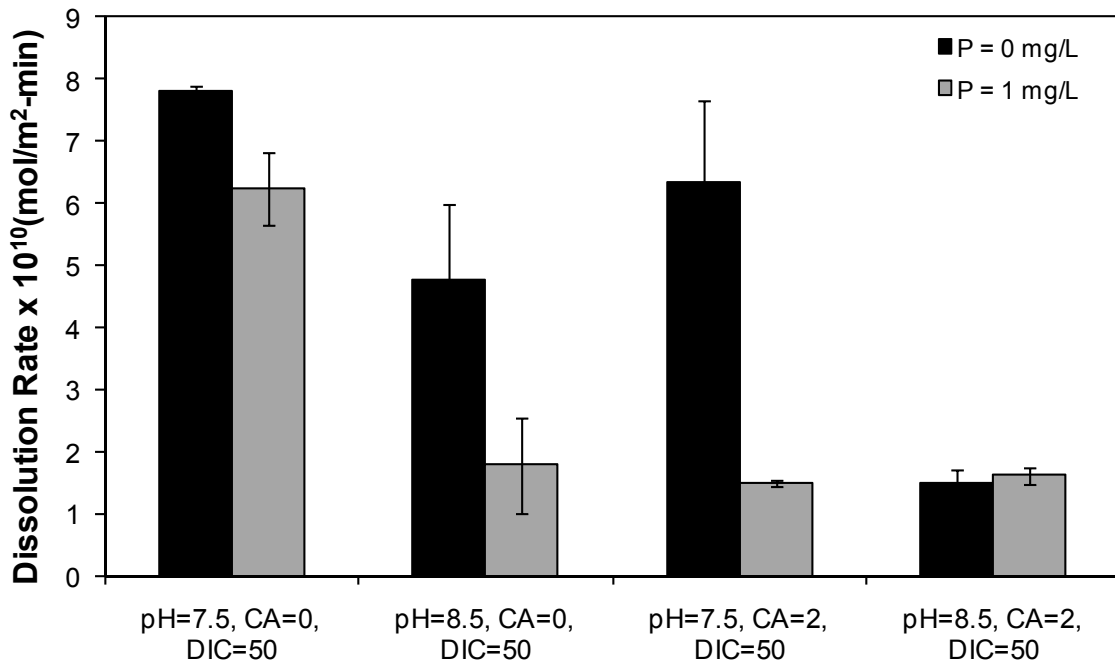
Figure 4.1. Effect of phosphate on dissolution rates of plattnerite. Conditions are listed on the x-axis with CA denoting the monochloramine concentration in mg/L as Cl_2 and DIC denoting the dissolved inorganic carbon concentration in mg C/L. Error bars represent one standard deviation. The pH indicated was the target pH of the influents, and the actual steady-state effluent pH values were within $\pm$ 0.22 pH units of the target value.

by monochloramine relative to no disinfectant at short residence time was caused by the elevated redox potential, which has been observed in Chapter 3. At long residence times, an intermediate species from monochloramine decay would reduce PbO_2 and enhance dissolution (Lin and Valentine 2008b).

The conditions and results of all dissolution experiments are summarized in Table 4.1. Replicate experiments conducted at each condition were generally in agreement; the largest differences among replicates were for the lowest overall lead concentrations, which were near the limit of quantification for lead. In the presence of DIC, the weighted averages of the pH (variation < 0.25 pH units) over the steady-state period used for rate calculations were within 0.22 pH units of the target value. In the absence of DIC, the pH varied up to 0.5 pH units over the assigned steady-state period and caused significant upward or downward trends of effluent lead concentrations for some conditions. The deviation of the weighted averages of the pH from the target value was also larger in the absence of DIC than in the presence of DIC. Due to the variation in pH, the effluent lead concentrations were variable and the reactors may not have reached steady state. Consequently, the results from experiments in the absence of DIC were not used to examine the impact of phosphate on rates.

Table 4.1. Conditions and results of plattnerite dissolution experiments

Experiment ID	pH	DIC (mg/L as C)	Orthophosphate (mg/L as P)	Chloramine (mg/L as Cl₂)	Measured pH†	Steady-State Effluent Lead (nM)	Equilibrium Lead (nM)‡	Net Lead Release Rate x 10^{10} (mol/min·m²)
			Influent Composition					
1A	7.5	50.0	0.0	0.0	7.62	83.8	23442	7.87
1B	7.5	50.0	0.0	0.0	7.68	82.7	23442	7.77
2A	8.5	50.0	0.0	0.0	8.36	41.5	2344	3.90
2B	8.5	50.0	0.0	0.0	8.42	59.9	2344	5.63
3A	7.5	50.0	1.0	0.0	7.72	70.9	23442	6.65
3B	7.5	50.0	1.0	0.0	7.70	62.1	23442	5.83
4A	8.5	50.0	1.0	0.0	8.50	24.7	2344	2.32
4B	8.5	50.0	1.0	0.0	8.55	13.1	2344	1.23
5A	7.5	50.0	0.0	2.0	7.30	77.5	NC	7.28
5B	7.5	50.0	0.0	2.0	7.58	57.2	NC	5.37
6A	8.5	50.0	0.0	2.0	8.53	14.0	NC	1.32
6B	8.5	50.0	0.0	2.0	8.52	17.6	NC	1.65
7A	7.5	50.0	1.0	2.0	7.66	16.4	NC	1.54
7B	7.5	50.0	1.0	2.0	7.65	15.4	NC	1.45
8A	8.5	50.0	1.0	2.0	8.52	16.2	NC	1.52
8B	8.5	50.0	1.0	2.0	8.53	18.2	NC	1.71
9A	7.5	0.0	0.0	0.0	7.58	2.0	2630	0.19
9B	7.5	0.0	0.0	0.0	7.52	11.6	2630	1.09
10A	8.5	0.0	0.0	0.0	8.57	5.7	123	0.53
10B	8.5	0.0	0.0	0.0	8.58	1.1	123	0.10
11A	7.5	0.0	1.0	0.0	7.20	17.2	2630	1.62
11B	7.5	0.0	1.0	0.0	7.11	31.2	2630	2.93
12A	8.5	0.0	1.0	0.0	8.68	8.4	123	0.78
12B	8.5	0.0	1.0	0.0	8.34	8.1	123	0.76
12A	7.5	0.0	0.0	2.0	7.30	36.9	NC	3.46
12B	7.5	0.0	0.0	2.0	7.58	8.5	NC	0.79
13A	8.5	0.0	0.0	2.0	8.85	1.4	NC	0.13
13B	8.5	0.0	0.0	2.0	8.69	1.6	NC	0.15
14A	7.5	0.0	1.0	2.0	7.42	15.5	NC	1.45
14B	7.5	0.0	1.0	2.0	7.45	14.6	NC	1.37
14C	7.5	0.0	1.0	2.0	7.64	15.4	NC	1.45
15A	8.5	0.0	1.0	2.0	8.44	8.3	NC	0.78
15B	8.5	0.0	1.0	2.0	8.07	7.8	NC	0.73

†The weighted average of the effluent pH during the steady-state period is indicated.

‡ Equilibrium lead concentrations were calculated using MINEQL+ software. NC = Not Calculated. Equilibrium lead concentrations were not calculated for influents containing chloramines because of the uncertainty of the equilibrium constants for the associated reactions.

4.3.2 Equilibrium versus kinetic control of dissolved lead concentrations

The O_2/H_2O couple controls the oxidation reduction potential (ORP) of the PbO_2 dissolution reaction in the absence of chloramines. The relevant half reactions are:

$$PbO_{2(s)} + 4H^+ + 2e^- = Pb^{2+} + 2H_2O \quad \log K_1 = 49.60 \quad E_H^0 = 1.46 \text{ V} \quad (4.2)$$

$$O_{2(aq)} + 4H^+ + 4e^- = 2H_2O \quad \log K_2 = 86.00 \quad E_H^0 = 1.27 \text{ V} \quad (4.3)$$

Therefore, the overall reaction and equilibrium constant are

$$2H^+ + PbO_{2(s)} = Pb^{2+} + \tfrac{1}{2} O_{2(aq)} + H_2O \quad \log K = 6.60 \quad (4.4)$$
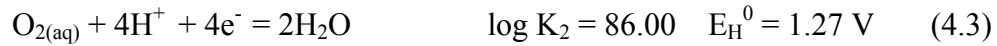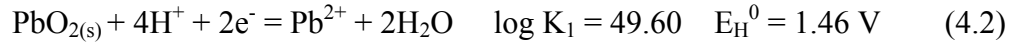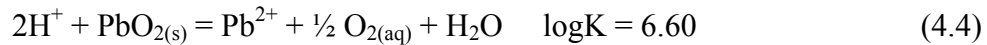
$$K = \frac{\{Pb^{2+}\}\{O_2\}^{1/2}}{\{H^+\}^2} = 10^{6.60} \quad (4.5)$$

The Pb^{2+} activity in equilibrium with plattnerite was calculated using Equation 4.5 assuming 0.001 atm P_{O_2} (1.26 µmol/L dissolved oxygen). The solution was purged with nitrogen immediately before it was pumped into the plastic bags, which should have decreased the dissolved oxygen concentration to below 1.26 µmol/L. Therefore, the equilibrium dissolved Pb(II) concentration calculated for P_{O_2} of 0.001 atm represents a lower bound. The reductive dissolution of PbO_2 produces O_2, but the highest O_2 concentration that could be generated from the dissolution reaction at steady state was 0.042 µmol/L. The solution was so dilute that activity coefficients of solutes can be approximated as 1 and the values of solute activities are equal to their molar concentrations. Based on the reactions in the Appendix, the dissolved Pb(IV) concentration is negligible compared to that of the dissolved Pb(II) species. The equilibrium dissolved Pb(II) concentration is the sum of all dissolved Pb(II) species concentrations, which were calculated from the reactions and equilibrium constants in the Appendix.

The steady-state effluent lead concentrations were about two orders of magnitude lower than the predicted equilibrium lead concentrations for plattnerite solubility (Figure 4.2). The equilibrium solubility of hydroxylpyromorphite, which could have formed in the presence of phosphate, is lower than that of plattnerite at both pH 7.5 and 8.5. At
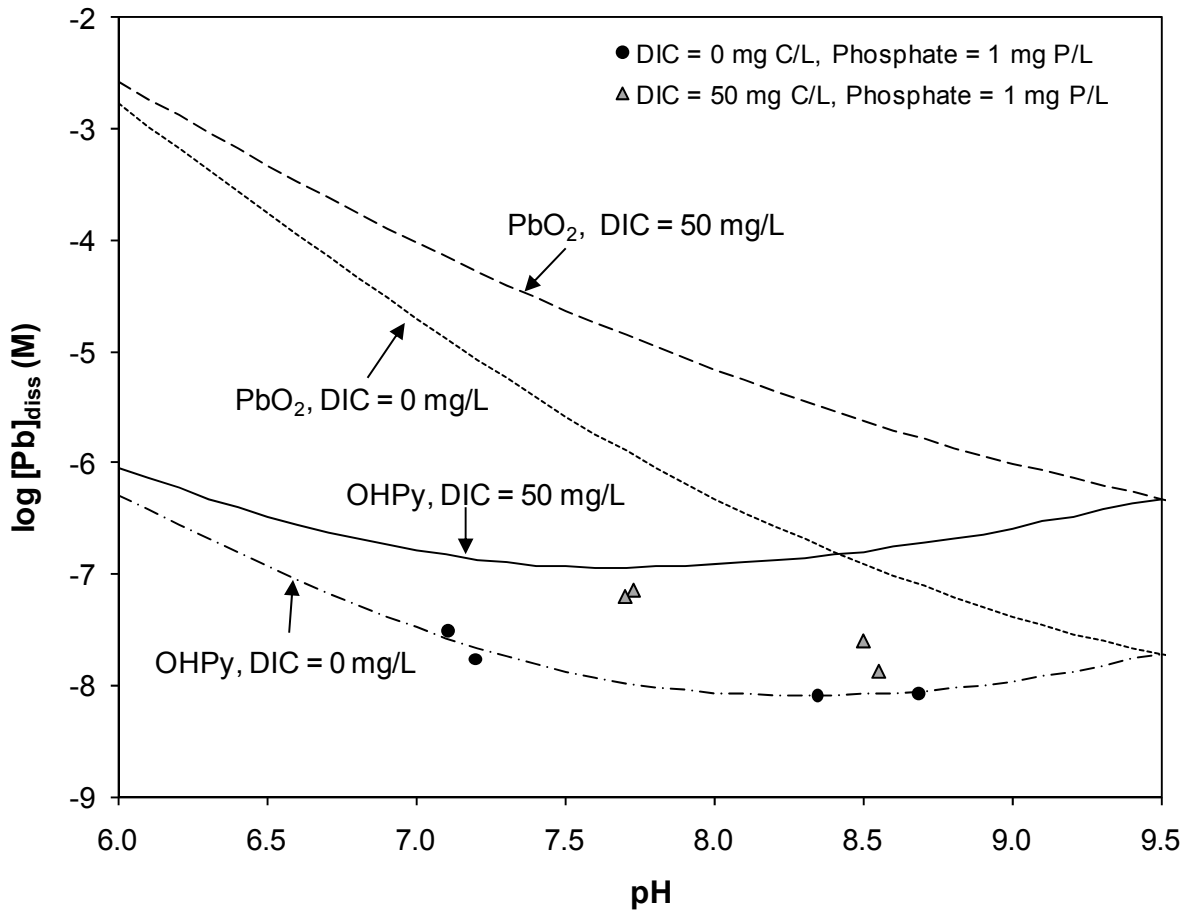
Figure 4.2. Steady-state and predicted equilibrium concentrations for plattnerite dissolution in the presence of 1 mg P/L phosphate. Calculations are made for an assumption of equilibrium with 0.001 atm O_2. Lines indicate the predicted equilibrium concentration as controlled by the solubility of plattnerite (β-PbO_2) or hydroxylpyromorphite (denoted as OHPy). Points identify the steady-state effluent lead concentrations at specific water chemistry conditions.

conditions with 1 mg P/L phosphate and in the absence of DIC, the final effluent

concentrations during plattnerite dissolution were similar to the calculated equilibrium

solubility of hydroxylpyromorphite, which suggests that hydroxylpyromorphite had

precipitated. Hydroxylpyromorphite would form by taking up lead released during

93

plattnerite dissolution. SEM showed the growth of small rod-shaped particles on the

tetragonal plattnerite particles (Figure 4.3a) after 24 hours of reaction in the absence of

DIC (Figure 4.3c); the sizes and shapes of these particles are consistent with

hydroxylpyromorphite (Figure 4.3b). Lytle and co-workers observed similar
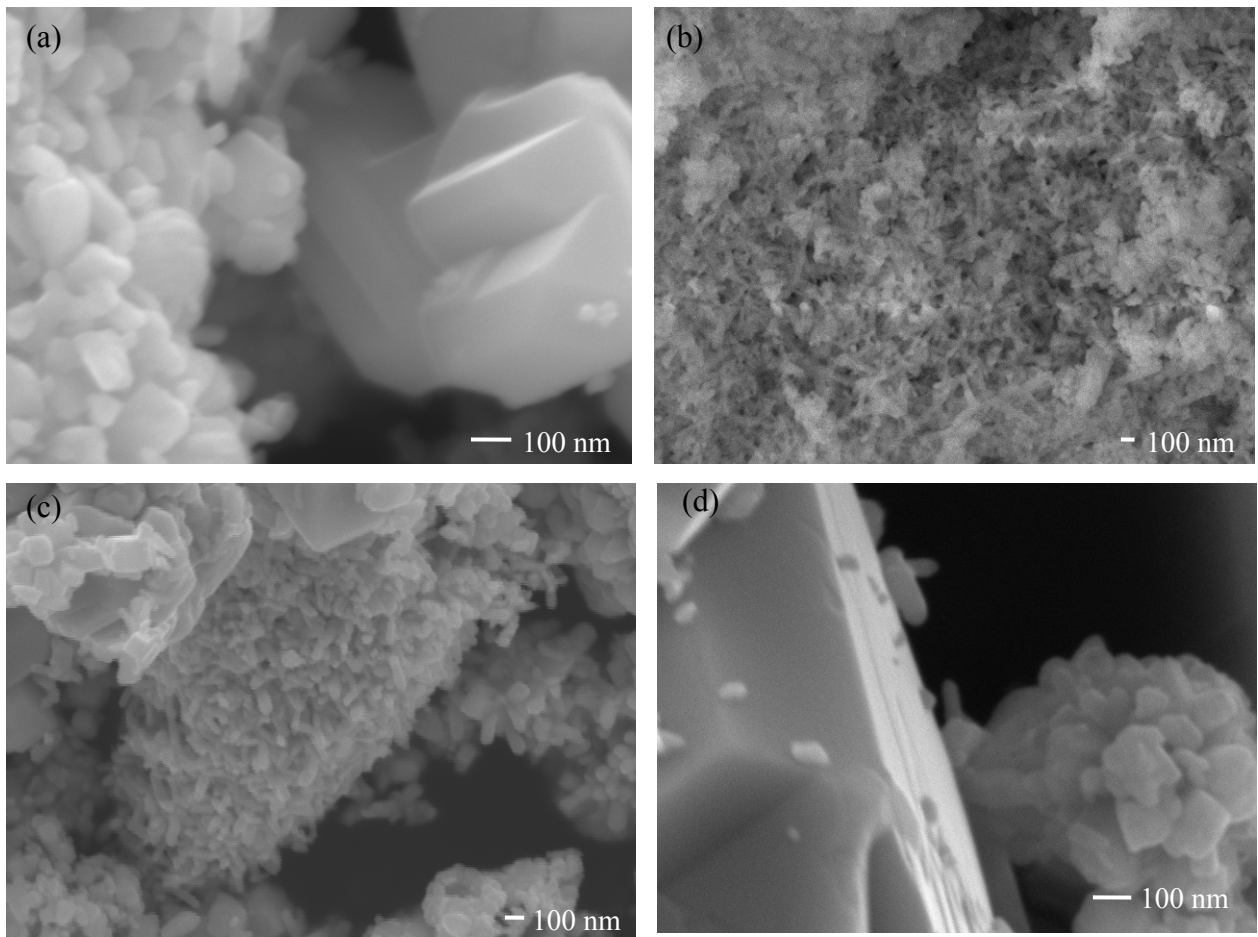
Figure 4.3. SEM images of (a) plattnerite before reaction, (b) hydroxylpyromorphite, (c) solids after reaction at pH 7.5, 0 mg C/L DIC, 1 mg P/L phosphate, and 2 mg-Cl$_2$/L monochloramine, and (d) solids after reaction at pH 8.5, 50 mg C/L DIC, 1 mg P/L orthophosphate, and 2 mg-Cl$_2$/L monochloramine

pyromorphite particles (< 50 nm) in the reaction of PbCl$_2$ solution with dissolved

phosphate (Lytle et al. 2009). Although X-ray diffraction analysis could not detect

hydroxylpyromorphite in these samples (Figure 4.4), the dissolution rates of plattnerite

were too small to generate sufficient lead(II) for the precipitation of

hydroxylpyromorphite amounts (< 0.17% of total lead by mass) that would be detectable by XRD.
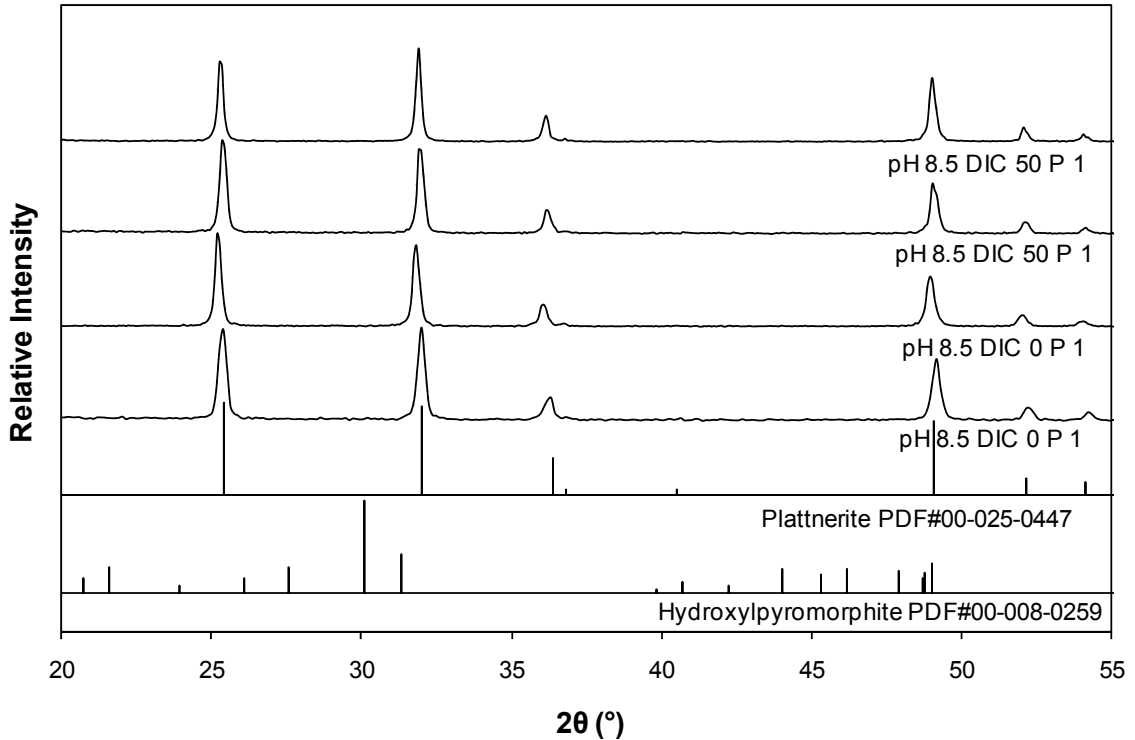
Figure 4.4. XRD of solids before and after reaction in the presence of orthophosphate for selected conditions. Reference patterns for plattnerite (PDF# 01-071-4820) and hydroxylpyromorphite (PDF# 00-008-0259) are included.

The equilibrium solubility of plattnerite and hydroxylpyromorphite are both higher in the presence of DIC due to the formation of lead carbonate complexes. At conditions with 1 mg P/L phosphate and 50 mg C/L DIC, the steady-state concentrations did not reach the equilibrium concentrations of hydroxylpyromorphite (Figure 4.2) but phosphate still lowered the dissolution rates. No secondary phases were observed following the reaction of plattnerite with phosphate in the presence of DIC (Figure 4.3d), which is consistent with the lead concentrations being undersaturated with respect to hydroxylpyromorphite (Figure 4.2). Phosphate could still inhibit dissolution of

plattnerite by adsorbing to the plattnerite surface and blocking access of a reductant or of a carbonate ion needed to extract Pb(II) from surface. Phosphate adsorption has also been shown to inhibit the dissolution of other metal oxides. Adsorption to block a reductant may explain the inhibition of plattnerite dissolution by phosphate in the presence of hydroquinone (Shi and Stone 2009a). Adsorbed phosphate present as binuclear surface complexes is particularly good at inhibiting both the reductive and nonreductive dissolution of iron(III) oxides (Bondietti et al. 1993; Stumm 1997).

Overall, there are two mechanisms through which phosphate can inhibit the reductive dissolution of PbO_2 (Figure 4.5). Dissolution of PbO_2 involves the reduction of Pb(IV) to Pb(II) at the surface of the solid followed by the release of Pb(II) to solution. In the presence of phosphate and in the absence of DIC, the formation of the lead(II) phosphate hydroxylpyromorphite limited lead release to solution (Mechanism A). With both phosphate and DIC present, the inhibition of plattnerite dissolution was probably caused by the adsorption of phosphate to the plattnerite surface to block sites of reduction or dissolution (Mechanism B).
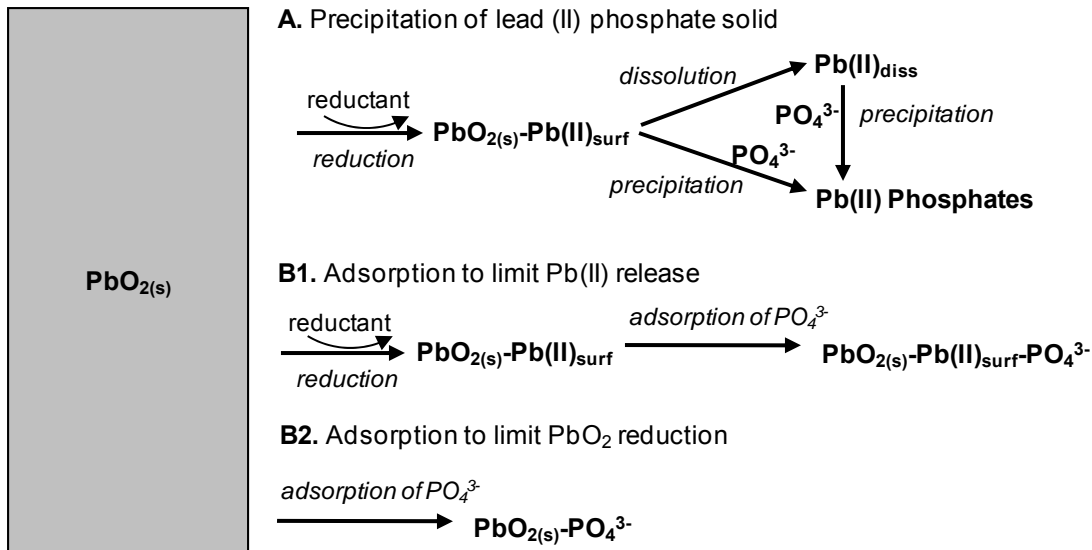
Figure 4.5. Conceptual model of PbO$_2$ dissolution showing different possible mechanisms and the potential role of phosphate.

4.4.   Conclusions

Phosphate has been an effective lead corrosion inhibitor in water distribution systems. The addition of phosphate significantly decreased the net rate of lead release from plattnerite by mechanisms of (a) precipitation of hydroxylpyromorphite and (b) adsorption to the plattnerite surface to block dissolution sites. As little as 1 mg P/L phosphate was needed to significantly inhibit plattnerite dissolution. Minimum effective doses may be even lower, and finding the optimal minimum dose can lower costs, reduce biofilm growth in distribution systems, and minimize needs for phosphate removal in wastewater treatment. Because it acts at the surface, phosphate addition could be beneficial even when PbO$_2$ is still the major component (by mass) of the materials of a pipe scale. When considering phosphate addition, the full water composition should be considered. The pH is still very important in controlling the lead concentration even

when phosphate is added. If the pH decreases along with the addition of phosphate, then a higher lead release rate may result.

Acknowledgements

Appendix

Table A-1. Equilibrium constants for aqueous species

#	Reaction	Log K	Source
1	$H_2O \rightarrow H^+ + OH^-$	-13.998	MINEQL+
2	$CO_2(g) + H_2O \rightarrow H_2CO_3^*$	-1.459	MINEQL+
3	$H_2CO_3^* \rightarrow 2H^+ + CO_3^{2-}$	-16.68	MINEQL+
4	$HCO_3^- \rightarrow H^+ + CO_3^{2-}$	-10.33	MINEQL+
5	$Pb^{2+} + H_2O \rightarrow PbOH^+ + H^+$	-7.597	MINEQL+
6	$Pb^{2+} + 2H_2O \rightarrow Pb(OH)_2^0 + 2H^+$	-17.12	Benjamin
7	$Pb^{2+} + 3H_2O \rightarrow Pb(OH)_3^- + 3H^+$	-28.06	Benjamin

8	$Pb^{2+} + 4H_2O \rightarrow Pb(OH)_4{}^{2-} + 4H^+$	-39.70	Benjamin
9	$Pb^{2+} + CO_3{}^{2-} \rightarrow PbCO_3{}^0$	6.478	MINEQL+
10	$Pb^{2+} + 2CO_3{}^{2-} \rightarrow Pb(CO_3)_2{}^{2-}$	9.38	MINEQL+
11	$Pb^{2+} + CO_3{}^- + H^+ \rightarrow PbHCO_3{}^+$	13.20	MINEQL+
12	$2Pb^{2+} + 3H_2O \rightarrow Pb_2(OH)^{3+} + H^+$	-6.397	MINEQL+
13	$3Pb^{2+} + 4H_2O \rightarrow Pb_3(OH)_4{}^{2+} + 4H^+$	-23.888	MINEQL+
14	$4Pb^{2+} + 4H_2O \rightarrow Pb_4(OH)_4{}^{4+} + 4H^+$	-19.988	MINEQL+
15	$Pb^{4+} + 3H_2O \rightarrow PbO_3{}^{2-} + 6H^+$	-23.06	Pourbaix
16	$Pb^{4+} + 4H_2O \rightarrow PbO_4{}^{4-} + 8H^+$	-63.94	Pourbaix
17	$HOCl \rightarrow OCl^- + H^+$	-7.60	Benjamin
18	$HOCl + 2e^- + H^+ \rightarrow Cl^- + H_2O$	50.20	Benjamin
19	$Pb^{2+} \rightarrow Pb^{4+} + 2e^-$	-28.64	Benjamin
20	$O_{2(aq)} + 4H^+ + 4e^- \rightarrow 2H_2O$	86.00	Benjamin
21	$2H^+ + 2e^- \rightarrow H_{2(aq)}$	3.10	Benjamin
22	$NH_2Cl + 2e^- + 2H^+ \rightarrow Cl^- + NH_4{}^+$	47.46	Switzer
23	$NH_2Cl + H_2O + 2e^- \rightarrow Cl^- + OH^- + NH_3$	23.39	Switzer

Benjamin = (Benjamin 2002)
MINEQL+ = (Schecher and McAvoy 1998b)
Switzer = (Switzer et al. 2006)
Pourbaix = (Pourbaix 1974)

Table A-2. Solubility products of selected lead solids

#	Solid	Reaction	Log K	Source
24	Massicot	$PbO_{(s)} + 2H^+ \rightarrow Pb^{2+} + H_2O$	12.91	MINEQL+
25	Litharge	$PbO_{(s)} + 2H^+ \rightarrow Pb^{2+} + H_2O$	12.72	MINEQL+
26	$Pb(OH)_{2(s)}$	$Pb(OH)_{2(s)} + 2H^+ \rightarrow Pb^{2+} + 2H_2O$	12.40	Stumm & Morgan
27	Cerussite	$PbCO_{3(s)} \rightarrow Pb^{2+} + CO_3{}^{2-}$	-13.13	Benjamin
28	Hydrocerussite	$Pb_3(CO_3)_2(OH)_{2(s)} + 2H^+ \rightarrow 3Pb^{2+} + 2CO_3{}^{2-} + 2H_2O$	-18.77	MINEQL+
29	$Pb_3(PO_4)_{2(s)}$	$Pb_3(PO_4)_{2(s)} \rightarrow 3Pb^{2+} + 2PO_4{}^{3-}$	-44.50	Benjamin
30	$PbHPO_{4(s)}$	$PbHPO_{4(s)} \rightarrow Pb^{2+} + PO_4{}^{3-} + H^+$	-37.80	MINEQL+

31	Hydroxyl-pyromorphite	$Pb_5(PO_4)_3OH_{(s)} + H^+ \rightarrow 5Pb^{2+} + 3PO_4^{3-} + H_2O$	-62.79	MINEQL+
32	Plattnerite	$PbO_{2\ (s)} + 4H^+ + 2e^- \rightarrow Pb^{2+} + 2H_2O$	49.60	MINEQL+
33	PbO_2	$Pb(IV)O_{2(s)} + 4H^+ \rightarrow Pb^{4+} + 2H_2O$	-8.26	Pourbaix

Benjamin = (Benjamin 2002); MINEQL+ = (Schecher and McAvoy 1998b); Stumm & Morgan = (Stumm and Morgan 1996); Pourbaix = (Pourbaix 1974)

References:

American Public Health Association, A.W.W.A., Water Environment Federation (1999) Standard Methods for the Examination of Water and Wastewater.

Benjamin, M.M. (2002) Water Chemistry, McGraw-Hill, New York, NY.

Bondietti, G., Sinniger, J. and Stumm, W. (1993) The Reactivity of Fe(Iii) (Hydr)Oxides - Effects of Ligands in Inhibiting the Dissolution. Colloids and Surfaces a-Physicochemical and Engineering Aspects 79(2-3), 157-167.

Edwards, M. and Dudi, A. (2004) Role of chlorine and chloramine in corrosion of lead-bearing plumbing materials. Journal American Water Works Association 96(10), 69-81.

Edwards, M. and McNeill, L.S. (2002) Effect of phosphate inhibitors on lead release from pipes. Journal American Water Works Association 94(1), 79-90.

Edwards, M., Triantafyllidou, S. and Best, D. (2009) Elevated blood lead in young children due to lead-contaminated drinking water: Washington, DC, 2001-2004. Environmental Science & Technology 43(5), 1618-1623.

Jafvert, C.T. and Valentine, R.L. (1992) Reaction scheme for the chlorination of ammoniacal water. Environmental Science & Technology 26(3), 577-586.

Lin, Y.P. and Valentine, R.L. (2008a) The release of lead from the reduction of lead oxide (PbO_2) by natural organic matter. Environmental Science & Technology 42(3), 760-765.

Lin, Y.P. and Valentine, R.L. (2008b) Release of Pb(II) from monochloramine-mediated reduction of lead oxide (PbO_2). Environmental Science & Technology 42(24), 9137-9143.
Lin, Y.P. and Valentine, R.L. (2010) Reductive Dissolution of Lead Dioxide (PbO_2) in Acidic Bromide Solution. Environmental Science & Technology 44(10), 3895-3900.

Lytle, D.A., Schock, M.R. and Scheckel, K. (2009) The Inhibition of Pb(IV) Oxide Formation in Chlorinated Water by Orthophosphate. Environmental Science & Technology 43(17), 6624-6631.

Nadagouda, M.N., Schock, M., Metz, D.H., DeSantis, M.K., Lytle, D. and Welch, M. (2009) Effect of Phosphate Inhibitors on the Formation of Lead Phosphate/Carbonate Nanorods, Microrods, and Dendritic Structures. Crystal Growth & Design 9(4), 1798-1805.

Noel, J.D. and Giammar, D.E. (2008) The influence of water chemistry on dissolution rates of Lead(II) carbonate solids found in water distribution systems, Water Quality Technology Conference, Cincinnati, OH.

Pourbaix, M. (1974) Atlas of Electrochemical Equilibrium in Aqueous Solutions, National Association of Corrosion Engineers, Houston, TX.

Schecher, W.D. and McAvoy, D.C. (1998a) MINEQL+: A chemical equilibrium modeling system, version 4.0, Environmental Research Software, Hallowell, ME.

Schecher, W.D. and McAvoy, D.C. (1998b) MINEQL+: A chemical equilibrium modeling system, version 4.5, Environmental Research Software, Hallowell, ME.

Schock, M., DeSantis, M.K., Lubbers, H. and Gerke, T. (2006) The occurrence and significance of tetravalent lead in New England, Proc. NEWWAAC, Danvers, MA.

Schock, M. and Giani, R. (2004) Oxidant/disinfectant chemistry and impacts on lead corrosion, Water Quality Technology Conference, San Antonio, TX.

Schock, M.R. (1999) Water quality and treatment. Letterman, R.D. (ed), McGraw-Hill, Inc., New York, New York.

Shi, Z. and Stone, A.T. (2009a) PbO_2(s, Plattnerite) Reductive Dissolution by Aqueous Manganous and Ferrous Ions. Environmental Science & Technology 43(10), 3596-3603.

Shi, Z. and Stone, A.T. (2009b) PbO_2(s, Plattnerite) Reductive Dissolution by Natural Organic Matter: Reductant and Inhibitory Subfractions. Environmental Science & Technology 43(10), 3604-3611.

Stumm, W. (1997) Reactivity at the mineral-water interface: dissolution and inhibition. Colloids and Surfaces A: Physicochemical and Engineering Aspects 120, 143-166.

Stumm, W. and Morgan, J.J. (1996) Aquatic chemistry, John Wiley & Sons, Inc., New York, NY.

Switzer, J.A., Rajasekharan, V.V., Boonsalee, S., Kulp, E.A. and Bohannan, E.W. (2006) Evidence that monochloramine disinfectant could lead to elevated Pb levels in drinking water. Environmental Science & Technology 40(10), 3384-3387.

U.S.EPA (1991) Maximum Contaminant Level Goals and National Primary Drinking Water Regulations for Lead and Copper. Final Rule. Federal Register 56, 26460.

U.S.EPA (2007) Review of the Interim Optimal Corrosion Control Treatment for Washington, D.C. U.S.EPA (ed), U.S.EPA.

Xie, Y., Wang, Y., Singhal, V. and Giammar, D.E. (2010) Effects of pH and carbonate concentration on dissolution rates of the lead corrosion product PbO_2 Environmental Science & Technology 44(3), 1093-1099.

Chapter 5. Role of water chemistry, stagnation time, and flow in lead release from pipe scales

Abstract

Lead release from pipe scales was investigated under different water chemistries, stagnation times, and flow velocities. Pipe scales were developed on lead pipes by conditioning the pipes with water containing free chlorine. After eight months of conditioning, the scales contained lead(IV) oxides and the lead(II) carbonate hydrocerussite. Water chemistry and the composition of the pipe scales are two key factors in lead release from pipe scales. The water in contact with pipe scales rarely reached equilibrium with lead corrosion products within one day, which makes solid-water contact time and dissolution rates of corrosion products the controlling factors of lead concentrations. Among five water chemistries that can affect lead concentrations, only a solution with orthophosphate was able to control the lead concentration below the action level. Flow can increase both dissolved and particulate lead release rates by accelerating the mass transfer of lead out of the pores in the pipe scales and physically destabilizing pipe scales. Dissolved lead comprised the majority of the lead released at stagnant and laminar flow conditions.

5.1.   Introduction

Lead concentrations in tap water are regulated by the Lead and Copper Rule, which set an action level of 15 μg/L for lead [1]. A recent study found that 50-75% of total lead in tap water can be attributed to lead release from lead service lines, while 25-30% can be contributed from premise piping [2]. Lead corrosion products that form scales on the interior pipe wall are in direct contact with water and control lead leaching to water [3]. Because lead release is controlled by reactions with corrosion products and not the elemental lead in the pipes, studies that use new lead pipes can not simulate the lead release expected in actual systems [4]. Conditioning of new lead pipes to develop corrosion products or using lead pipe sections removed from actual distribution systems provides more realistic solid phases for assessing lead release from pipe scales [5, 6].

Lead release from lead pipes is influenced by stagnation time, flow velocity, and water chemistry. The stagnation time was found to substantially affect lead release from pipes, with most of the release occurring within the first 24 hours [7]. Schock pointed out that lead concentrations rarely reach equilibrium in distribution systems (Schock, 1989). The dissolution rates of corrosion products and stagnation time can be more important than equilibrium in controlling the lead concentrations in tap water [8].

Flow velocity can influence erosion mechanisms of corrosion products and can affect the development of pipe scales [9]. At stagnant conditions, immobile water inside or adjacent to porous scales contains high concentrations of solutes and is not well mixed with bulk water, which may limit lead release rates and the lead concentrations [10]. At flow conditions, lead release can be accelerated because of enhanced mass transfer rate of lead from the immobile water in the porous pipe scales to the mobile bulk water in the

pipes. Lead-rich particles could also detach from pipe scales during flow and contribute significantly to the total lead concentration [11].

With respect to water chemistry, disinfectants, dissolved inorganic carbon (DIC), pH, and phosphate inhibitors are important parameters in controlling lead concentrations in tap water. Free chlorine and chloramines are commonly used residual disinfectants. Free chlorine can oxide Pb(II) to PbO_2, but chloramines cannot [12]. Therefore, PbO_2 has been found only on lead pipes of distribution systems with a history of free chlorine usage [13]. The dissolution of PbO_2 would be accelerated if the residual disinfectant is switched from free chlorine to chloramines [14]. A switch of disinfectants, as may be done to limit disinfection byproduct formation, can influence lead concentrations in tap water. The incident of high lead concentrations in Washington D.C. from 2001-2004 is an example of increased lead release following a switch from free chlorine to chloramines [15, 16].

The effect of carbonate, which is related to pH and alkalinity, on lead release depends on the specific lead corrosion products present in the pipe scales. Lead carbonate solids, such as cerussite ($PbCO_3$) and hydrocerussite ($Pb_3(CO_3)_2(OH)_2$), have been found in lead pipe scales [17]. Initial increases in DIC can lower the solubility of these lead carbonate solids, although further increases in DIC can actually enhance their solubility by forming soluble lead carbonate complexes [18]. If PbO_2 or hydroxylpyromorphite ($Pb_5(PO_4)_3(OH)$) is the dominant lead corrosion product, then carbonate from DIC can enhance the lead release from pipes scales by forming soluble lead carbonate complexes [8, 19].

The pH effect on lead release is connected with the effect of DIC and depends on the specific corrosion product in pipe scales. Increasing pH from near neutral generally lowers the lead release rates from hydrocerussite and PbO_2 at high DIC levels, while increasing pH from 8.5 to 10 may slightly enhance the lead release rates from hydrocerussite and PbO_2 at low DIC levels [8, 20]. In a study of hydroxylpyromorphite dissolution, the dissolution rate was lower at pH 8.5 than at pH 7.5 or 10.0, which parallels the trends in the equilibrium solubility of hydroxylpyromorphite [19].

Orthophosphate have been used as a lead corrosion inhibitor to maintain lead concentrations below the action level in water utilities. Orthophosphate has been demonstrated to inhibit lead release from new pipes [5]. The effect of orthophosphate is believed to result from the precipitation of lead phosphate solids, such as hydroxylpyromorphite, and hydroxylpyromorphite has been identified in some pipe scales [21]. The precipitation of hydroxylpyromorphite dramatically decreased the net lead release rate during hydrocerussite dissolution in solutions with orthophosphate [20]. Zinc orthophosphate has the same effects as sodium orthophosphate or phosphorus acid [22]. Orthophosphate concentrations higher than 0.4 mg/L have been observed to be effective in controlling lead concentrations [23].

In this study, lead corrosion products that developed as scales on lead pipe in the presence of free chlorine were identified and characterized. The roles of water chemistry, solid-water contact time, and flow on lead release from the pipe scales were then evaluated. Mechanisms of dissolved and particulate lead release were proposed for different water chemistries.

5.2.   Experimental Section

5.2.1. Development of pipe scales.

Corrosion products were developed on the interiors of new lead pipes. Three 24-inch long new lead pipe were reacted with solutions designed to promote the formation of lead(IV) oxides. The lead pipes were fixed at an inclined angle of 20° in a holding rack. The pipes were filled with an aqueous solution at pH 10 with 10 mg C/L DIC and 3.5 mg/L free chlorine, kept stagnant for a day, and then emptied. The filling and emptying procedure was repeated daily (five days per week) for eight months of conditioning. Effluent samples were collected for analysis once every week with the exception of the first month, during which samples were collected daily (five days per week). For these samples the pH and concentrations of residual chlorine and dissolved lead were measured.

At the conclusion of the conditioning period, one pipe was used for characterization of the pipe scale. The pipe cross-section and interior wall were prepared for imaging. A 2 inch section of the pipe was filled with epoxy to retain the pipe scale before a cross-section was cut and polished. The pipe cross-section was imaged using scanning electron microscopy (SEM) to see the layers and thickness of the pipe scale. A 12 inch section of the pipe was cut lengthwise to visually observe the scale that developed on the insides of the pipes. The scale materials were then gently scraped off with a metal spatula. The crystalline phases in the pipe scales were identified with X-ray diffraction (XRD), and the size and morphology of the scale particles were determined with SEM.

5.2.2. Lead release experiments from pipe scales.

Duplicate lead release experiments were conducted using the two pipe sections that were not used for characterization. Experiments examined the effects of water chemistry, stagnation time, and flow on lead release from the pipes (Table 5.1). These experiments examined the release of lead from pipe scales in response to a change in the water chemistry relative to the condition with which the scales had acclimated during conditioning.

Before conducting lead-release experiments, the pipes were reconditioned for 2 weeks because they had been stored between the initial 8-month conditioning period and the time of the release experiments. The tests with different experimental conditions were sequenced to avoid altering the pipe scales. Experiments with flow were conducted after stagnation time experiments to avoid potential problems of physically disturbing the scales. To recondition the pipes between experiments and provide a uniform starting point, they were filled and contacted for 1 day with an aqueous solution with the same composition as the original conditioning solution.

Table 5.1. Factors evaluated in experiments with pipe reactors

Factor	Conditions Evaluated					Application to Investigation
water chemistry	pH	DIC (mg C /L)	Cl_2 (mg/L)	NH_2Cl (mg/L as Cl_2)	PO_4^{3-} (mg/L as P)	Represent five water chemistries that may affect lead release from corrosion products.
	10	10	0	0	0	
	10	10	2	0	0	
	10	10	0	2	0	
	8.5	50	0	0	0	
	7.5	10	0	0	1	
stagnation time	0, 1, 2, 4, 8, 24 hours					Stagnation time can control the dissolved lead concentration in household plumbing.
flow velocity	0, 0.1 m/s					Flow may mechanically degrade pipe scales and accelerate the mass transfer of dissolved lead out of porous pipe scales.

For evaluation of the effect of stagnation time, the water in the pipe section was sampled after the prescribed periods through valves at the bottom of the pipes. The pH of the solution was measured, and the water collected was split into filtered (0.02 μm polyethersulfone membrane) and unfiltered samples. Filtered samples were analyzed for dissolved lead, orthophosphate, and free chlorine or monochloramine concentrations. Unfiltered samples were analyzed for total lead and orthophosphate concentrations. Before analysis of dissolved and total lead and phosphorus, samples were acidified to 2% nitric acid.

For evaluation of the effect of flow, fresh solution of the desired chemistry was recirculated through the pipe sections at a flow velocity of 0.1 m/s, which gave a Reynolds number of 953 and was in the laminar flow regime. In actual distribution systems, both laminar and turbulent flow regimes are possible. The pipe reactor system consisted of a 1.15 L reservoir that had the target water chemistry, a lead pipe with a volume of 250 mL, and a peristaltic pump that provided flow through the system. Effluent samples were collected after one and two hours of recirculation for analysis of pH and concentrations of dissolved and total lead, free chlorine, monochloramine, and orthophosphate. Only for the high orthophosphate condition, the recirculation time was extended to 24 hours with sampling at 4 and 24 hours. The recirculation experiments were conducted to assess the impact of flow on lead release rates; however, the configuration of water recirculation through a pipe section is not representative of the flow path through an actual lead service line. Two hours of recirculation allow much more extensive lead release than could occur during the much shorter contact time of water flowing through a pipe section without recirculation. The only exception to more extensive lease release during recirculation would occur if the dissolution rate was sufficiently fast to closely approach equilibrium at both the short contact time during once-through flow and the longer contact times of recirculation.

5.2.3. Analytical methods.

Dissolved concentrations of lead and phosphorus were determined by inductively coupled plasma mass spectrometry (ICP-MS). The ICP-MS has an instrument detection limit of 9 ppt (ng/L) and a method detection limit of 50 ppt (ng/L) for lead. The pH of

solutions was measured with a glass pH electrode and pH meter. Free chlorine and

monochloramine concentrations were measured using the standard DPD colorimetric

method [24]. A scanning ultraviolet/visible spectrophotometer was used for analysis.

XRD was performed on an instrument that uses Cu-Kα radiation and has a vertical

goniometer and a scintillation counter. A field emission scanning electron microscope

was used to view the size and morphology of the solids.

5.3.   Results and Discussion

5.3.1. Water chemistry during development of pipe scales

During the first 10 days of the conditioning period, the total lead concentration of the water in the pipes after one day of stagnation initially increased to more than 500 µg/L (Figure 5.1a-c). The lead concentration dropped significantly after this initial period, and for the remaining 230 days it was stable around 50 µg/L. The pH increased from the initial value of 10 to 11 and then dropped back to 10 during the first two weeks. The residual chlorine concentration after one day of contact was always in the range of 0 to 1 mg/L as Cl_2, which indicates consumption of free chlorine from reaction with the lead pipe. The residual chlorine concentration was close to 0 during the first 10 days. After 10 days, it increased from 0 to 0.5 mg/L as Cl_2 and then fluctuated around 0.5 mg/L as Cl_2.
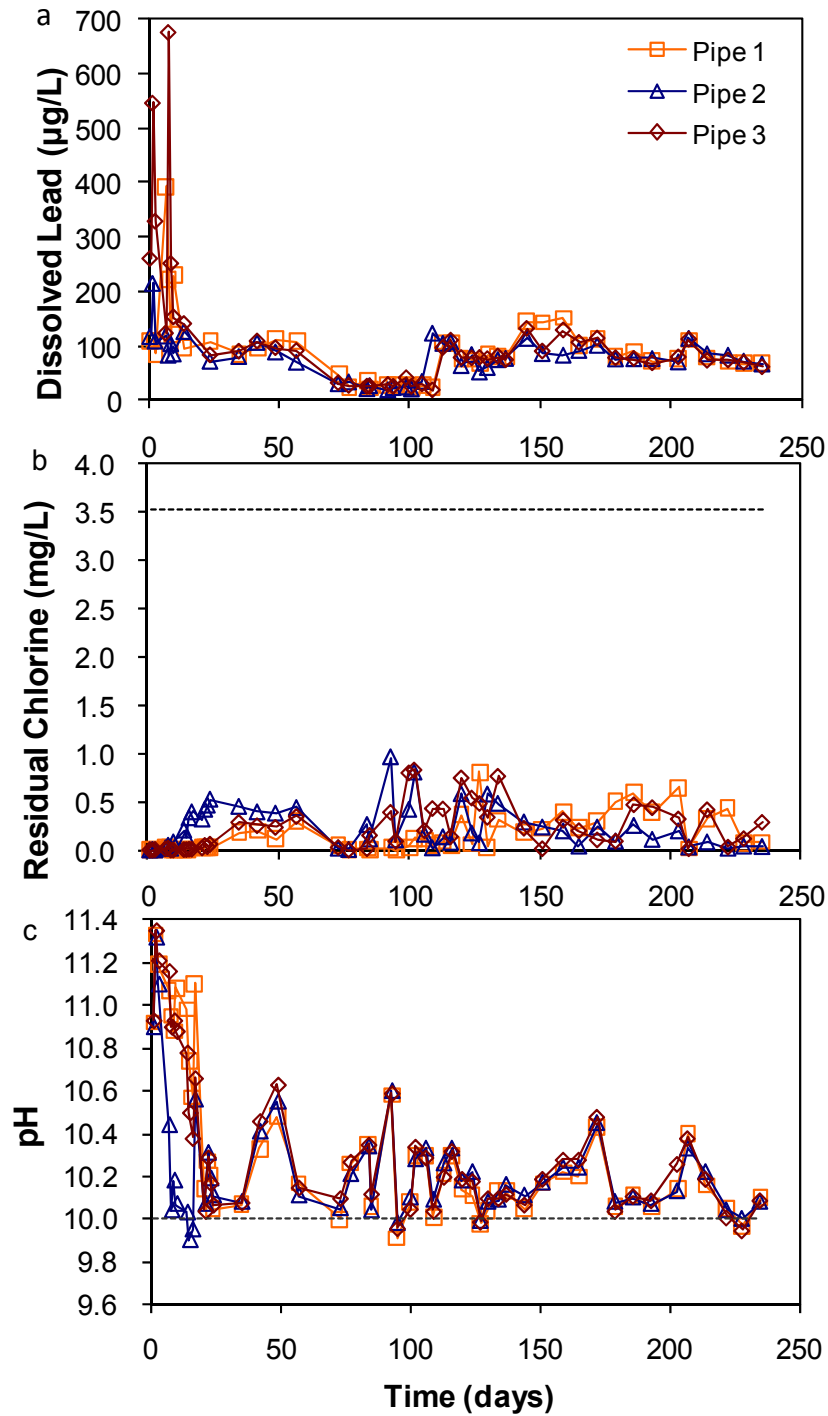
Figure 5.1. Evolution of (a) lead concentration, (b) residual free chlorine concentration, and (c) pH in three lead pipes during eight months of conditioning. The initial pH and free chlorine concentration of the filling solution are indicated by the dashed lines.

5.3.2. Characterization of lead pipe scales

The interior wall of an eight-month conditioned pipe had red islands in a white and red background (Figure 5.2). The reddish color in the ends and the islands of the pipe is characteristic of lead(IV) oxides [25].

XRD analysis of the scale materials (Figure 5.3) showed that the red islands and end sections contained the lead(IV) oxides scrutinyite and plattnerite, but the major component of the scale was hydrocerussite. Very little lead(IV) oxide was identified in other areas. In the presence of 3.5 mg/L as Cl_2 free chlorine, equilibrium calculations predict that lead(IV) oxide should be the only lead phase. However, the metallic lead of the pipe is oxidized first to lead(II) before reaching the lead(IV) state. Since hydrocerussite is the predicted Pb(II) phase at pH 10 and 10 mg/L DIC, hydrocerussite formed before any lead(IV) oxide was produced. The production of lead(IV) oxides on the pipes may be limited by the rate of reaction with free chlorine and by the once daily resupply of free chlorine. Previous research has observed the coexistence of lead(II) and lead(IV) phases in pipe scales, and layers of different corrosion products can develop in
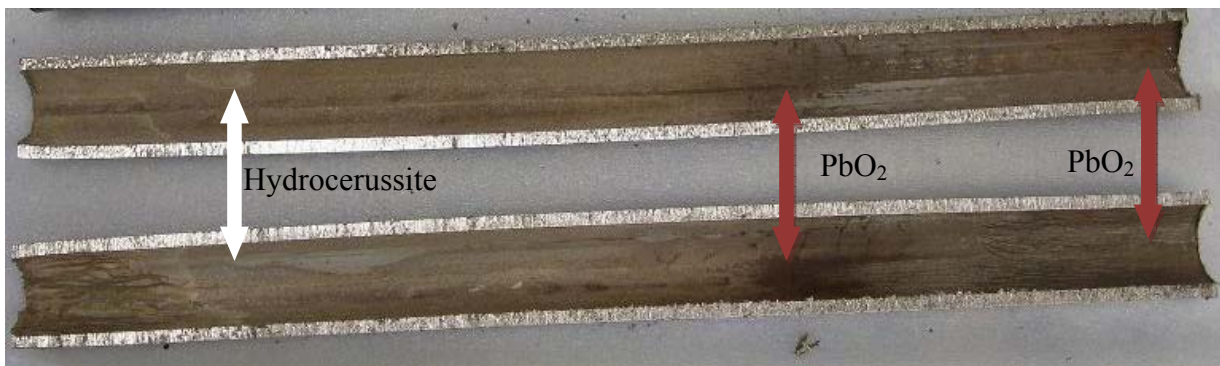
Figure 5.2. Inside of 12 inch section of pipe that had been conditioned for eight months with a solution of pH 10, 10 mg/L DIC, and 3.5 mg/L free chlorine.

pipe scales [26]. Elemental lead peaks were found in most patterns because portions of

unaltered pipe were scraped off while collecting materials of the pipe scale.
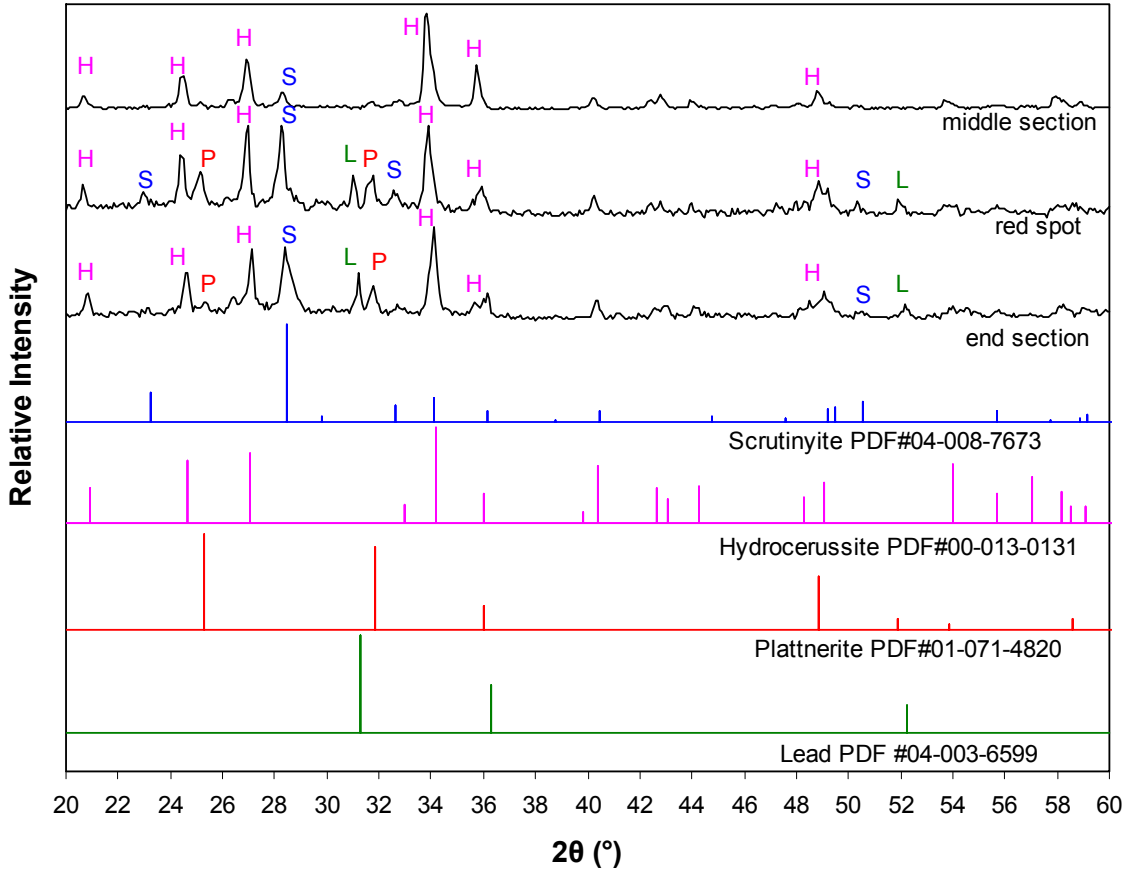
Figure 5.3. X-ray diffraction patterns of pipe scale formed after conditioning for eight months. The reference patterns of scrutinyite (S), hydrocerussite (H), plattnerite (P), and elemental lead (L) are included for comparison. The peaks of the sample patterns corresponding to different phases are noted.

Electron micrographs of the pipe scale particles and the cross section of the pipe

scale are shown (Figure 5.4). The pipe scale contains large platy particles and aggregates

of smaller tiny particles. The large particles are hydrocerussite, which usually forms with

a platy shape [27]. The smaller particles are probably plattnerite and scrutinyite. The

larger particles are more abundant than the aggregated smaller particles, which is

consistent with the predominance of hydrocerussite in the XRD patterns. The pipe scale

was about 24 μm thick and had gaps and pores that would allow water infiltration.

Materials of different shapes in different regions were indicative of layers.
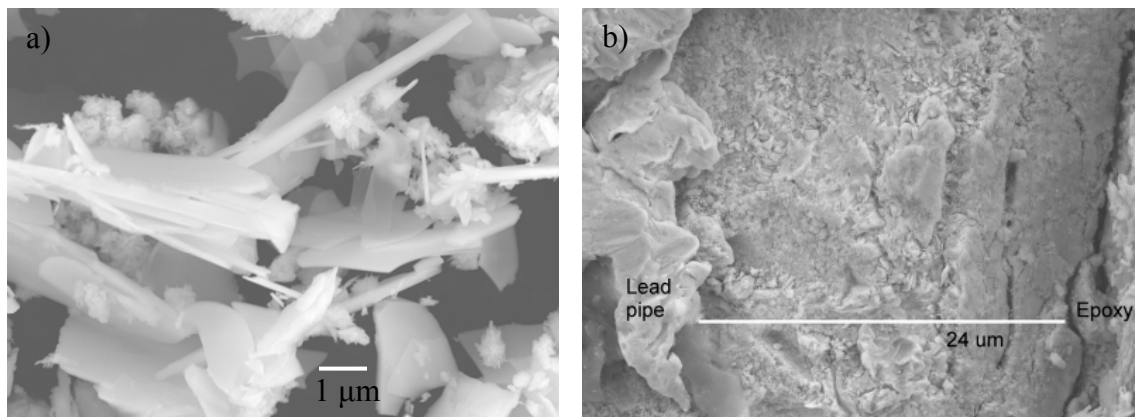
Figure 5.4. Electron micrographs of a) particles in the pipe scale and b) cross section of pipe surface with development of corrosion products. In the cross section, unaltered lead pipe is visible on the left and the epoxy used to fill the pipe prior to cutting and polishing is on the right.

5.3.3. Effects of water chemistry on dissolved lead concentrations in pipes

When the conditioned pipes were contacted with five different solutions in stagnation experiments, the solution with orthophosphate yielded the lowest dissolved lead concentration (Figure 5.5a). Orthophosphate effectively controlled the dissolved lead concentration below the 15 μg/L action level for the first 8 hours of the stagnation experiments, but the dissolved lead concentration after 24 hours exceeded the action level. The experiment with the high DIC solution had the highest dissolved lead concentration. Dissolved lead concentrations in solutions with high pH, monochloramine, or free chlorine were in between. The impact of the residual disinfectant can be assessed by comparing lead release in these three solutions, which are all at pH 10 with 10 mg/L DIC. The dissolved lead concentrations decreased from

monochloramine to no disinfectant to free chlorine. Similar trends were observed for

flow experiments (Figure 5.5b).
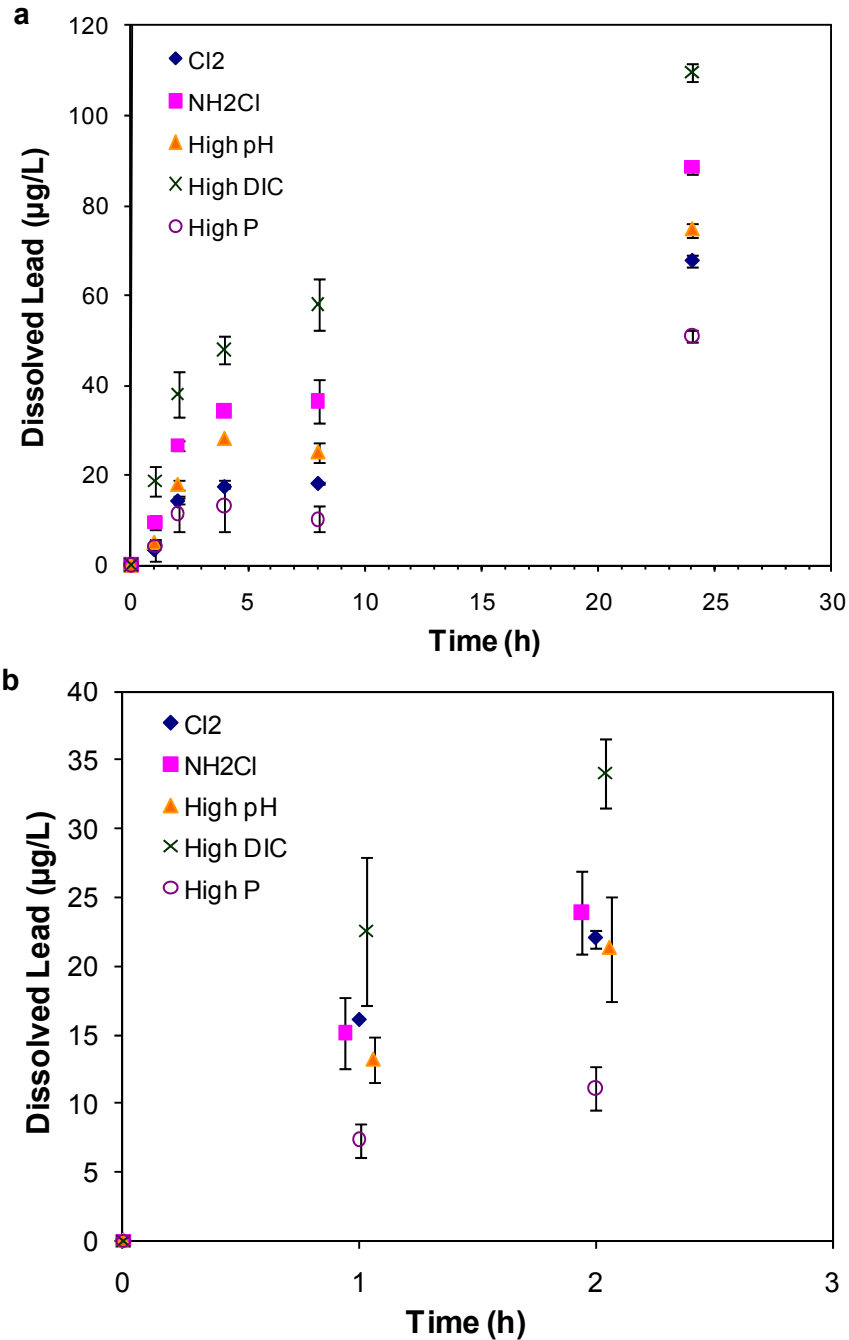
Figure 5.5. Effects of reaction time and water chemistry on the dissolved lead released from pipe scales in (a) stagnation and (b) flow experiments. Error bars represent one standard deviation of duplicate experiments. Although the points in panel b are slightly staggered to avoid overlap in the plot, the reaction times shown for all five water conditions are for 1.0 hour and 2.0 hours.

The dissolved lead concentrations kept increasing with time in stagnation and flow experiments, except in the first 8 hours when orthophosphate was present, which indicates that the water in the pipes had not reached equilibrium with the pipe scales (Figure 5.5). Therefore, the dissolved lead concentrations in both stagnation and flow experiments without orthophosphate were controlled by the dissolution rates and not by the equilibrium solubility of the corrosion products.

The effects of water chemistry on lead release from pipe scales were consistent with the effects of water chemistry on dissolution of individual lead corrosion products. Orthophosphate can decrease the net lead release from lead(II) carbonates by forming lead phosphate precipitates [20], and in the present experiments the solutions containing orthophosphate had the lowest dissolved lead concentrations. Increasing DIC from 10 to 50 mg/L can enhance dissolution of hydrocerussite and PbO_2 by forming soluble Pb(II) carbonate complexes, and decreasing the pH from 10 to 8.5 could also enhance dissolution of hydrocerussite and PbO_2 [8, 18]. Switching from 10 mg/L DIC at pH 10 to 50 mg/L DIC at pH 8.5 increased the dissolution rates of hydrocerussite and PbO_2 and resulted in the highest lead release observed in this study. Free chlorine can raise the redox potential and inhibit PbO_2 dissolution, and it can oxidize Pb(II) released from hydrocerussite to PbO_2. Monochloramine increased lead concentrations relative to the solution without disinfectant; the effect of monochloramine was probably caused by the reduction of PbO_2 by an intermediate species produced during monochloramine decay [14].

The pH was stable and did not vary more than 0.5 pH units except after 24 hours of stagnation in the experiments with orthophosphate solution (Figure 5.6). Therefore,

the observed effects of water chemistry on the lead release cannot be attributed to the changes in pH during experiments. After 24 hours of reaction in the orthophosphate solution, the dissolution of lead corrosion products and precipitation of lead phosphate solids had increased the pH from 7.5 to 8.7.
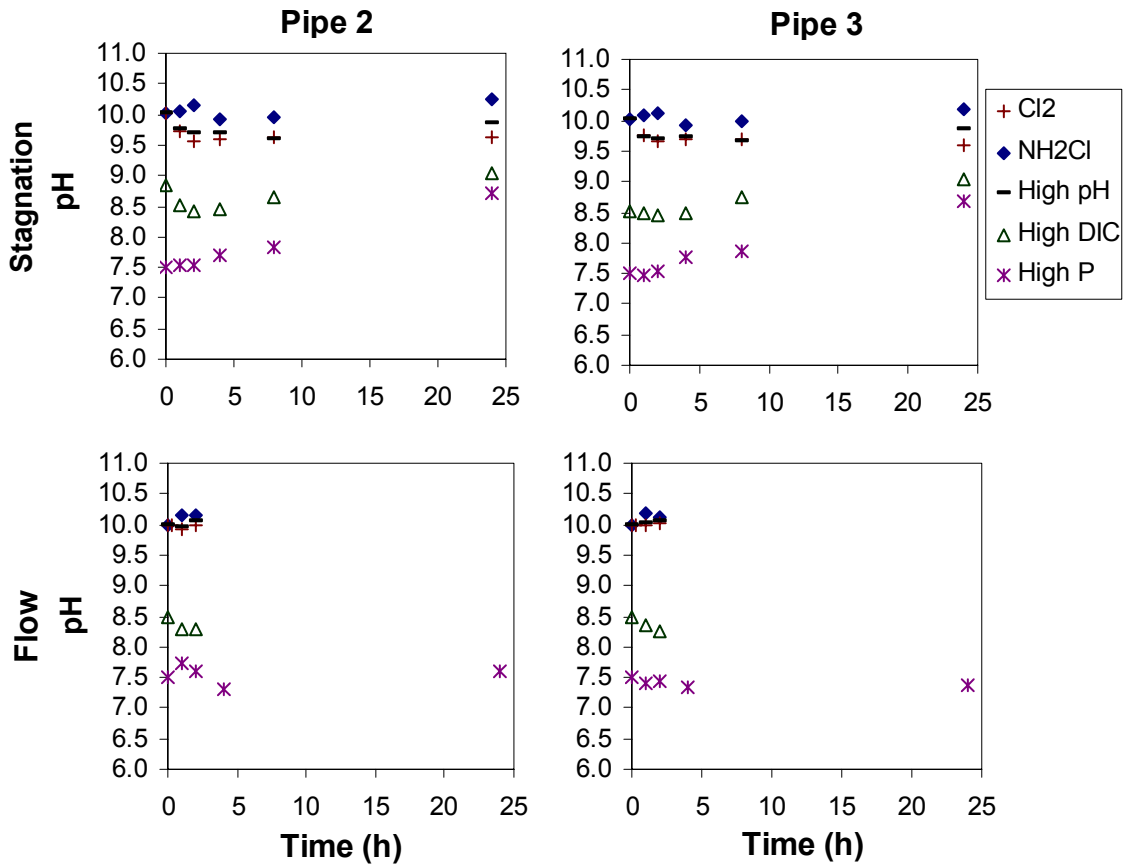
Figure 5.6. The pH profile during stagnation and flow experiments in Pipe 2 and Pipe 3.

5.3.4. Effects of water chemistry on particulate lead concentrations in pipes

Lead-containing suspended particles could come from (a) remobilization of lead corrosion products in pipe scales and (b) precipitation of new lead-containing solids in solution. The solution with orthophosphate generated the highest particulate lead concentration in both flow and stagnation experiments (Figure 5.7). PbO_2 is negatively

charged at pH > 7 [28], and phosphate adsorption to lead corrosion products in the pipe

scales can change the surface charge of the particles. The increased negative surface

charge from phosphate adsorption can cause stronger electrostatic repulsion between

particles, which consequently could have destabilized the aggregates and mobilized small

particles. The precipitation of lead phosphate solids may also contribute to the particulate

lead in the presence of orthophosphate, and this possibility is discussed more in a later

section.
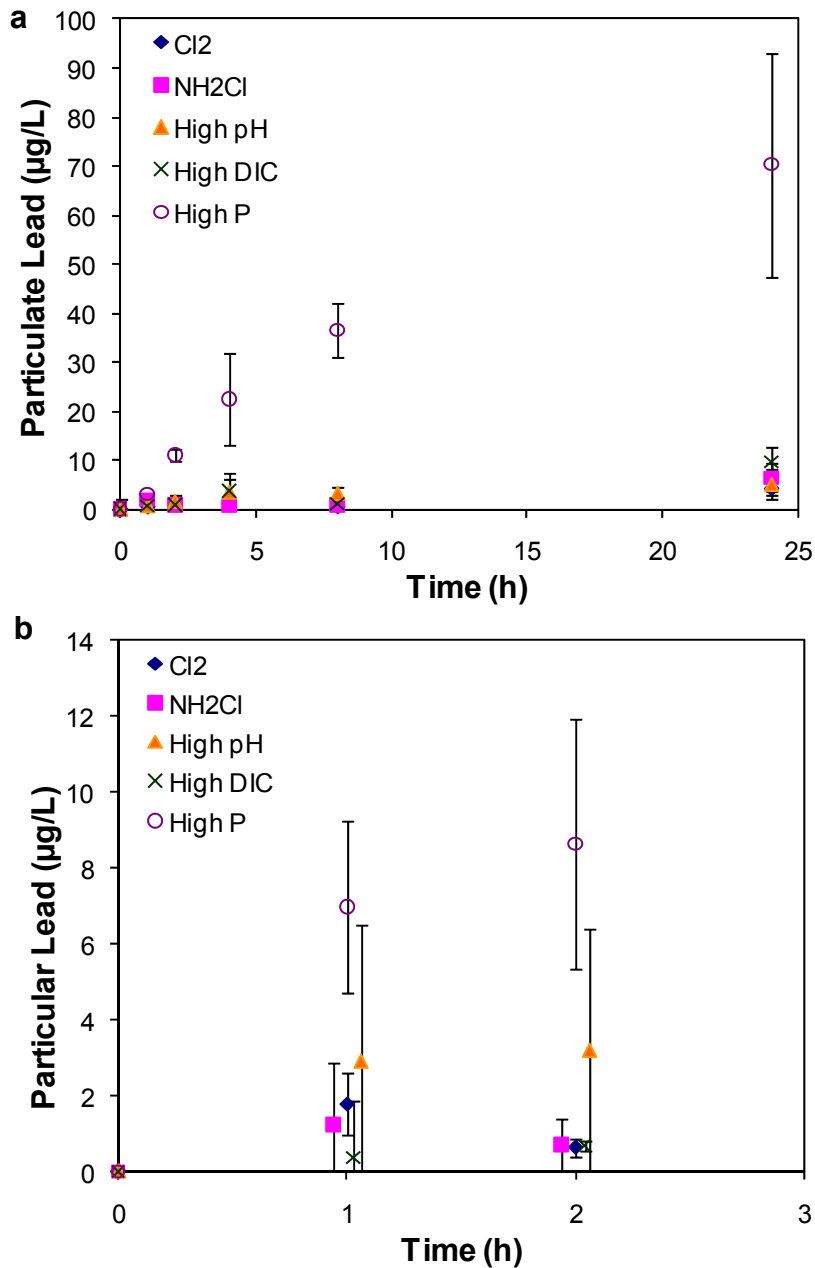
Figure 5.7. Effects of reaction time and water chemistry on the particulate lead concentrations released from pipe scales in (a) stagnation and (b) flow experiments. Error bars represent one standard deviation of the duplicates. Although the points in panel b are slightly staggered to avoid overlap in the plot, the reaction times shown for all five water conditions are for 1.0 hour and 2.0 hours.

5.3.5. Effects of flow on lead release rates from pipe scales

The average lead release rate (mol s^{-1} or µg h^{-1}) over a prescribed period can be determined using Equation 5.1, in which C_s is the dissolved or particulate lead concentration, V is the volume of the pipe system, and t_{rxn} is the time for reaction between the water and pipe scale. For stagnation experiments, V is the volume of water in the pipe; while for experiments with recirculating flow, V is the total volume of the pipe and the reservoir.

$$R_{measured} = \frac{C_s \cdot V}{t_{rxn}}$$

(5.1)

Dissolved lead. The dissolved lead release rates in flow experiments were one order of magnitude higher than in stagnation experiments (Figure 5.8a). Flow probably enhanced dissolved lead release rates by accelerating mass transfer of dissolved lead out of porous scales . A recent experimental study has shown that immobile water inside porous pipe scales is not well mixed with bulk water. The immobile water contains high solute concentrations released from scales, and it mixes much better with the bulk water at flow conditions [29]. In Appendix 5A, better mixing at flow conditions than stagnant conditions has been proven to cause higher lead release rates in terms of accelerating the mass transfer of lead in the immobile water to bulk water .

Although the flow condition yielded higher lead release rates than the stagnant condition, the recirculation configuration has a much longer reaction time than the once-through configuration of an actual distribution system. If the flow were in a once-through configuration, the calculated dissolved lead concentrations from a 24-inch pipe section based on the lead release rates determined in the present study and the reaction

time range from 0.08 to 0.3 μg/L, which is far less than the dissolved lead concentration after stagnation for 1 hour (8-25 μg/L). So although lead release rates are higher with flow, the dissolved lead concentrations reached in pipe sections will still be higher during stagnation.

Particulate lead. The particulate lead release rates at flow conditions were also about one order of magnitude higher than at stagnation conditions (Figure 5.8b). Flow could mechanically or chemically destabilize the pipe scales and mobilize particles in the scales at the first few hours. There was more fluctuation in particulate lead concentrations than in dissolved lead concentrations.
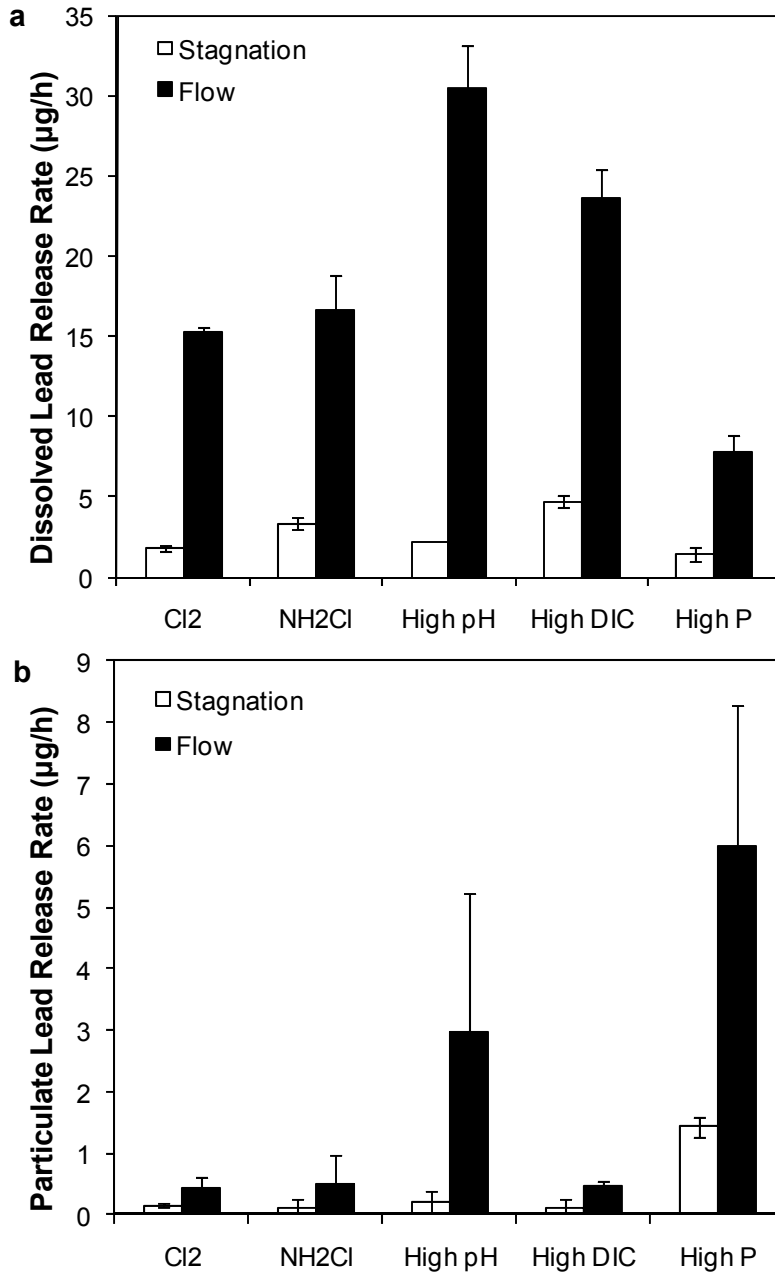
Figure 5.8. Effects of flow on (a) dissolved and (b) particulate lead release rates from scales over the first 2 hours of experiments. Error bars represent one standard deviation of the duplicates.

5.3.6. Effects of stagnation time on dissolved lead release rates from pipe scales

For all five solutions, the dissolved lead release rates were highest during the first 2 hours (Figure 5.9). The dissolved lead release rates decreased from 2 hours on. The decreasing lead release rates could be caused by (a) accumulation of dissolved lead and approaching equilibrium or (b) fast initial dissolution of very small particles or labile surface phases. Faster initial dissolution than later steady-state dissolution of pure PbO_2 has been observed previously in flow-through experiments [8].
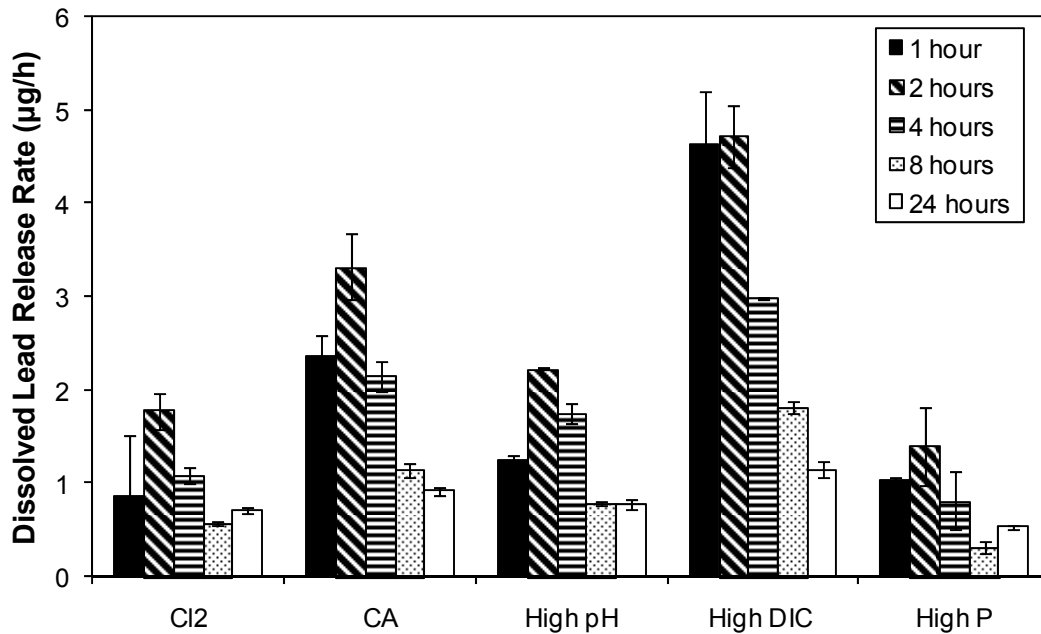
Figure 5.9. Effects of stagnation time on dissolved lead release rates from pipe scales in stagnation experiments. Error bars represent one standard deviation of the duplicates.

5.3.7 Lead profile in stagnation experiments

In stagnation experiments, most of the lead released was dissolved except in the experiment with orthophosphate (Figure 5.10a). Particulate lead constituted less than

10% of the total lead in solutions without phosphate. For solutions with phosphate, particulate lead accounted for 49% of the total lead.

In flow experiments, the majority of the released lead was also dissolved except in the experiment with orthophosphate (Figure 5.10b). Particulate lead made up less than 5% of the total lead in high DIC, free chlorine, and monochloramine solutions. For solutions with phosphate, particulate lead was 46% of the total lead. In the high pH solution without disinfectant, 13% of the total lead was present as particulate.
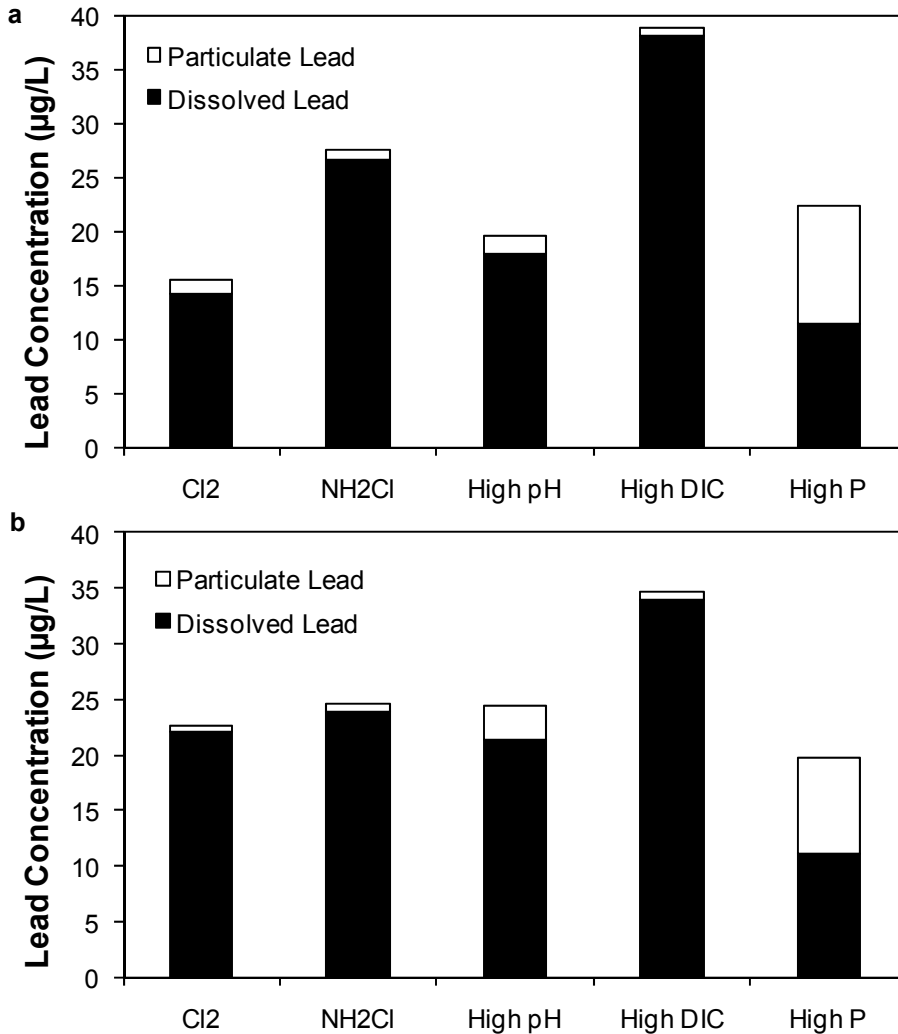
Figure 5.10. Lead profile of 2-hour samples in (a) stagnation and (b) flow experiments.

5.3.8. Orthophosphate case

The solution with orthophosphate controlled dissolved lead concentrations below the action level for the first few hours, and the trends of orthophosphate and dissolved lead provide insights into the mechanism of the orthophosphate effect. In both stagnation and flow experiments, the decreasing trend of phosphate correlated with an increasing trend of dissolved lead (Figure 5.11a-b). Before the phosphate concentration dropped below 100 µg/L, the dissolved lead concentration did not reach 20 µg/L, which is close to the solubility of hydroxylpyromorphite in the presence of 0.3 mg/L orthophosphate as P at the pH and DIC of the experiment. The precipitation of hydroxylpyromorphite probably controlled the dissolved lead concentration until the orthophosphate was depleted below a critical level.

The precipitation of hydroxylpyromorphite probably contributed to the particulate lead release, which made the total lead release in the presence of orthophosphate as high as and higher than in other solutions (Figure 5.10). The particulate lead release in the presence of orthophosphate could cause potential water safety issues, although lead solids, especially lead phosphates, are less bioavailable than dissolved lead [30, 31].
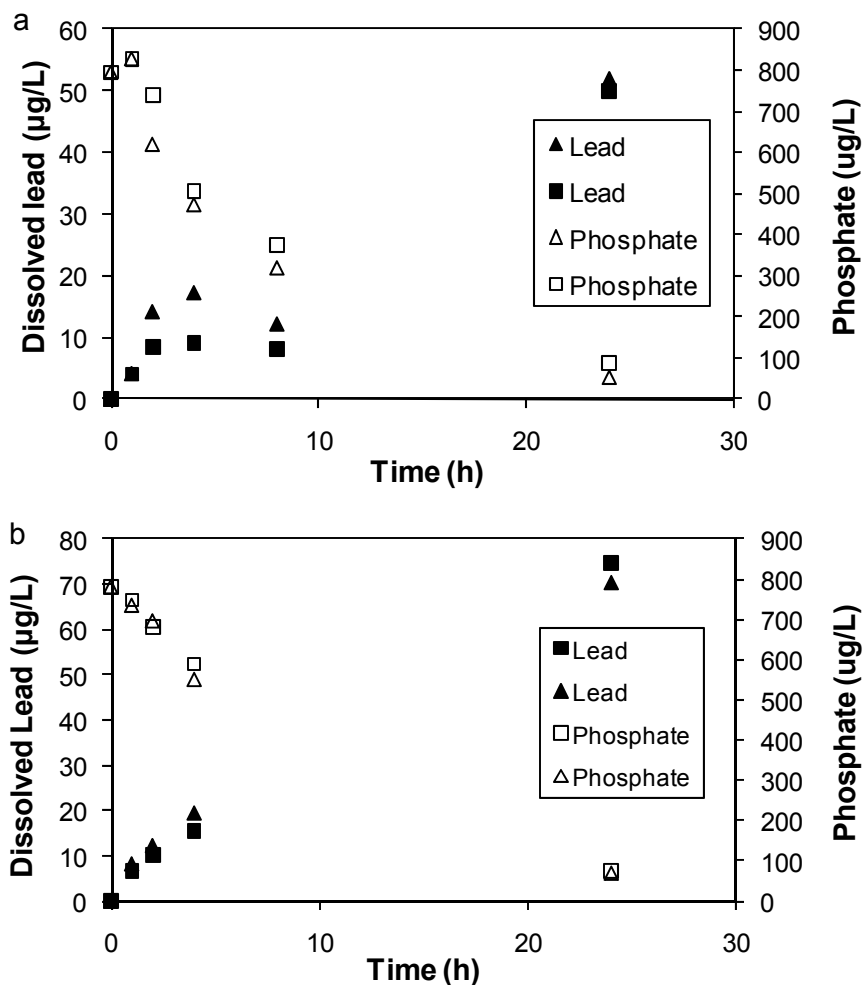
Figure 5.11. Dissolved lead and orthophosphate concentrations in high orthophosphate solution during (a) stagnation and (b) flow experiments. Data are shown for duplicate experiments.

5.3.9. Free chlorine case

In stagnation experiments, the decreasing trend of free chlorine correlated with the increasing trend of dissolved lead (Figure 5.12). The dissolved lead did not reach 25 µg/L in the first 8 hours, which was probably due to the oxidation of Pb(II) to PbO_2 by free chlorine. The free chlorine concentration dropped over time because of the consumption of free chlorine in the oxidation of Pb(0) to Pb(II) and Pb(II) to PbO_2. Free

chlorine concentrations higher than 1 mg/L as Cl_2 were able to maintain low lead levels. The stagnation time affects the disinfectant levels in distribution systems and consequently the lead concentrations. Free chlorine levels will also vary with water age in a distribution system, and the most distant connections may be most vulnerable to lead release because of lowered residual free chlorine concentrations.
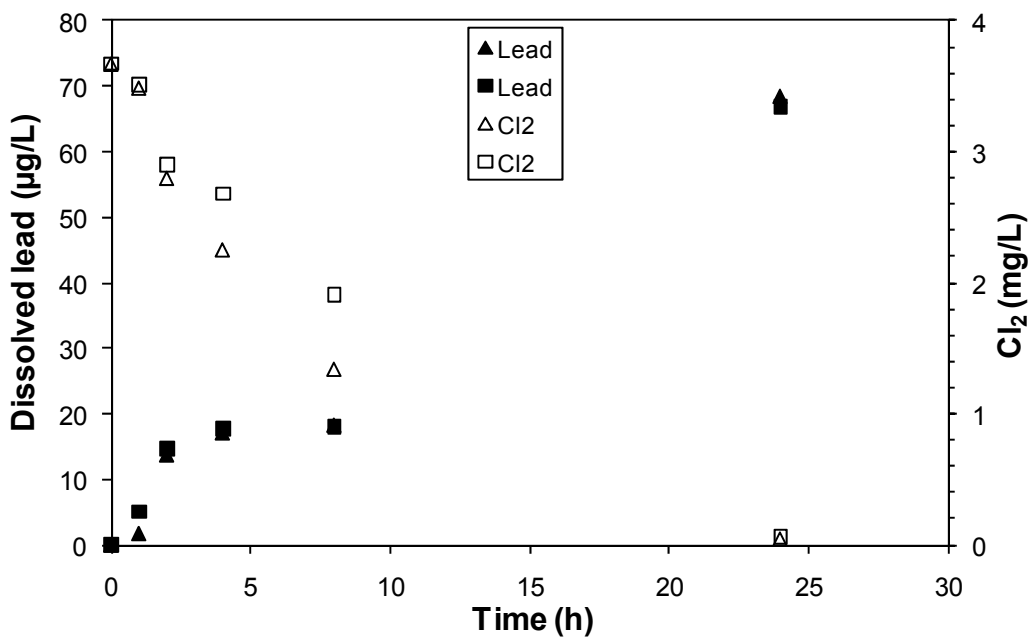
Figure 5.12. Dissolved lead and free chlorine concentrations in solution with free chlorine during stagnation experiments. Results are shown for both duplicate experiments.

5.4. Conclusions

Lead release from pipe scales is related to the dissolution and precipitation of lead corrosion products. Knowledge of the corrosion products in the pipe scales is key to understanding the response of lead release to water chemistry. Orthophosphate can be used as a lead corrosion inhibitor for pipes with scales comprised of hydrocerussite and

PbO$_2$. Orthophosphate concentrations higher than 0.3 mg P/L were necessary to maintain

the dissolved lead concentration below the action level, although orthophosphate did

increase particulate lead.   For pipe scales consisting of hydrocerussite (major) and PbO$_2$

(minor), solutions with and without disinfectant at pH 10 and DIC 10 mg/L and a solution

at pH 8.5 with DIC 50 mg/L were not effective in controlling the dissolved lead

concentrations below the action level. A switch of disinfectant from free chlorine to

monochloramine increased the lead release in stagnation experiments.

Laminar flow accelerated both dissolved and particulate lead release rates from

pipe scales. Stagnation time and dissolution rate control the dissolved lead

concentrations within 1 day in the absence of orthophosphate, since equilibrium is not

reached. Stagnation time also influenced the dissolved lead concentration by affecting

the concentrations of residual disinfectant or orthophosphate. The total lead

concentration was primarily dissolved lead under both no-flow and laminar flow

conditions.

Acknowledgement

Michael Shock, Leland Harms, and Windsor Sung and the laboratory assistance of Yin

Wang.

References:

1.   U.S.EPA, Maximum Contaminant Level Goals and National Primary Drinking Water Regulations for Lead and Copper. Final Rule. *Federal Register* **1991,** *56*, 26460.

2.   Sandvig, A.; Kirmeyer, G. In *Contribution of lead sources to lead levels at the tap*, Water Quality Technology Conference, Cincinnati, OH, 2008.

3.   Schock, M. R.; Hyland, R. N.; Welch, M. M., Occurrence of contaminant accumulation in lead pipe scales from domestic drinking-water distribution systems. *Environ. Sci. Technol.* **2008,** *42*, (12), 4285-4291.

4.   Sharp, R.; Rosenfeldt, B.; Glaser, C.; Freud, S.; Laun, S.; Becker, W. In *Impact of disinfection type, stagnation time, and scale chemistry on lead leaching from lead service lines*, Water Quality Technology Conference, Seattle, WA, 2009.

5.   Edwards, M.; McNeill, L. S., Effect of phosphate inhibitors on lead release from pipes. *J. Am. Water Works Assoc.* **2002,** *94*, (1), 79-90.

6.   Schock, M. R.; Lytle, D. A.; Sandvig, A. M.; Clement, J.; Harmon, S. M., Replacing polyphosphate with silicate to solve lead, copper, and source water iron problems. *J. Am. Water Works Assoc.* **2005,** *97*, (11), 84-93.

7.   Lytle, D. A.; Schock, M. R., Impact of stagnation time on metal dissolution from plumbing materials in drinking water. *Journal of Water Supply Research and Technology-Aqua* **2000,** *49*, (5), 243-257.

8.   Xie, Y.; Wang, Y.; Singhal, V.; Giammar, D. E., Effects of pH and carbonate concentration on dissolution rates of the lead corrosion product PbO_2 *Environ. Sci. Technol.* **2010,** *44*, (3), 1093-1099.

9.   Schock, M. R., Internal corrosion and deposition control. In *Water quality and treatment*, Fifth ed.; Letterman, R. D., Ed. McGraw-Hill, Inc.: New York, New York, 1999.

10.   Hyacinthe, C.; Bonneville, S.; Van Cappellen, P., Reactive iron(III) in sediments: Chemical versus microbial extractions. *Geochim. Cosmochim. Acta* **2006,** *70*, (16), 4166-4180.

11.   Triantafyllidou, S.; Parks, J.; Edwards, M., Lead particles in potable water. *J. Am. Water Works Assoc.* **2007,** *99*, (6), 107-117.

12.   Switzer, J. A.; Rajasekharan, V. V.; Boonsalee, S.; Kulp, E. A.; Bohannan, E. W., Evidence that monochloramine disinfectant could lead to elevated Pb levels in drinking water. *Environ. Sci. Technol.* **2006,** *40*, (10), 3384-3387.

13.   Schock, M.; Giani, R. In *Oxidant/disinfectant chemistry and impacts on lead corrosion*, Water Quality Technology Conference, San Antonio, TX, 2004.

14.   Lin, Y. P.; Valentine, R. L., Release of Pb(II) from monochloramine-mediated reduction of lead oxide (PbO_2). *Environ. Sci. Technol.* **2008,** *42*, (24), 9137-9143.

15.   Boyd, G. R.; Dewis, K. M.; Korshin, G. V.; Reiber, S. H.; Schock, M. R.; Sandvig, A. M.; Giani, R., Effects of changing disinfectants on lead and copper release. *J. Am. Water Works Assoc.* **2008,** *100*, (11), 75-87.

16.   Edwards, M.; Dudi, A., Role of chlorine and chloramine in corrosion of lead-bearing plumbing materials. *J. Am. Water Works Assoc.* **2004,** *96*, (10), 69-81.

17.   Schock, M. R., Understanding corrosion control strategies for lead. *J. Am. Water Works Assoc.* **1989,** *81*, (7), 88-100.

18.   Noel, J. D.; Giammar, D. E. In *The influence of water chemistry on dissolution rate of lead corrosion products*, Water Quality Technology Conference, Charlotte, NC, 2007.

19.   Giammar, D.; Nelson, K.; Noel, J.; Xie, Y. In *Role of Phosphate in Mitigating Lead Release from Corrosion Products*, Water Quality Technology Conference, Cincinnati, OH, 2008.

20.   Noel, J. D.; Giammar, D. E. In The influence of water chemistry on dissolution rates of Lead(II) carbonate solids found in water distribution systems, Water Quality Technology Conference, Cincinnati, OH, 2008.

21.   Schock, M.; DeSantis, M. K.; Lubbers, H.; Gerke, T. In *The occurrence and significance of tetravalent lead in New England*, Proc. NEWWAAC, Danvers, MA, 2006.

22.   Schneider, O. D.; Lechevallier, M. N.; Reed, H. F.; Corson, M. J., A comparison of zinc and nonzinc orthophosphate-based corrosion control. *J. Am. Water Works Assoc.* **2007,** *99*, (11), 103-113.

23.   McNeill, L. S.; Edwards, M., Phosphate inhibitor use at US utilities. *J. Am. Water Works Assoc.* **2002,** *94*, (7), 57-63.

24.   Clesceri, L. S.; Greenberg, A. E.; Eaton, A. D., *Standard Methods for the Examination of Water and Wastewater*. Twentieth ed.; American Public Health Association, American Water Works Association, Water Environment Federation: Washington, DC, 1999.

25.   Lytle, D. A.; Schock, M. R., Formation of Pb(IV) oxides in chlorinated water. *J. Am. Water Works Assoc.* **2005,** *97*, (11), 102-114.

26.   Schock, M. R.; Scheckel, K. G.; DeSantis, M.; Gerke, T. In *Mode of occurrence, treatment, and monitoring significance of tetravalent lead*, Water Quality Technology Conference, Quebec, Canada, 2005.

27.   Korshin, G. V.; Ferguson, J. F.; Lancaster, A. N., Influence of natural organic matter on the morphology of corroding lead surfaces and behavior of lead-containing particles. *Water Research* **2005,** *39*, (5), 811-818.

28.   Shi, Z.; Stone, A. T., PbO_2(s, Plattnerite) Reductive Dissolution by Aqueous Manganous and Ferrous Ions. *Environ. Sci. Technol.* **2009,** *43*, (10), 3596-3603.

29.   Nawrocki, J.; Raczyk-Stanislawiak, U.; Swietlik, J.; Olejnik, A.; Sroka, M. J., Corrosion in a distribution system: Steady water and its composition. *Water Res. 44*, (6), 1863-1872.

30.   Ryan, J. A.; Scheckel, K. G.; Berti, W. R.; Brown, S. L.; Casteel, S. W.; Chaney, R. L.; Hallfrisch, J.; Doolan, M.; Grevatt, P.; Maddaloni, M.; Mosby, D., Reducing children's risk from lead in soil. *Environ. Sci. Technol.* **2004,** *38*, (1), 18A-24A.

31.   Sonmez, O.; Pierzynski, G. M., Phosphorus and manganese oxides effects on soil lead bioaccessibility: PBET and TCLP. *Water Air and Soil Pollution* **2005,** *166*, (1-4), 3-16.

Appendix 5A. Models of lead release from pipe scales

1. Introduction

Previous studies provided qualitative analysis of water chemistry effects on the

dissolved lead concentrations released from pipes [1-6]. Quantitative prediction of

dissolved lead concentrations in pipes has been developed using an equilibrium model

based on the lead corrosion products present in pipe scales. However, dissolved lead

concentrations are often not in equilibrium with the lead corrosion products at normal

solid-water contact times of seconds to hours [7]. Therefore, for non-equilibrium

conditions equilibrium concentrations cannot accurately predict dissolved lead

concentrations in pipes.

Methods for predicting lead release rates from pipes have been pursued and are

still being developed. In 1983, Kuch and Wagner proposed two mass transfer models to

fit lead concentrations in drinking water at turbulent and stagnant conditions [8]. In

Lytle and Schock examined the effectiveness of the diffusion model developed by Kuch

and Wagner in predicting lead and copper release at various stagnation times [9]. In

Van Der Leer et al developed an exponential model and proposed the idea of combining

the exponential model or the diffusion model with flow models, such as no-flow,

laminar-flow, and turbulent-flow conditions [10]. Cardew extended the diffusion model

with a convection term and applied it to laminar flow conditions [11]. Previous models,

except the exponential model, assumed that equilibrium lead concentrations were reached

at the pipe walls as a boundary condition. When the dissolution reaction is rate limiting,

dissolution rates rather than equilibrium need to be used set the boundary condition. Although the exponential model used a mass transfer rate, which has a similar impact as using a dissolution rate, the mechanistic rationale for using such a mass transfer rate was not explained [10]. In Kuch and Wagner's diffusion model for stagnant conditions, an additional mass transfer coefficient was used to fit the data based on the assumption that there could be a secondary layer of iron or manganese oxides on top of the lead corrosion product layer [8]. However, the assumption can only be valid when there is experimental evidence of a secondary top layer. The mass transfer models are all based on lead acting as a single species from a uniform source, whereas lead actually dissolves from different lead corrosion products in pipe scales.

In this chapter, mass transfer models incorporating dissolution rates as well as diffusion are developed and compared to predict lead release rates from pipe scales for stagnant and flow conditions. Lead release from pipe scales is predicted using the dissolution rates of individual lead corrosion products in pipe scales at different water chemistry conditions. The type, concentration, and surface area of two pipe scale components, PbO_2 and hydrocerussite, were considered in the proposed model to predict the lead release rates. The model also accounts for the impact of water chemistry for the calculation of dissolution rates.

2. Models of dissolved lead release from pipe scales
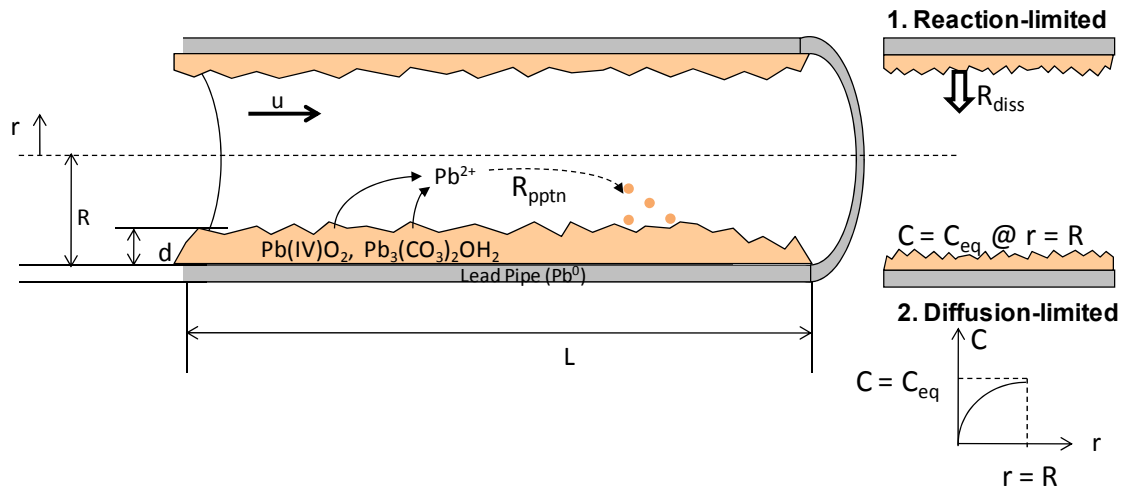
Figure 5A-1. Conceptual diagram of lead release from pipe scales. The parameters

shown in the diagram are listed in Table S1 of the Supporting Information.

Figure 5A-1 illustrates the dissolution and precipitation reactions and mass

transfer involving lead in a lead pipe. Dissolved lead release from pipe scales can be

viewed as dissolution of lead corrosion products in pipe scales. Inside the lead pipe, lead

is first dissolved from corrosion products (PbO_2 and hydrocerussite) in the pipe scales,

and then it diffuses to the bulk water. The dissolved lead can also precipitate and be

removed from solution.

A reversible dissolution-precipitation reaction $AB_{(s)} \Leftrightarrow A + B$ includes a forward

reaction (dissolution) and a backward reaction (precipitation). The dissolution and

precipitation reactions can be written as:

Dissolution: $$AB_{(s)} \xrightarrow{k_0} A + B$$

135

Precipitation: $\qquad\qquad\qquad A + B \xrightarrow{k_1} AB_{(s)}$

Where k_0 and k_1 are the dissolution and precipitation rate constants, respectively. The dissolution rate ($RATE_d$) can be derived from the rate constant

$$RATE_d = k_0 \cdot SSA \cdot [solids] \qquad\qquad (1)$$

Where SSA is the specific surface area of the dissolving solid, and [solids] is the solid content in the solution ($\frac{m_{solids}}{V_{solution}}$). The precipitation rate can be written as

$$RATE_p = k_1 \cdot \{A\} \cdot \{B\} \qquad\qquad (2)$$

At equilibrium, the forward dissolution rate should be equal to the backward precipitation rate. Therefore,

$$k_0 \cdot SSA \cdot [solids] = k_1 \cdot \{A\}_{eq} \cdot \{B\}_{eq} \qquad\qquad (3)$$

$$\frac{k_1}{k_0 \cdot SSA \cdot [solids]} = \frac{1}{\{A\}_{eq} \cdot \{B\}_{eq}} \qquad\qquad (4)$$

Therefore, the net rate of release from the solid ($RATE_{tot}$) is:

$$RATE_{tot} = RATE_d - RATE_p = k_0 \cdot SSA \cdot [solids] - k_1 \cdot \{A\} \cdot \{B\}$$

$$= k_0 \cdot SSA \cdot [solids] \cdot \left(1 - \frac{k_1 \cdot \{A\} \cdot \{B\}}{k_0 \cdot SSA \cdot [solids]}\right)$$

$$= k_0 \cdot SSA \cdot [solids] \cdot \left(1 - \frac{\{A\} \cdot \{B\}}{\{A\}_{eq} \cdot \{B\}_{eq}}\right) \qquad\qquad (5)$$

For undersaturated conditions, $RATE_{tot}$ is greater than zero because the precipitation rate is smaller than the dissolution rate.

In the lead release experiments, lead dissolves from PbO_2 and hydrocerussite in pipe scales, and the dissolution/precipitation reactions follow the same relationship assuming that the precipitation reaction is first order to lead and dissolution is first order

136

with respect to surface area. If the anions that are precipitating with lead are abundant with respect to dissolved lead, then Equation 5 can be simplified as:

$$RATE_{tot} = k_0 \cdot SSA \cdot [solids] \cdot \left(1 - \frac{\{Pb\}}{\{Pb\}_{eq}}\right) \tag{6}$$

The fact that the lead concentrations are on the order of 10^{-7} mol/L and other anions, such as carbonate, are on the order of 10^{-3} mol/L validates the assumption of abundant anions. Equation 6 is a classic rate model for dissolution and precipitation that has been employed in many dissolution/precipitation studies, including investigations of PbO_2 dissolution (Chapter 2) [12, 13].

In a pipe, dissolution is assumed to occur at the pipe wall where most lead solids are. Precipitation could occur anywhere in the pipe system. By assuming precipitation as a first order reaction, the precipitation rate is generally higher at positions close to pipe wall than at the center of the pipe since lead concentration is higher when closer to pipe wall. Therefore, the precipitation term accounted for the heterogeneity of the precipitation reaction in the solution.

Inside the pipe, the general mass balance equation for lead can be written as:

$$\frac{\partial C}{\partial t} = -(\nabla C \cdot V^*) - (\nabla \cdot J^*) - R_{pptn} \tag{7}$$

Where C (mol/L) is the dissolved lead concentration, t (s) is the time, V^* is the vector of velocity, and J^* is the vector of flux of lead from pipe scales, and R_{pptn} is the rate of precipitation of any lead-containing solid. In this equation, $\frac{\partial C}{\partial t}$ is the net rate of

accumulation of dissolved lead in moles per unit volume, $-(\nabla C \cdot V^*)$ is the rate of addition by convection, $-(\nabla \cdot J^*)$ is the rate of addition by diffusion.

Before proceeding to the specific models, the characteristic times for convection, diffusion, and reaction are compared. Such a comparison can help to distinguish which process is rate-limiting and whether any terms can be neglected. For experiments at flow conditions, the hydraulic residence time of the pipe section can be derived from the length of the pipe (L) and the velocity of the flowing water (u). In actual pipes of distribution systems, the velocity of the flowing water can range from 0 to higher than 1 m/s, which may result in laminar flow or turbulent flow.

$$\tau_f = \frac{L}{u} = \frac{24\ inch \times 0.0254\frac{m}{inch}}{360\ m/h} = 1.7 \times 10^{-3}\ h \tag{8}$$

The diffusion coefficient of lead in water is 1×10^{-9} m^2/s. Since the thickness of the scale (2.4×10^{-5} m) is much smaller than the radius of the pipe ($\sim 10^{-2}$ m), the time for diffusion of lead through the scale is negligible compared to the time for diffusion of lead from the pipe wall to the center of the pipe. The characteristic time of diffusion can then be calculated as

$$\tau_d = \frac{R^2}{D} = \frac{(\frac{3}{8}\ inch \times 2.54 \times 10^{-2}\frac{m}{inch})^2}{1 \times 10^{-9}\ m^2/s} = 9.07 \times 10^4\ s = 25.2\ h \tag{9}$$

The characteristic reaction time can be calculated as

$$\tau_r = \frac{C_{eq}}{R_{scale}} \tag{10}$$

Where C_{eq} is the equilibrium concentration of lead, R_{scale} is the total dissolution rate of lead from the corrosion products in pipe scales. C_{eq} is assumed to be equal to the lead concentration after 24 hours, which is a common assumption in previous studies. For the estimation of characteristic reaction time, $5.29*10^{-4}$ mol/m^3 lead (the 24-hour lead concentration in high DIC solution) is used. R_{scale} is calculated in a later section as the sum of dissolution rates of individual corrosion products, and it ranges from $1.6*10^{-6}$ to $7.0*10^{-7}$ mol/m^3–h at different water chemistry assuming 30% scale porosity. Depending on water chemistry, the characteristic reaction time ranges from 5.2 to 11.8 hours.

The characteristic reaction time is similar as the characteristic diffusion time. Both characteristic reaction time and characteristic diffusion time are much larger than the hydraulic residence time. Therefore, both the dissolution rate and diffusion can play important roles in mass transfer, and either one of them may control the rates of lead release. Therefore, dissolution rates need to be used in predicting lead concentrations released from pipe scales.

In this chapter, multiple models were developed and compared to predict the dissolved lead concentration released from pipe scales at stagnant and flowing conditions. At stagnant conditions, there is no convection term, so a diffusion-limited model and a reaction-limited model were built and compared. At flow conditions, dissolution rates of lead corrosion products in pipe scales are shown to control the dissolved lead concentrations and a mass transfer model incorporating dissolution rates and flow is proposed to predict lead release.

2.1 Modeling of lead release from pipe scales at stagnant conditions

At stagnant conditions, there is no convection term. The mass transfer equation of lead at stagnant conditions can be simplified as

$$\frac{\partial C}{\partial t} = -(\nabla \cdot J^*) + R_{pptn} \tag{11}$$

Where C (mol/L) is the dissolved lead concentration, t (s) is the time, J^* (mol/m^2-hr) is the vector of flux by diffusion, and R_{pptn} (mol/m^3-hr) is the rate of precipitation. In the tubular pipe, no concentration gradients in the axial or angular direction were assumed at stagnation conditions. The only concentration gradient is in the radial direction. Therefore, there is no net flux by diffusion in the axial or angular direction.

$$J^* = -D \cdot \nabla C \tag{12}$$

D is the diffusion coefficient of lead through water (3.6×10^{-6} m^2/hr) [9, 11].

Assuming precipitation is a first order reaction with respect to lead, the precipitation rate can then be written as

$$R_{pptn} = -k_1 \cdot C \tag{13}$$

Substituting Equations 12 and 13 into Equation 11 in cylindrical coordinate gives

$$\frac{\partial C}{\partial t} = D \cdot \nabla^2 C - k_1 \cdot C = D \left[\frac{\partial^2 C}{\partial r^2} + \frac{1}{r} \frac{\partial C}{\partial r} \right] - k_1 \cdot C \tag{14}$$

Equation 14 is the governing equation for both the reaction-limited model and the diffusion-limited model presented in sections 2.1.1 and 2.1.2, respectively. The only difference between these two models is the difference in the boundary conditions.

2.1.1 Reaction-limited model at stagnant conditions

For reaction-limited conditions, the dissolution of corrosion products in pipe scales provides a constant flux of lead to the bulk water. The net flux by diffusion of lead through water must equal the macroscopic dissolution rate per surface area of the pipe wall R_{diss} (mol/m²-h). The macroscopic dissolution rate can be related to the dissolution rates of individual corrosion products (PbO$_2$ and hydrocerussite) by Equation 15.

$$R_{diss} \cdot S = RATE_{scale} \cdot V_p = (RATE_{PbO_2} + RATE_{HC}) \cdot V_p \qquad (15)$$

Where S (m²) is the surface area of the interior pipe wall, V_p is the volume of the pipe (m³) and $RATE_{scale}$ (mol/m³-h) is the dissolution rate not normalized to surface area. HC denotes hydrocerussite.

The net flux of lead being the dissolution rate per surface area of pipe wall can be one of the boundary conditions, which is written as $-D \frac{\partial C}{\partial r} = -R_{diss}$ @ $r = R$. Since the pipe system is symmetric, the other boundary condition is $\frac{\partial C}{\partial r} = 0$ @ $r = 0$. The initial condition is C = 0 @ t = 0. Equation 14 can be solved numerically to get the dissolved lead concentration $C(r, t)$ as a function of t and r. The profile of lead concentration $C(r, t)$ over t and r in high DIC solution is illustrated in Figure 5A-2.
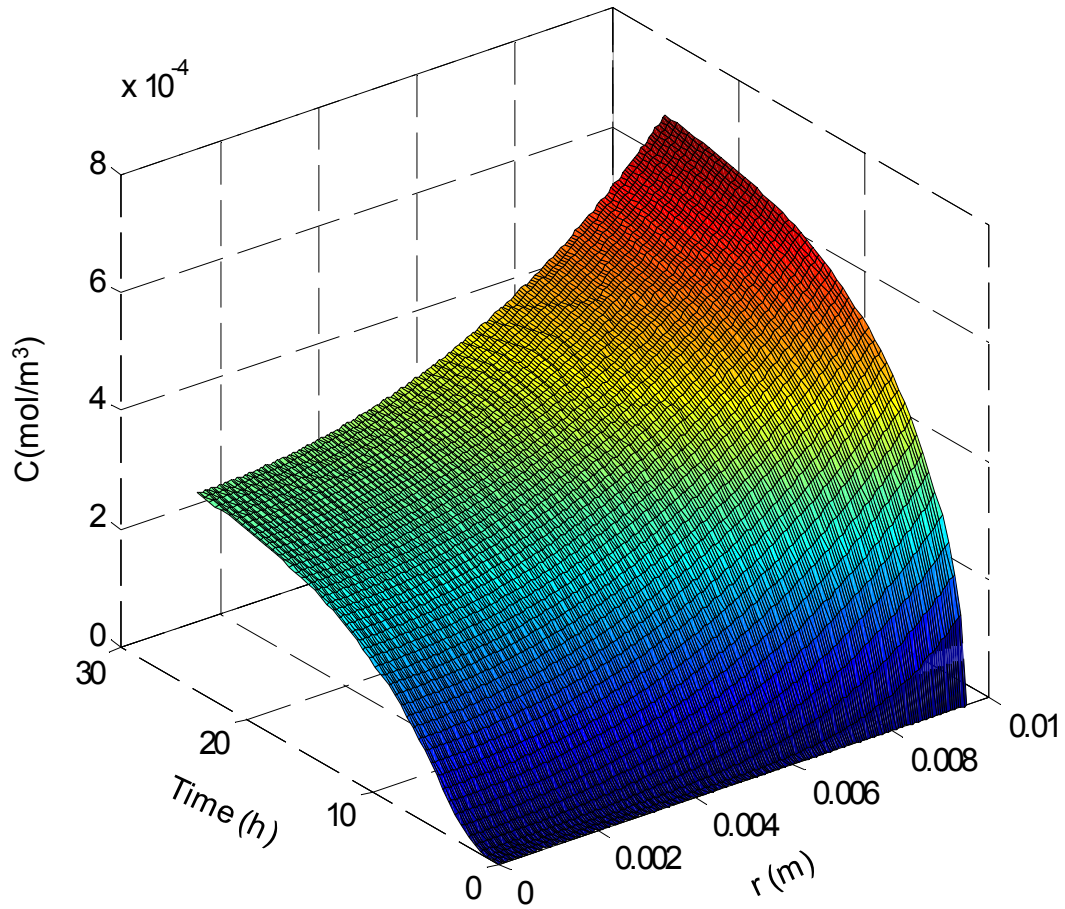
Figure 5A-2. Illustration of lead concentration profile with time and radial distance from the center of the pipe in high DIC solution using the reaction-limited model at stagnant conditions.

The sampled lead concentration is the average lead concentration over a cross section. The change of average lead concentration with time can be derived from the concentration profile by Equation 16.

$$\bar{C}(t) = \frac{\int_0^R 2\pi r C(r,t)dr}{\pi R^2} \qquad (16)$$

The evolution of $\bar{C}(t)$ with time can be solved numerically using MATLAB programming. There are two fitting parameters in this model, R_{diss} and k_1. k_1 can be related to R_{diss} by macroscopic mass balance at equilibrium. At equilibrium, the addition of lead by dissolution should be equal to the subtraction of lead by precipitation.

$$0 = R_{diss} \cdot S - k_1 \cdot C_{eq} V_p \tag{17}$$

Where V_p is the volume of the pipe. Therefore, the ratio of k_1 to R_{diss} is fixed.

$$\frac{R_{diss}}{k_1} = \frac{C_{eq} V_p}{S} \tag{18}$$

The values of k_1 and R_{diss} with constant ratio of R_{diss} to k_1 were varied to fit the experiment data with this model.

2.1.2   Diffusion-limited model at stagnation conditions

If diffusion is rate limiting, then equilibrium would be reached at the pipe wall after a short time. Consequently, the boundary condition for equilibrium at the pipe wall can be written as $C_0 = C_{eq}$ at $r = R$. Where C_{eq} is the equilibrium dissolved lead concentration, and R is the radius of the pipe. Another boundary condition is $\frac{\partial C}{\partial r} = 0$ at $r = 0$. The initial condition is $C = 0$ at t = 0.

The governing equation (Equation 14) is solved using MATLAB based on the boundary conditions. The numerical solution gives a lead concentration profile with time and radial distance (Figure 5A-3). Then, Equation 16 is used to get the average lead concentration over time.
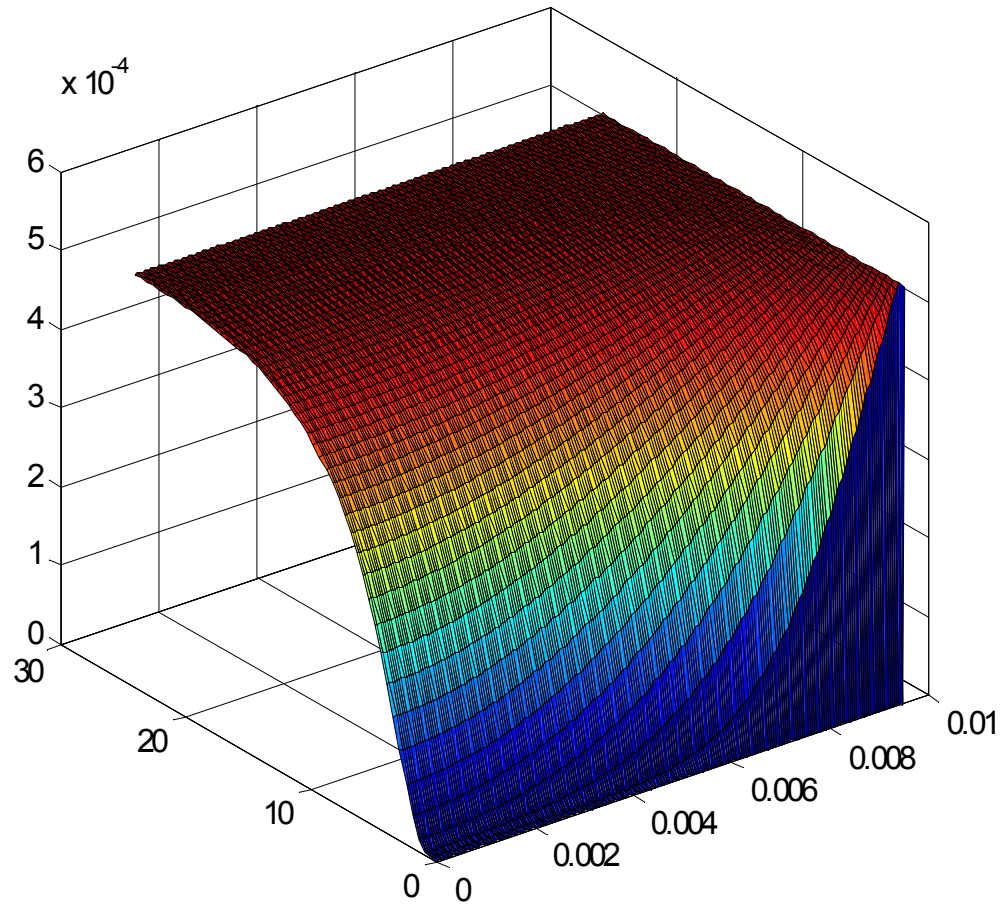
Figure 5A-3. Illustration of lead concentration profile with time and radial distance from the center of the pipe in high DIC solution using the diffusion-limited model at stagnant conditions.

2.1.3   Previous diffusion-limited model

Previous studies developed a diffusion-limited model with the assumption that equilibrium is reached at the pipe wall.

$$\frac{\partial C}{\partial t} = D\left[\frac{\partial^2 C}{\partial r^2} + \frac{1}{r}\frac{\partial C}{\partial r}\right] \qquad (19)$$

144

The boundary conditions are the same as the diffusion-limiting model in section 2.1.2. The solution of Equation 19 has been developed by Crank to describe the dependence of radial distance on concentration. The change of the volumetric average lead concentration over time (Equation 16) is more relevant, and has been studied by Kuch and Wagner [8].

$$\bar{C}(t) - C_{t=0} = \left(C_{eq} - C_{t=0}\right) \times \left\{1 - \sum_{s=1}^{\infty} \frac{4}{\alpha_s^2 R} \exp(-D\alpha_s^2 t)\right\} \qquad (20)$$

Where $\alpha_1, \alpha_2, \cdots, \alpha_s$ are positive roots of the equation $J_0(R\alpha) = 0$, where J_0 is the Bessel function of the first kind of zero order. Based on Equation 17, the average lead concentration profile only depends on the equilibrium lead concentration and time for a known pipe inner diameter and diffusion coefficient. Since equilibrium lead concentration can be determined and is often calibrated to measured lead concentrations after 24 hours, the lead concentration profile is hard to match the experimental observation with no fitting parameters [8, 9]. An addition parameter β_a, which accounts for additional resistance from a secondary layer of deposits (e.g. iron or manganese oxides) on top of the pipe scales, was introduced to fit the experimental data better. In previous studies, a simplified equation incorporating a coefficient of additional resistance β_a has been developed to simplify Equation 20 and is used in fitting experimental data [8].

$$\frac{\bar{C}(t) - C_{t=0}}{C_{eq} - C_{t=0}} = 1 - \exp \frac{-4F_o{'}}{\frac{1}{Bi{'}} + \frac{1}{\sqrt{(5.78)^2 + \frac{1}{\pi}\frac{1}{F_o{'}}}}} \qquad (21)$$

Where Bi' is the Biot number (Equation 22), and Fo' is the Fourier number (Equation 23).

$$Bi' = \frac{\beta_a 2R}{D} \tag{22}$$

Where β_a is the coefficient of additional resistance caused by a second layer of corrosion deposits on the inner surface of the pipe. The Biot number gives the ratio of the mass-transfer rate at the interface to the mass-transfer rate in the interior of the second layer of corrosion deposits.

$$F_o' = \frac{Dt}{4R^2} \tag{23}$$

The Fourier number represents the ratio of the rate of diffusion transport to the rate of accumulation.

2.2 Modeling of lead release from pipe scales at flow conditions

At flowing conditions, a recirculation system including a tubular pipe and a reservoir is used in the present study. To simplify the system (Figure 5A-4), the pipe can be considered as a plug flow reactor (PFR), while the reservoir acts as a continuously-stirred tank reactor (CSTR).
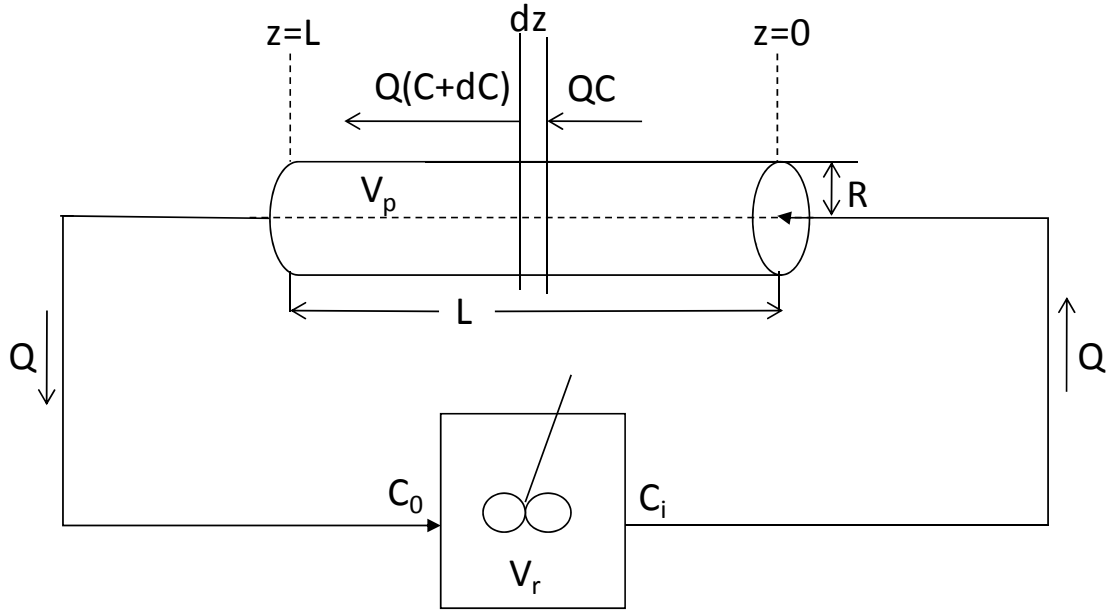
Figure 5A-4. Schematic of the recirculation system at flow conditions.

2.2.1 Reaction-limited model at flow conditions

For the reservoir (CSTR),

$$\frac{d(C_i \cdot V_r)}{dt} = QC_0 - QC_i + R_{pptn} \cdot V_r \tag{24}$$

$$\frac{dC_i}{dt} = \frac{Q}{V_r}(C_0 - C_i) - k_1 \cdot C_i \tag{25}$$

Where $\frac{Q}{V_r}$ is the hydraulic residence time τ_c for the reservoir.

For the pipe (PFR), lead concentration at a finite cross section (dz) is assumed to reach pseudo-steady-state with respect to the hydraulic residence time of the pipe τ_p, since τ_p (6 seconds) is much smaller than the characteristic diffusion time (hours) and the characteristic reaction time (hours). Therefore, the change of lead concentration in each

147

finite pipe cross section over hydraulic residence time of the pipe τ_p can be neglected.

Lead concentration does change over the length of the pipe since lead is dissolving, which is accounted in Equation 27.

$$\frac{\pi R^2 \cdot L \cdot dC}{dt} = 0 = Q \cdot C - Q \cdot (C + dC) + 2\pi R \cdot dz \cdot R_{diss} - \pi R^2 \cdot dz \cdot k_1 \cdot C \quad (26)$$

Simplifying Equation 26 yields

$$Q \cdot dC = (2\pi R \cdot R_{diss} - \pi R^2 \cdot k_1 \cdot C) \cdot dz \quad (27)$$

The boundary conditions are C = C_i @ z = 0 and C = C_0 at z = L.

Solving the equation yields

$$C_0 = \frac{2R_{diss}}{Rk_1}\left[1 - \exp\left(-\frac{\pi R^2 L k_1}{Q}\right)\right] + C_i \cdot \exp\left(-\frac{\pi R^2 L k_1}{Q}\right) \quad (28)$$

Where $\frac{\pi R^2 L}{Q}$ is the hydraulic residence time τ_p of the pipe section. Equation 28 indicates

that the dissolution and precipitation reactions result in a concentration difference

between inlet and outlet of the pipe. Plugging Equation 28 into Equation 25 gives

$$\frac{dC_i}{dt} = \frac{1}{\tau_c}\left\{\frac{2R_{diss}}{Rk_1} \cdot [1 - \exp(-k_1\tau_p)] + C_i \cdot \exp(-k_1\tau_p) - C_i\right\} - k_1 \cdot C_i \quad (29)$$

Although the change of lead concentration in each finite pipe cross section over hydraulic

residence time of the pipe (τ_p) can be neglected, Equation 29 shows that lead

concentration does accumulate over a longer period of time.

The initial condition is C_i = 0 @ t = 0. Equation 29 can be solved analytically,

and the solution is given below.

$$C_i = \frac{\frac{1}{\tau_c} \cdot \frac{2R_{diss}}{Rk_1} \cdot [1 - \exp(-k_1\tau_p)]}{-k_1 - \frac{1}{\tau_c} \cdot [1 - \exp(-k_1\tau_p)]} \cdot \left\{\exp\left\{\left\langle -k_1 - \frac{1}{\tau_c} \cdot [1 - \exp(-k_1\tau_p)]\right\rangle \cdot t\right\} - 1\right\} \quad (30)$$

Since the precipitation rate constant k_1 can be determined from fitting the reaction-limited model at stagnant conditions with experimental data, the only fitting parameter is the dissolution rate R_{diss}.

3. Results and Discussion

In diffusion-limited models, lead concentrations were assumed to reach equilibrium after 24 hours of stagnation, which is a common assumption in previous models [9-11]. To compare the reaction-limited model with diffusion-limited models at stagnation condition, equilibrium lead concentrations were assumed to be equal to the lead concentrations after 24 hours at stagnation condition.

In the model fitting, only experimental data for the high DIC and high pH solutions were used in most of the cases, since the dissolution rates of both PbO_2 and hydrocerussite at only these two conditions were available. In the previous diffusion-limited model, extra data for the high monochloramine solution was used together with the data for the high DIC and high pH solutions since dissolution rate is not needed.

3.1 Prediction of lead release from stagnation experiments

The fitting results by one reaction-limited model and two diffusion-limited models were compared.

3.1.1 Predicted lead release by the reaction-limited model at stagnant conditions

Figure 5A-5 shows the predicted lead release profile based on the reaction-limited model together with the experimental data. The predicted lead release profiles are quite close to the experimental data. Because the reaction-limited model uses the mass transfer equation (Eqn. 14), it accounts for diffusion. The main difference between the reaction-limited model and the diffusion-limited model is different boundary conditions.

Figure 5A-5. Comparison of the predicted lead release profiles by the reaction-limited model and the experimental lead release profiles at stagnant conditions. The points are experimental dissolved lead concentrations, and the lines are predicted lead release profiles. High pH and High DIC in the graph refer to the high pH solution and high DIC solution, respectively.

The best fit values of k_1 and R_{diss} are included in Table 5A-1. Only R_{diss} value was varied to optimize the fit and the k_1 value was constrained by the R_{diss} value. Comparison of R_{diss} values among different water chemistries shows that the lead release

rate is highest for high DIC solution and lowest at high pH solution, which is consistent

with the relationship between determined dissolution rates of PbO_2 and hydrocerussite

and pH or DIC in the CFSTR studies (Chapter 2).

Table 5A-1. Fitted values of dissolution rate R_{diss} and precipitation rate constant k_1.

	R_{diss} (mol/m^2-hr)	k_1 (/hr)	C_{eq} (mol/m^3)	V_p/S (m)
High pH	1.50E-07	8.75E-02	3.60E-04	4.76E-03
High DIC	3.40E-07	1.35E-01	5.29E-04	4.76E-03

3.1.2   Predicted lead release by the diffusion-limited model at stagnant conditions
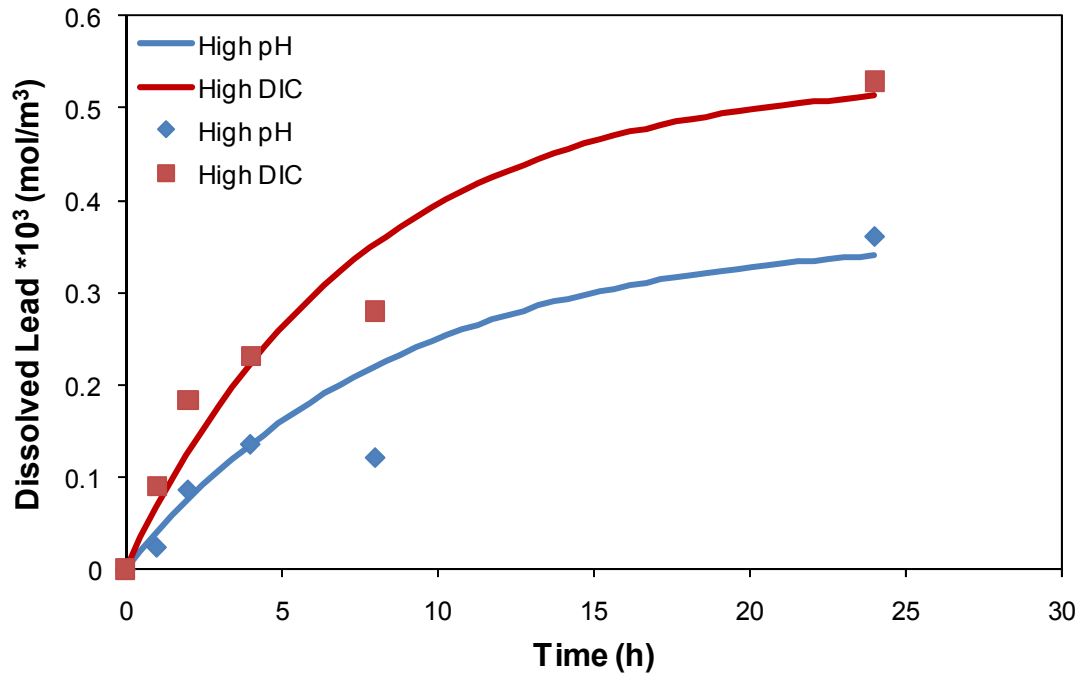

Figure 5A-6. Comparison of the predicted lead release profiles by the diffusion-limited model and the experimental lead release profiles at stagnant conditions. The points are experimental dissolved lead concentrations, and the lines are predicted lead release profiles. High pH and High DIC in the graph refer to the high pH solution and high DIC solution, respectively.

The diffusion-limited model overpredicted the lead release for all solutions, especially at the beginning several hours (Figure 5A-6). The overprediction by the diffusion-limited model indicates that diffusion from a wall with concentrations at equilibrium solubility allows higher lead release than the experimental lead release. Therefore, diffusion was not rate-limiting in the experiments of lead release from pipe scales.

3.1.3 Fitting of lead release data by the diffusion-limited model developed by Kuch and Wagner

The use of this model is limited to conditions without significant precipitation, since this model does not consider precipitation as a sink. Therefore, it would not predict the lead release well for the high phosphate and high free chlorine solution because precipitation may be significant in these two solutions. In this model fitting, only lead release data in high pH, high DIC, and high chloramines solutions were used since precipitation in these three solutions could be negligible.

Figure 5A-7 shows the diffusion model fitting results by least squares optimization of the β_a term. The model result generally describes the experimental data for all three concentrations. The best fit β_a values range from 1×10^{-7} to 3×10^{-7} m/s, which is not uniform among all solutions and indicates that the model cannot explain the experimental results well by a uniform β_a value. The fitted β_a values are consistent with the fitted β_a values (4.4×10^{-8} to 5.8×10^{-6}) in Lytle and Schock's study, and the fitted

β_a values in Lytle and Schock's work varied over a broader range. Lytle and Schock reached the same conclusion as the present study that this diffusion-limited model by Kuch and Wagner is not a good predictive tool for estimating stagnation behavior, although the fitting of β_a allows the diffusion model to describe the lead release from pipe scales. This conclusion here can be further explained by experimental evidence. The physical meaning of β_a is additional resistance by a secondary layer (such as iron or manganese oxides), which indicates the models are best suited to pipe scales with a secondary layer of iron or manganese oxides. For the lead pipe scales used in the present study, no secondary layer was found, which hinders the ability to explain the experimental data with this model.
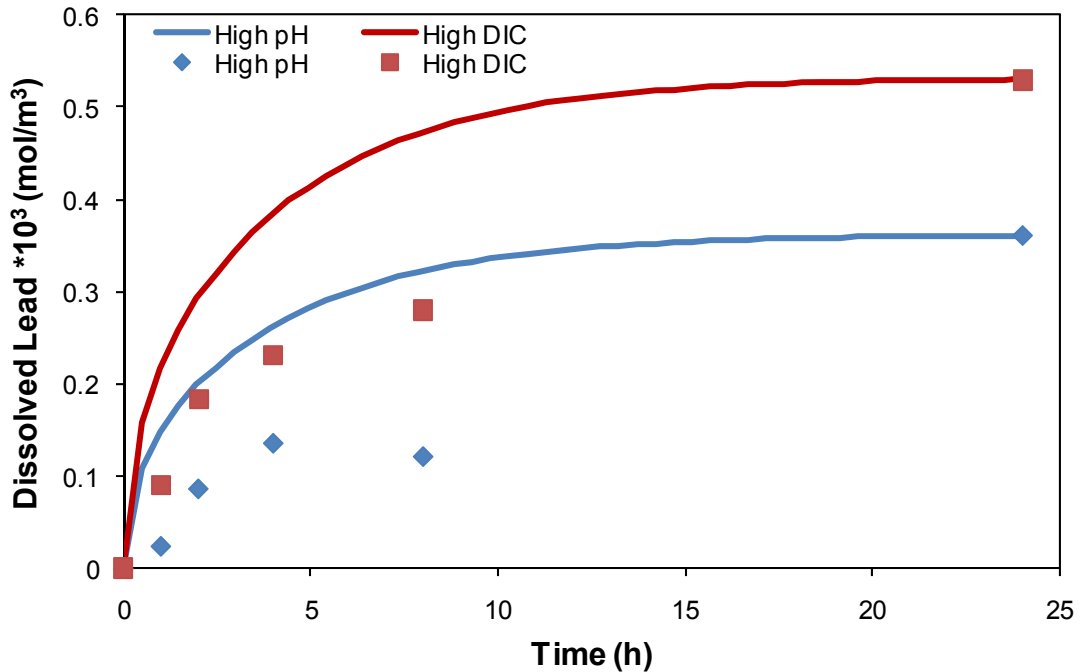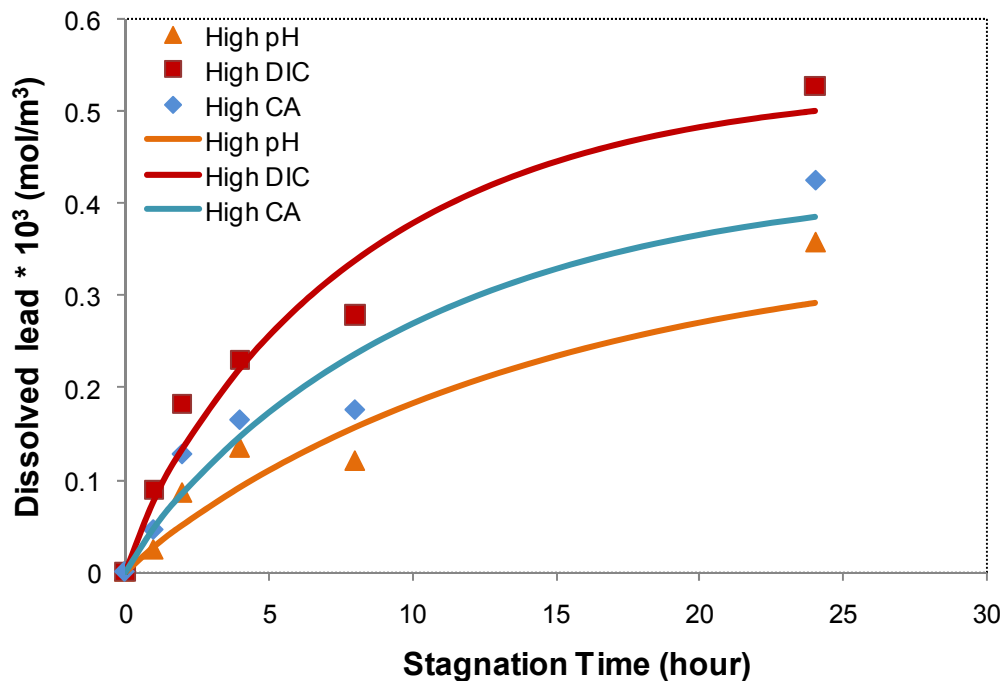

Figure 5A-7. Comparison of the predicted lead release profiles by the diffusion-limited model and the experimental lead release profiles. The points are experimental dissolved lead concentrations, and the lines are predicted lead release profiles. High pH, High DIC,

and High CA in the graph refer to the high pH solution, high DIC solution, and high monochloramine solution, respectively.

The comparison of these three models showed that the reaction-limited model fits the experimental data best with reasonable explanation. Therefore, the stagnant experiments were probably reaction-limited.

3.2. Prediction of lead release in flow experiments

The model fitting of the stagnant experiments showed that the lead release rates from pipe scales were limited by dissolution reaction rather than by diffusion. The pipe system with flowing water has better transport properties than the pipe system with stagnant water. Therefore, the reaction should also be the rate-limiting step in flow experiments.

3.2.1 Fitting of experimental data with the reaction-limited model at flow conditions

The predicted lead release profile matches very well with the experimental lead release in the first 2 hours (Figure 5A-8a). The fitting and simplification of the analytical solution showed that the lead release in the first two hours depends mostly on the dissolution rates R_{diss}, which explained why the lead release profile in the first two hours was close to linear with time. The precipitation term is negligible because the concentrations in the first two hours were far below equilibrium solubility. Although the fitted curves match well with the experimental data, there are uncertainties in the fitted

R_{diss} values since limited experimental data were obtained for the purpose of the present study. Recirculation experiments lasting for a longer time are recommended to further verify the prediction of the reaction-limited model at flow conditions (Figure 5A-8b).
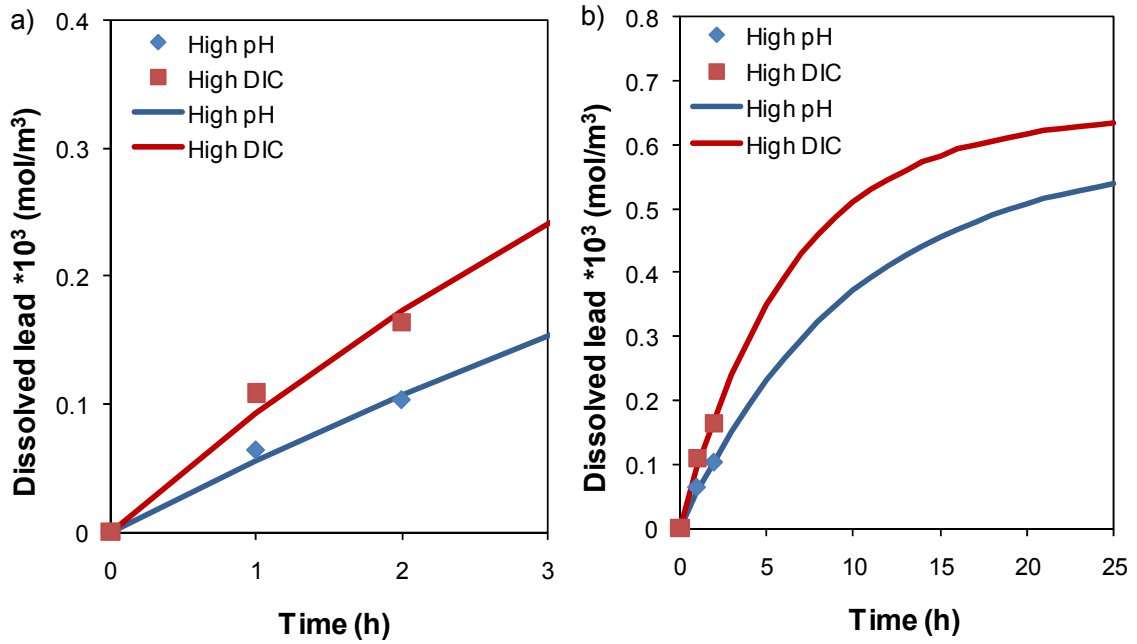
Figure 5A-8. Comparison of the predicted lead release profiles for a) 2 hours and b) 24 hours by the reaction-limited model and the experimental lead release profiles at flow conditions. The points are experimental dissolved lead concentrations, and the lines are predicted lead release profiles. High pH and High DIC in the graph refer to the high pH solution and high DIC solution, respectively.

The best fit values of R_{diss} are included in Table 5A-2. Comparison of R_{diss} values among different water chemistries shows that the total lead release rate is higher for the high DIC solution than for the high pH solution, which is consistent with the relationship between determined dissolution rates of PbO_2 and hydrocerussite and pH or DIC from CFSTR studies.

Table 5A-2. Fitted R_{diss} values by the reaction-limited model for flow experiments using k_1 values obtained from stagnation experiments.

	R_{diss} (mol/m²-hr)	k_1 (/hr)
High pH	1.84E-06	8.75E-02
High DIC	3.13E-06	1.35E-01

3.3. Mechanistic explanation of fitted rates

3.3.1 Derivation of observed rates from dissolution rates of corrosion products

The macroscopic fitted dissolution rate can be related to the sum of dissolution rates of individual corrosion products in pipe scales (Equation 15). The dissolution rates of individual corrosion products in pipe scales can be calculated from the determined surface area normalized rates of PbO_2 dissolution in CFSTR studies in Chapters 2, 3 and 4 and the surface area normalized rates of hydrocerussite dissolution.

From X-ray diffraction analysis, the pipe scales consist of hydrocerussite ($Pb_3(CO_3)_2(OH)_2$), plattnerite (β-PbO_2), and scrutinyite (α-PbO_2), and elemental lead. Since the Gibbs free energy of scrutinyite is similar to that of plattnerite, the surface area normalized dissolution rate constants of scrutinyite and plattnerite are assumed to be the same. The SEM images of the scale material provided evidence that elemental lead is isolated from water by a 24 µm thick scale of lead corrosion products. The elemental lead identified in the sample pattern was probably introduced to the sample by cutting and scraping during collection of scale materials. Assuming no elemental lead in pipe

scales, the overall dissolution rates from pipe scales can then be derived from the

dissolution rates of hydrocerussite and PbO_2 as follows:

$$RATE_{scale} = RATE_{PbO_2} + RATE_{HC} \qquad (31)$$

Where $RATE_{scale}$ (mol/L-min) is the net rate of lead release from pipe scales, $RATE_{PbO_2}$

(mol/L-min) is the dissolution rate of PbO_2, $RATE_{HC}$ (mol/L-min) is dissolution rate of

hydrocerussite.

The volumetric dissolution rates of individual lead corrosion products can be

determined from the surface area normalized dissolution rates, the solid contents, and the

effective specific surface areas in the following equation.

$$RATE = rate \cdot [\text{solids}] \cdot \theta \cdot \text{SSA} \qquad (32)$$

Where *rate* (mol/m^2-min) is the surface area normalized dissolution rate, *[solids]* (g/L) is

the solid content ($\frac{m_{solids}}{V_{solution}}$), *SSA* (m^2/g) is the specific surface area, θ is the effective

solid-water contact ratio of the whole surface area for hydrocerussite or PbO_2. The

specific surface area of individual corrosion product can be estimated according to the

geometries of the hydrocerussite and PbO_2 particles.

The surface area normalized dissolution rates of plattnerite (β-PbO_2) have been

determined in Chapters 2, 3, and 4. The surface area normalized dissolution rates of

hydrocerussite have been determined by Noel and Giammar [14, 15]. The surface area

normalized rate is specific to water chemistry. Among the five water chemistries

examined for lead release from pipe scales, the dissolution rates of both plattnerite and

hydrocerussite have been determined in two water chemistries (high pH solution and high

157

DIC solution). Therefore, we are only able to use the dissolution rates of both plattnerite and hydrocerussite at these two water chemistries to predict lead release from pipe scales. To predict lead release at other conditions, the dissolution rates of PbO_2 and hydrocerussite at these exact conditions need to be determined.

The total solid content can be calculated as follows.

$$[solids]_{tot} = \frac{\rho_{solids} \cdot V_{solids}}{V_{solution}} = \frac{\rho_{solids} \cdot (1 - \eta) \cdot V_{scale}}{V_{solution}}$$

$$= \frac{\rho_{solids} \cdot (1 - \eta) \cdot 2\pi \cdot r \cdot d \cdot L}{\pi \cdot r^2 \cdot L} = \frac{\rho_{solids} \cdot (1 - \eta) \cdot 2d}{r} \qquad (33)$$

Where ρ_{solids} (g/m^3) is the density of the solids in the scale, V_{solids} (m^3) is the volume of solids in pipe scale, $V_{solution}$ (m^3) is the volume of solution in the pipe section, V_{scale} (m^3) is the total volume of pipe scale including pores, η is the porosity of the scales, d (m) is the thickness of the scale, r (m) is the inner diameter, and L (m) is the length of the pipe.

$$\rho_{solids} = \frac{\rho_{HC} \cdot \rho_{PbO_2}}{\alpha_{PbO_2} \cdot \rho_{HC} + \alpha_{HC} \cdot \rho_{PbO_2}} = 7.09 \times 10^6 \ (g/m^3) \qquad (34)$$

Where α_{PbO_2} is the molar percentage of the PbO_2 in the corrosion products of the scales, ρ_{PbO_2} (9.06×10^6 g/m^3) is the density of pure PbO_2, α_{HC} is the molar percentage of the PbO_2 in the corrosion products of the scales, and ρ_{HC} (6.8×10^6 g/m^3) is the density of pure hydrocerussite. α_{PbO_2} and α_{HC} were determined by X-ray absorption near edge spectroscopy (XANES). Figure 5A-9 shows the XANES spectra of the scale material and the reference spectra of PbO_2, hydrocerussite, and elemental lead. The linear combination fitting of the sample XANES spectra gave a molar percentage of 14 %

Pb(IV), 67% Pb(II), and 19% Pb(0). The goodness-of-fit can also be seen from the

reduced chi-square value of 0.001. Assuming no actual elemental lead in pipe scales and

that all of Pb(II) is present as hydrocerussite, the composition of the pipe scales in molar

percentage is 38.5% PbO_2 and 61.5% hydrocerussite.
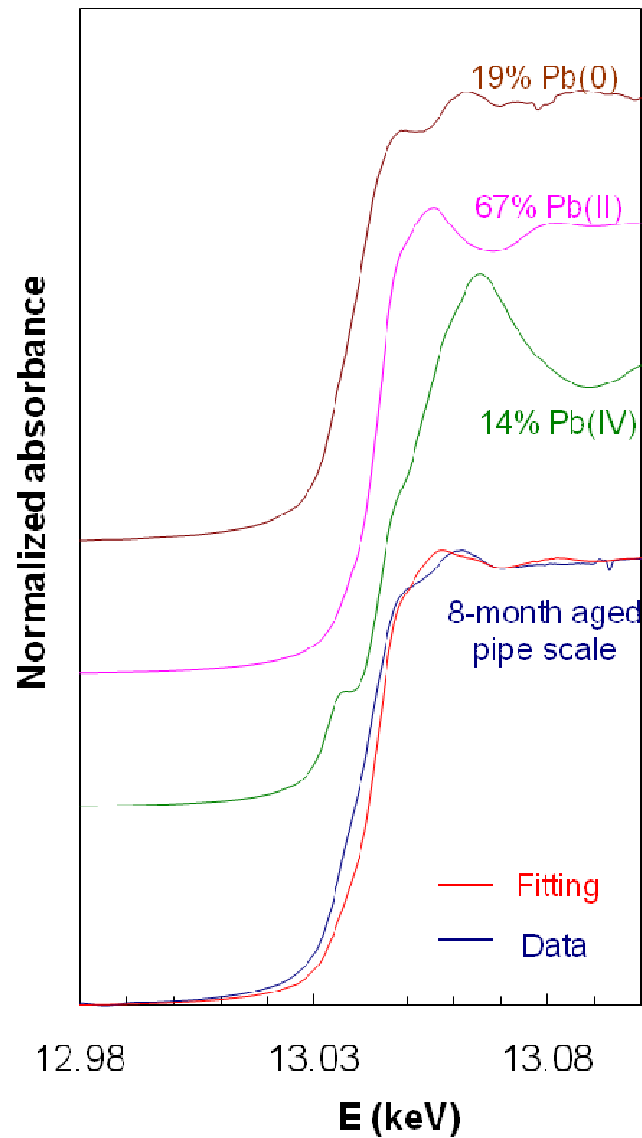
Figure 5A-9. Linear combination fitting of the pipe scale XANES spectrum using reference spectra of PbO_2, hydrocerussite, and elemental lead. The percentages shown are the molar lead percentage of each end member in the pipe scale.

Therefore,

$$[solids]_{tot} = \frac{(1 - \eta) \times 7.09 \times 10^6 \frac{g}{m^3} \times 2 \times 24 \times 10^{-6} m}{\frac{3}{8} inch \times 2.54 \times 10^{-2} \frac{m}{inch}}$$

$$= 3.58 \times 10^4 \times (1 - \eta) \left(\frac{g}{m^3}\right) \tag{35}$$

The solid content of each solid, hydrocerussite or PbO_2, can then be calculated based on their densities and molar percentages.

$$[solids]_{PbO_2} = \beta_{PbO_2} \cdot [solids]_{tot}$$

$$= \frac{\alpha_{PbO_2} \cdot M_{PbO_2}}{\alpha_{PbO_2} \cdot M_{PbO_2} + \alpha_{HC} \cdot M_{HC}} [solids]_{tot} = 16.2\% [solids]_{tot} \tag{36}$$

$$[solids]_{HC} = \beta_{HC} [solids]_{tot}$$

$$= \frac{\alpha_{HC} \cdot M_{HC}}{\alpha_{PbO_2} \cdot M_{PbO_2} + \alpha_{HC} \cdot M_{HC}} [solids]_{tot} = 83.8\% [solids]_{tot} \tag{37}$$

The specific surface area of hydrocerussite and PbO_2 can be estimated from the geometry of the hydrocerussite and PbO_2 particles. From SEM images, average PbO_2 particles are estimated to be cubic particles with 100 nm sides (a), and hyrocerussite particles are approximated by thin hexagonal plates with side length (b) of 1 μm and height (h) of 200 nm. Then, the specific surface of PbO_2 can be derived from the volume of an individual PbO_2 particle divided by its mass.

$$SSA_{PbO_2} = \frac{S_{PbO_2}}{m_{PbO_2}} = \frac{6a^2}{\rho_{PbO_2} \cdot \pi a^3} = \frac{6}{\rho_{PbO_2} \cdot \pi a}$$

$$= \frac{6}{9.06 \times 10^6 \frac{g}{m^3} \times 3.14 \times 10^{-7} m} = 2.11 \frac{m^2}{g} \tag{38}$$

Similarly, the specific surface area of hydrocerussite can be derived from the volume of an individual hydrocerussite particle divided by its mass.

$$SSA_{HC} = \frac{S_{HC}}{m_{HC}} = \frac{3\sqrt{3}b^2 + 6bh}{\rho_{HC} \cdot \frac{3\sqrt{3}b^2h}{2}} = \frac{2\sqrt{3}b + 4h}{\rho_{HC} \cdot \sqrt{3}bh}$$

$$= \frac{2\sqrt{3} \times 1 \times 10^{-6}m + 4 \times 2 \times 10^{-7}m}{6.8 \times 10^6 \frac{g}{m^3} \times \sqrt{3} \times 10^{-6}m \times 2 \times 10^{-7}m} = 1.81 \frac{m^2}{g} \qquad (39)$$

Therefore, the estimated volumetric dissolution rates (mol/m³-h) are

$$RATE_{PbO_2} = rate_{PbO_2} \cdot [solids]_{PbO_2} \cdot \theta_{PbO_2} \cdot SSA_{PbO_2}$$

$$= 16.2\% \times 3.58 \times 10^4 \times (1 - \eta)\frac{g}{m^3} \times 2.12 \frac{m^2}{g} \times \theta_{PbO_2} \cdot r_{PbO_2}$$

$$= 1.23 \times 10^4 m^{-1} \times (1 - \eta)\theta_{PbO_2} \cdot r_{PbO_2} \qquad (40)$$

$$RATE_{HC} = rate_{HC} \cdot [solids]_{HC} \cdot \theta_{HC} \cdot SSA_{HC}$$

$$= 83.8\% \times 3.58 \times 10^4 \times (1 - \eta)\frac{g}{m^3} \times 1.81 \frac{m^2}{g} \times \theta_{HC} \cdot r_{HC}$$

$$= 5.43 \times 10^4 m^{-1} \times (1 - \eta)\theta_{HC} \cdot r_{HC} \qquad (41)$$

Where $rate_{PbO_2}$ is the surface area normalized dissolution rate of PbO_2 determined in CFSTR experiments (Chapters 2), and r_{HC} is the surface area normalized dissolution rate of hydrocerussite determined in CFSTR experiments by Noel et al [14]. The surface area normalized dissolution rates are listed in Table 5A-3.

Table 5A-3. Surface area normalized dissolution rates of PbO_2 and hydrocerussite in CFSTR experiments.

Solution	$rate_{PbO_2}$ (mol/m²-h)	r_{HC} (mol/m²-hr)
High DIC	2.86E-08	1.70E-07
High pH	1.05E-08	7.56E-08

Therefore, the volumetric dissolved lead release rate (mol/m³-h) from pipe scales can be estimated by the sum of the dissolution rates of hydrocerussite and PbO_2 in the absence of orthophosphate.

$$RATE_{scale} = RATE_{PbO_2} + RATE_{HC}$$

$$= 1.23 \times 10^4 m^{-1} \cdot (1 - \eta)\theta_{PbO_2} \cdot r_{PbO_2} +$$

$$5.43 \times 10^4 m^{-1} \cdot (1 - \eta)\theta_{HC} \cdot r_{HC} \qquad (42)$$

3.3.2 Role of contact ratio in lead release rates from pipe scales

Combining macroscopic fitted dissolution rates with microscopic total dissolution rates, we can obtain the contact ratio from the following equation.

$$R_{diss} \cdot S = RATE_{scale} \cdot V_p \qquad (43)$$

Where R_{diss} (mol/m²-h) is the dissolution rate per unit surface area of the pipe wall, S (m²) is the surface area of interior pipe wall, $RATE_{scale}$ (mol/m³-h) is the net volumetric dissolution rate from pipe scales, and V_p (m³) is the volume of the pipe.

For a known pipe, the porosity of scales η is fixed, and it is estimated to be from 10% to 70% based on the SEM images of the pipe scales. Assuming the contact ratios

162

θ_{PbO_2} and θ_{HC} are the same for a fixed water chemistry and flow condition, the contact

ratio can then be derived from Equation 44.

$$\theta = \frac{R_{diss} \cdot S}{(1.23 \times 10^4 m^{-1} \cdot r_{PbO_2} + 5.43 \times 10^4 m^{-1} \cdot r_{HC}) \cdot V_p} \cdot (1 - \eta)^{-1} \qquad (44)$$

Where the values of r_{HC} and $rate_{PbO_2}$ are listed in Table 5A-3.

Table 5A-4. The contact ratios for different water chemistries at stagnant and flow
conditions

	Stagnation		Flow	
Conditions	Contact Ratio θ	Fitted R_{diss}	Contact Ratio θ	Fitted R_{diss}
pH	7.43E-03$(1-\eta)^{-1}$	1.50E-07	6.9E-02$(1-\eta)^{-1}$	1.84E-06
DIC	7.48E-03$(1-\eta)^{-1}$	3.40E-07	9.1E-02$(1-\eta)^{-1}$	3.13E-06

For all water chemistries, the contact ratios increased about one order of

magnitude at flow conditions compared to those at stagnant conditions (Table 5A-4).

The reason why flow increased lead release rates by one order of magnitude is probably

that mixing of water with solids is better at flow conditions than at stagnant conditions,

which is indicated by the higher contact ratio at flow conditions. A recent experimental

study has shown that immobile water inside porous pipe scales is not well mixed with

bulk water (Figure 5A-10). The immobile water contains high solute concentrations

released from scales, and it exchanges solutes more rapidly with the bulk water at flow

conditions [16]. The fact that contact ratio is much higher at flow conditions than

stagnant conditions is consistent with better mixing of the steady water at flow

conditions.
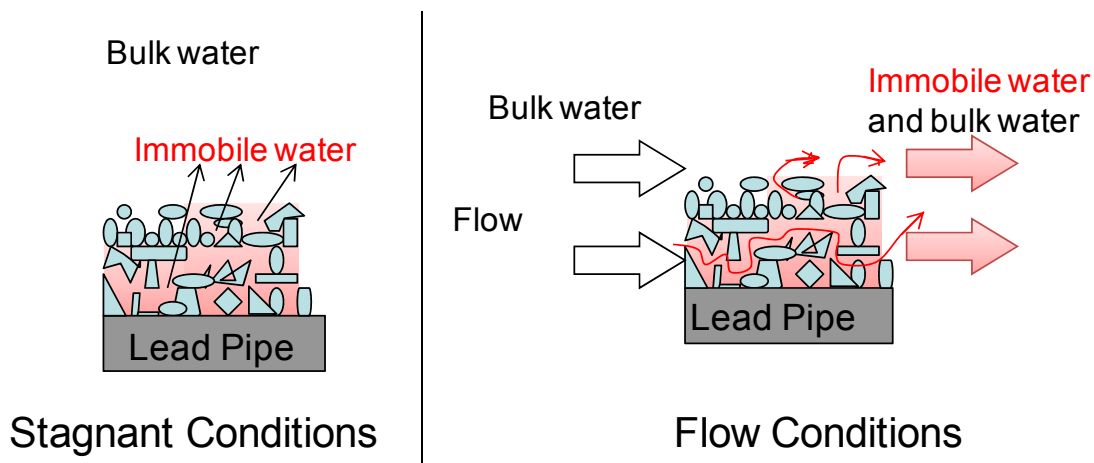
Figure 5A-10. Illustration of the effect of flow on effective water-solid contact ratio and lead release from porous pipe scales. The red area indicates zones with immobile water that are not readily exchanged with the bulk water at stagnant condition. At flow conditions, bulk water mixes better with porous scales (larger contact area) and brings out the immobile water that has high lead concentrations released from scales.

For different water chemistries at the same flow condition, the contact ratios are very similar. The little variation of the contact ratio at flow condition could be caused by the uncertainty introduced by limited data points. The uniform contact ratio at the same flow condition provide further support that the dissolution rates of individual corrosion products were proportional to the surface area of solids in contact with water and can be used in predicting lead release from pipe scales.

4. Conclusion

Reaction-limited models for stagnation and flow are more accurate than diffusion models in predicting the lead release from pipe scales containing PbO_2 and hydrocerussite. Hence, the lead release is probably surface reaction limited. The measured surface area normalized dissolution rates can be incorporated into mass transfer

164

models to quantify and interpret the lead release from pipe scales. To fully predict the lead release rates from pipe scales, the porosity of pipe scales and the contact ratios of water with corrosion products in pipe scales need to be determined at different flow conditions.

Supporting Information

Table S1. Parameters used in the model

Parameters	Physical Meaning	Dimensions
$RATE_d$	Dissolution rate	mol/m^3-hr
$RATE_d$	Precipitation rate	mol/m^3-hr
$RATE_{tot}$	Overall accumulation rate	mol/m^3-hr
k_0	Dissolution rate constant	mol/m^2-hr
k_1	Precipitation rate constant	/hr
SSA	Specific surface area of a solid	m^2/g
$\{A\}$	Activity of A	mol/m^3
$\{A\}_{eq}$	Equilibrium activity of A	mol/m^3
R	Radius of the pipe	m
r	Radial distance from the center of the pipe	m
D	Difussion coefficent	m^2/hr
u	Flow velocity	m/hr
τ_f	Hydraulic residence time	hr
τ_d	Characteristic diffusion time	hr
τ_r	Characteristic dissolution reaction time	hr
R_{diss}	Macroscopic dissolution rate per unit surface area of the pipe wall	mol/m^2-hr
R_{pptn}	Precipitation rate	mol/m^3-hr
C	Concentration of soluble lead	mol/m^3
C_{eq}	Equilibrium concentration of lead	mol/m^3
$\bar{C}(t)$	Volumetric average concentration of lead	mol/m^3
t	time	hr
β_a	Coefficient of additional resistance	m/s
Bi'	Biot number	
F_o'	Fourier number	
Q	Volumetric flow rate	m^3/hr
C_i	Pipe influent lead concentration	mol/m^3

C_0	Pipe effluent lead concentration	mol/m^3
V_p	Volume of Pipe	m^3
V_r	Volume of Resevoir	m^3
S	Surface area of interior pipe wall	m^2
z	Distance from the end of the pipe	m
M	Molecular weight	g/mol
α	Molar percentage	
ρ	Density	g/m^3
β	mass percentage	
a	PbO_2 particle side length	m
b	Hydrocerussite particle side length	
h	Hydrocerussite particle height	m
[solids]	Solid concentration/content	g/m^3
$J*$	Flux vector by diffusion	$mol/m^2\text{-hr}$
$RATE_{scale}$	Volumetric dissolution rate of pipe scales	$mol/m^3\text{-hr}$
$RATE_{HC}$	Volumetric dissolution rate of hydrocerussite	$mol/m^3\text{-hr}$
$RATE_{PbO2}$	Volumetric dissolution rate of PbO_2	$mol/m^3\text{-hr}$
$rate_{scale}$	Surface area normalized dissolution rate of pipe scales	$mol/m^2\text{-hr}$
$rate_{HC}$	Surface area normalized dissolution rate of hydrocerussite	$mol/m^2\text{-hr}$
$rate_{PbO2}$	Surface area normalized dissolution rate of PbO_2	$mol/m^2\text{-hr}$
V_{scale}	Volume of the pipe scales in a pipe section	m^3
$V_{solution}$	Volume of the solution in a pipe section	m^3
η	porosity	
θ	contact ratio	

References

1. Boyd, G. R.; Dewis, K. M.; Korshin, G. V.; Reiber, S. H.; Schock, M. R.; Sandvig, A. M.; Giani, R., Effects of changing disinfectants on lead and copper release. *J. Am. Water Works Assoc.* **2008,** *100*, (11), 75-87.
2. Vasquez, F. A.; Heaviside, R.; Tang, Z. J.; Taylor, J. S., Effect of free chlorine and chloramines on lead release in a distribution system. *J. Am. Water Works Assoc.* **2006,** *98*, (2), 144-154.
3. Hozalski, R. M.; Esbri-Amador, E.; Chen, C. F., Comparison of stannous chloride and phosphate for lead corrosion control. *J. Am. Water Works Assoc.* **2005,** *97*, (3), 89-103.
4. Edwards, M.; Dudi, A., Role of chlorine and chloramine in corrosion of lead-bearing plumbing materials. *J. Am. Water Works Assoc.* **2004,** *96*, (10), 69-81.

5.   Cantor, A. F.; Park, J. K.; Vaiyavatjamai, P., Effect of chlorine on corrosion in drinking water systems. *J. Am. Water Works Assoc.* **2003,** *95*, (5), 112-123.

6.   McNeill, L. S.; Edwards, M., Phosphate inhibitor use at US utilities. *J. Am. Water Works Assoc.* **2002,** *94*, (7), 57-63.

7.   Schock, M. R., Understanding corrosion control strategies for lead. *J. Am. Water Works Assoc.* **1989,** *81*, (7), 88-100.

8.   Kuch, A.; Wagner, I., A mass transfer model to describe lead concentrations in drinking water. *Water Res.* **1983,** *17*, (10), 1303-1307.

9.   Lytle, D. A.; Schock, M. R., Impact of stagnation time on metal dissolution from plumbing materials in drinking water. *Journal Of Water Supply Research And Technology-Aqua* **2000,** *49*, (5), 243-257.

10.   Van der Leer, D.; Weatherill, N. P.; Sharp, R. J.; Hayes, C. R., Modelling the diffusion of lead into drinking water. *Applied Mathematical Modelling* **2002,** *26*, (6), 681-699.

11.   Cardew, P. T., Development of a convective diffusion model for lead pipe rigs operating in laminar flow. *Water Res.* **2006,** *40*, (11), 2190-2200.

12.   Lasaga, A. C., *Kinetic theory in the earth sciences*. Princeton University Press: Princeton, New Jersey, 1998; p 811.

13.   Xie, Y.; Wang, Y.; Singhal, V.; Giammar, D. E., Effects of pH and carbonate concentration on dissolution rates of the lead corrosion product PbO_2 *Environ. Sci. Technol.* **2010,** *44*, (3), 1093-1099.

14.   Noel, J. D.; Giammar, D. E. In *The influence of water chemistry on dissolution rate of lead corrosion products*, Water Quality Technology Conference, Charlotte, NC, 2007;

15.   Noel, J. D.; Giammar, D. E. In The influence of water chemistry on dissolution rates of Lead(II) carbonate solids found in water distribution systems, Water Quality Technology Conference, Cincinnati, OH, 2008;

16.   Nawrocki, J.; Raczyk-Stanislawiak, U.; Swietlik, J.; Olejnik, A.; Sroka, M. J., Corrosion in a distribution system: Steady water and its composition. *Water Res.* **2010.** *44*, (6), 1863-1872.

Chapter 6.   Conclusions and recommendations

6.1 Conclusions

This study investigated lead release from corrosion products in distribution systems in three experimental tasks. The first task was studying the effects of water chemistry on dissolution rates of the lead corrosion product PbO_2. The second task measured the equilibrium solubility of PbO_2 in the presence of free chlorine and compared the experimental results with thermodynamic predictions. The third task investigated lead release rates from pipe scales containing PbO_2 and assessed the possibility of predicting lead concentrations in pipe sections using dissolution rates determined in the first task.

Task 1: Investigate the effects of water chemistry on dissolution rates of PbO_2

In the first task, dissolution rates of the lead corrosion product PbO_2 were determined as a function of pH and concentrations of carbonate, free chlorine, monochloramine, and orthophosphate. The PbO_2 dissolution rates were determined using continuous-flow stirred tank reactors at a hydraulic residence time of half an hour. Complementary batch studies that followed the flow-through experiments were conducted to examine the effects of water chemistry at a longer residence time of 24 hours. The effects of water chemistry parameters on dissolution rates of PbO_2 provided insights into the mechanisms and rate-limiting steps of PbO_2 dissolution.

Higher carbonate concentration or lower pH increased PbO_2 dissolution rates. Carbonate accelerated PbO_2 dissolution by forming Pb(II)-carbonate complexes and detaching Pb(II) from the PbO_2 surface. The results indicated that PbO_2 dissolution occurs in two steps: first, PbO_2 is reduced to Pb(II) on the surface, and then Pb(II) detaches from the surface to solution. The detachment of Pb(II) from the surface was shown to be the rate-limiting step in the absence of chlorine disinfectants. An empirical dissolution rate model was developed to predict PbO_2 dissolution rates at different pH values and carbonate concentrations.

In flow-through experiments, both free chlorine and monochloramine inhibited PbO_2 dissolution by raising the redox potential relative to no disinfectant. The reduction of PbO_2 to Pb(II) on the surface was shown to be the rate-limiting step in the presence of chlorine disinfectants. Complementary batch studies have shown that monochloramine has two effects on PbO_2 dissolution. At short residence times, monochloramine inhibited PbO_2 dissolution by raising the redox potential relative to no disinfectant. At long residence times, an intermediate from monochloramine decay reduced PbO_2 and enhanced PbO_2 dissolution.

Orthophosphate significantly decreased net lead release rates to solution during PbO_2 dissolution by inducing the precipitation of hydroxylpyromorphite and by adsorbing to the plattnerite surface to block dissolution or reduction sites. As little as 1 mg P/L phosphate was needed to significantly inhibit PbO_2 dissolution. In the absence of carbonate, precipitation was the likely mechanism responsible for slowing net lead

release to solution from PbO_2. In the presence of carbonate, adsorption was probably the mechanism that inhibited PbO_2 dissolution.

Task 2: Determine equilibrium solubility of PbO_2 in the presence of free chlorine

Batch studies were conducted at different pH values in the presence of free chlorine to determine the equilibrium solubility of PbO_2. Although free chlorine was commonly believed to keep the lead concentrations under the action level, the lead concentrations released from PbO_2 in the presence of free chlorine can still exceed the action level at long residence times. Calculations using the thermodynamic constants of PbO_2 and $Pb(IV)$ species failed to predict PbO_2 equilibrium solubility in the presence of free chlorine. The equilibrium constants of PbO_2 and $Pb(IV)$ species were developed at extremely acidic or basic conditions, which were far away from environmentally-relevant conditions.

Task 3: Evaluate lead release rates from pipe scales containing PbO_2

Lead release from pipe scales with PbO_2 and hydrocerussite was examined under different water chemistry conditions, stagnation times, and flow velocities. The effectiveness of five water chemistry conditions as potential lead corrosion control strategies was investigated. The effects of stagnation time and flow on lead release from pipe scales were also studied.

170

Lead release from pipe scales is related to the dissolution and precipitation of lead corrosion products. Orthophosphate can be used as a lead corrosion inhibitor for pipes with hydrocerussite and PbO_2 scales. Orthophosphate concentrations higher than 0.3 mg P/L kept the dissolved lead concentration below the action level. For pipe scales consisting of hydrocerussite and PbO_2, the solutions that did not contain orthophosphate were not effective in controlling the dissolved lead concentrations below the action level. A switch of disinfectant from free chlorine to monochloramine increased the lead release in stagnation experiments.

Laminar flow accelerated both dissolved and particulate lead release from pipe scales. Turbulent flow would possibly increase the lead release rates even more. Dissolved lead contributed to most of the total lead concentration under both no-flow and laminar flow conditions. Stagnation time affected lead release from pipe scales by limiting the concentrations of residual disinfectant or corrosion inhibitor and by accumulating released lead when equilibrium was not reached.

The lead release rates from pipe scales were then predicted based on the dissolution rates of PbO_2 and the other lead corrosion product hydrocerussite. Reaction-limited and diffusion-limited models were developed and compared to predict the lead release from pipe scales. At stagnation conditions, the reaction-limited model accounting for both diffusion of lead and the rate of the dissolution reaction is better than the diffusion-limited model in describing the lead concentration change with time. At flow conditions, dissolution rate can be combined with mass transfer equations to predict the

lead concentration over time. The surface area normalized dissolution rates determined in flow-through experiments can be used in the reaction-limited models to predict lead release from pipe scales and explain the different observed rates at flow and stagnant conditions.

6.2 Recommendations for future work

Further research on the effects of different concentrations of monochloramine and phosphate on the dissolution of PbO_2 can be helpful to fully quantify the effects of these parameters. Since there is a difference in the Gibbs free energy of the two polymorphs of PbO_2, studies on the dissolution rate and equilibrium solubility of scrutinyite would complement the present study's focus on plattnerite. Determining the reaction constants of PbO_2 and $Pb(IV)$ species and consequently predicting the equilibrium solubility of PbO_2 can provide valuable information and guidance for lead corrosion control.

Investigation of the effects of various water chemistry conditions on lead release from other pipe scales containing cerussite, hydroxylpyromorphite, or litharge, would extend the information obtained from the present study to apply to more types of pipe scales. Knowledge of the effects of water chemistry on lead release from pipe scales with different corrosion products would assist water utilities in making decisions about water chemistry changes based on the composition of their corrosion scales. Examining the effect of turbulent flow on the lead release from pipe scales would extend the results to the full range of flow regimes that are possible in a distribution system.

172

For modeling lead release from pipe scales at flow or no-flow conditions, considering the flux of lead from the pipe wall to the water when the dissolution reaction is rate-limiting rather than setting the lead concentration at the pipe walls to the equilibrium lead concentration is recommended for the boundary condition assumption. Future research on incorporating dissolution rates into a turbulent mass transfer model for predicting lead release at turbulent flow conditions is needed.